R006-01
Zoom meeting B ：11/1　AM1　(9:00-10:30)
09:00-09:15

SC の PI 期に現れる 2 つの電流系について

#藤田　茂 [1)2)]
気象大,[2)]極地研

Two current systems in the PI phase of the Sudden Commencement

#Shigeru Fujita[1),2)]
Meteorological College,[2)]National Institute of Polar Research

In the Preliminary Impulse (PI) phase of the Sudden Commencement (SC), the dayside magnetopause is suddenly compressed. Then, the induced magnetosonic wave propagates in the magnetosphere around the Earth. The field-perpendicular current flowing along the wavefront of the magnetosonic wave is converted into the field-aligned current in the inner magnetosphere. This field-aligned current reaches the ionosphere. Thus, the upward field-aligned current on the prenoon side, the perpendicular current of the magnetosonic wavefront in the magnetosphere, and the downward field-aligned current on the post noon side form a PI-phase current circuit [Araki, 1994; Fujita et al., 2003a]. The PI signal in the magnetosphere propagates at the speed of the magnetosonic speed.　This fast propagation of the SC signal is detected by the satellite observation [Takahashi et al., 2017].
Besides, the ground network observation indicates that the duration of the PI magnetic signal on the ground is longer in the higher latitude [Araki, 1992].　This feature is also confirmed by the simulation [Fujita et al., 2003a].　It seems hard to explain this feature by the scenario of the magnetosonic wave propagation described above.　Thus, we intend to reveal this feature based on the MHD simulation study.
In order to determine the PI current system from the simulation results, the current system from the point with the strongest PI field-aligned current in the ionosphere is usually selected as the starting point. This time, we select the high latitude area and the low latitude area where the PI current system is relatively strong, and the current line was traced starting from that location. As a result, the field-aligned current from the high latitude region is a current system consisting of the perpendicular current that connects the field-aligned currents in the prenoon and postnoon. While the current system from the low latitude region crosses the magnetopause. This current is connected to the magnetosheath current in the region where the magnetosheath is strongly deformed by solar wind shock passing through it. This PI current system was first discovered this time.
Further results will be open in the talk.
Araki, T., H. Shimazu, T. Kamei, and H. Hanado, Scandinavian IMS magnetometer array data and their use for studies of geomagnetic rapid variations. Proc. NIPR Symp. Upper Atmos. Phys., 5, 10-20, 1992.
Araki, T., A physical model of the geomagnetic sudden commencement. In Solar Wind Sources of Magnetospheric Ultra-Low-Frequency Waves, ed. by M. J. Engebretson, K. Takahashi, and M. Scholer, American Geophysical Union, Washington, D.C., 183-200, 1994.
Fujita, S., T. Tanaka, T. Kikuchi, K. Fujimoto, K. Hosokawa, and M. Itonaga (2003a), A numerical simulation of the geomagnetic sudden commencement: 1. Generation of the field-aligned current associated with the preliminary impulse, J. Geophys. Res., 108(A12), 1416, doi:10.1029/2002JA009407.
Takahashi, N., Y. Kasaba, Y. Nishimura, A. Shinbori, T. Kikuchi, T. Hori, Y. Ebihara, and N. Nishitani (2017), Propagation and evolution of electric fields associated with solar wind pressure pulses based on spacecraft and ground-based observations, J. Geophys. Res. Space Physics, 122, 8446-8461, doi:10.1002/2017JA023990.

R006-02
Zoom meeting B ：11/1 AM1 (9:00-10:30)
09:15-09:30

The location of auroral oval depending on the tilt and precession of dipole axes deduced from global magnetosphere model

#Aoi Nakamizo[1)], Yasubumi Kubota[1)], Tsutomu Nagatsuma[1)], Takashi Tanaka[2)]
[1)]NICT,[2)]REPPU code Institute

Global magnetosphere simulation is one of the useful ways to complement observations and to know deductively what is going on in the magnetosphere-ionosphere. However, there has been much room for improvement of our simulation code to reproduce the realistic space environment. In order to simulate the magnetosphere more realistically, we introduced the inclination of the magnetic axis (tilt) and the precession between the magnetic and rotation axis, which have been coincided with each other and orthogonal to the ecliptic plane in the original REPPU code [Tanaka et al., 2015].
Although the tilt and precession may be thought to be less effective, it is expected to affect the simulation result because it alters the ionospheric conductance distribution, which largely modify the ionosphere-magnetosphere convection field through the M-I coupling processes [Nakamizo and Yoshikawa, 2019].
With this improved code, we examine how the distribution of large-scale FAC and associated conductance enhancement changes with/without the tilt and precession. Hereafter we call these regions as auroral oval. Because the location and intensity of FACs and conductances are the source of the disturbances of high-latitude ionosphere and primary energy input from the magnetosphere to the ionosphere, the improvement of predictability contributes to the practical use. We compare the locations of auroral ovals in simulations with tilt and precession (we use winter solstice conditions) and without tilt and precession (no seasonal and time dependence of conductance distribution) under the same solar wind and IMF input. In the northern hemisphere (dark winter hemisphere), the auroral oval tends to contract poleward in the dayside and expand equatorward in the nightside. This tendency become clearer for intense solar wind and IMF parameters. We discuss the result in terms of the solar wind-magnetosphere-ionosphere coupling.
References:
Tanaka, T. (2015). Substorm Auroral Dynamics Reproduced by Advanced Global Magnetosphere－Ionosphere (M?I) Coupling Simulation. In Auroral Dynamics and Space Weather (eds Y. Zhang and L.J. Paxton). doi:10.1002/9781118978719.ch13
Nakamizo, A., & Yoshikawa, A. (2019). Deformation of ionospheric potential pattern by ionospheric Hall polarization. Journal of Geophysical Research: Space Physics, 124, 7553? 7580. https://doi.org/10.1029/2018JA026013

R006-03
Zoom meeting B ：11/1 AM1 (9:00-10:30)
09:30-09:45

3D-current structure associated with auroral electrojet

#Yuto Yano[1)], Yusuke Ebihara[2)]
[1)]RISH, Kyoto Univ.,[2)]RISH, Kyoto Univ.

We developed a simplified Hall-MHD simulation to understand the magnetosphere-ionosphere coupling in the polar region during the auroral substorm. The governing equations were derived from the law of conservation of momentum of ions and electrons, the equation of continuity of plasma, the law of Ohm, the law of Ampere, and the law of Faraday. The Hall effect is included because it retains the Hall term in the governing equations. The advection in the governing equations were solved by using the implicit scheme and the Lax-Wendroff scheme and the Superbee limiter function. We imposed a flow shear on the topside boundary to excite Alfven wave. First, we ran the simulation under the condition that the ionospheric plasma density is uniform in the horizontal space. It was confirmed that the Alfven wave propagated downward and the FACs were closed by the Pedersen current in the lower ionosphere. Secondly, we introduced a high-density channel. The secondary electric field is confirmed to appear due to the blockage of the Hall current (polarization), which intensifies the ionospheric current. This is similar to the auroral electrojet. In addition, we found the additional FAC confined at limited altitude and this current may connect the Pedersen current and the Hall current.

R006-04
Zoom meeting B ：11/1 AM1 (9:00-10:30)
09:45-10:00

North-south asymmetric auroral surge development as reproduced by global MHD simulation

#Kiyoka Murase[1)], Ryuho Kataoka[1),2)], Herbert Akihito Uchida[1)], Yusuke Ebihara[3)], Shigeru Fujita[2),4)], Takashi Tanaka[5)]
[1)]Polar Science, SOKENDAI,[2)]NIPR,[3)]RISH, Kyoto Univ.,[4)]Meteorological College,[5)]REPPU code Institute

Uchida et al. (2020) reported observational evidence that auroral surges expanded in opposite direction in the northern and southern hemispheres simultaneously. The directions of the surges corresponded to those of the Hall current in the vicinity of surges in each hemisphere, as expected from the results from a recent global magnetohydrodynamic (MHD) simulation (Ebihara and Tanaka, 2018). The asymmetric Hall current direction in conjugate area can be originated from the difference of two-cell convection patterns in the ionosphere because of the strong y-component of the interplanetary magnetic field (~6 nT in GSM). In this presentation, we show the example of the asymmetrically expanding surges as reproduced by the REPPU Level 7 code (Tanaka, 2015), which essentially support the above mentioned idea. We also quantitatively compare the simulation results with the observed features such as displacement of the initial brightening and the difference in the traveling speed of the surges in both hemispheres. This study implies that the cutting-edge MHD simulation can be used to precisely predict such a dynamic mesoscale auroral variation if computational resource is large enough.

R006-05
Zoom meeting B ：11/1　AM1　(9:00-10:30)
10:00-10:15

沿磁力線方向の磁気圏・電離圏不均一性を考慮したフィードバック不安定性理論

#渡邉　智彦[1),]樋渡　淳也[1),]前山　伸也[1)]
[1)]名大・理・物理

Feedback instability theory including field-aligned inhomogeneity of the magnetosphere and ionosphere

#Tomo-Hiko Watanabe[1)], Junya Hiwatari[1)], Shinya Maeyama[1)]
[1)]Dept. Physics, Nagoya Univ.

We have recently extended the feedback instability theory, including inhomogeneity of the magnetosphere and the ionosphere. The detailed　eigenvalue analysis clarifies that the altitude dependence of the ionospheric collision frequency may lead to stabilization of the ionospheric Alfven resonator (IAR) mode which stems from the non-uniform Alfven velocity profile in the magnetosphere. The theoretical analysis confirms that the stabilization is brought by an effective internal resistivity due to the ionospheric inhomogeneity, not by a shear of the ionospheric current in contrast to a previous study. Nevertheless, the filed line resonance (FLR) type mode with lower frequency remains unstable even when the high frequency IAR modes are stabilized, as confirmed by the eigenmode analysis and the numerical simulation. The present study demonstrates a robustness of the feedback instability mechanism providing spontaneous growth of the auroral arc structure in the magnetosphere-ionosphere coupling through the FLR type modes even with strong inhomogeneity in the magnetosphere and the ionosphere.

R006-06
Zoom meeting B ：11/1　AM2　(10:45-12:30)
10:45-11:00

#田中　杜雄[1)],田口　聡[1)],細川　敬祐[2)]
[1)]京大理,[2)]電通大

The characteristics of the inverted-V event accompanying the downward return field-aligned current

#Morio Tanaka[1)], Satoshi Taguchi[1)], Keisuke Hosokawa[2)]
[1)]Grad school of Science, Kyoto Univ.,[2)]UEC

The inverted-V is an energetic electron precipitation event, which can be seen as a V-shape structure in electron flux spectrograms, and causes intense auroral arcs. Previous satellite observations have suggested that some inverted-V structures, corresponding to the upward field-aligned current (FAC), would accompany the downward FAC adjacent to them [Marklund et al., 1997, 2004, 2011; Baddeley et al., 2017]. Marklund et al. [2011] conducted the in-situ observation of the parallel electric field in the auroral acceleration region, which was associated with the inverted-V, and reported that the structure would be stable for some minutes at least. However, the detail characteristics of the inverted-V phenomena that accompany the downward FAC adjacent to them are still unclear. In this study we conducted a statistical analysis to identify the characteristics of these current systems, using precipitating electron and magnetic field data from the DMSP spacecrafts (F16, F17, F18) in 2015 and 2016. Aurora image data (557.7 nm and 630 nm) from an all-sky imager at Longyearbyen, Svalbard are also used to track the time evolution of the upward current region.The result of the analysis indicates that the upward FAC density, i.e., the inverted-V current density is much correlated with the?density of the downward FAC located equatorward of the V-shape structure. We also identified the auroral events that in which the auroral black structure appeared on the equatorward side of the intense aurora arc, corresponding to the inverted-V. These facts suggest that the downward FAC equatorward of and adjacent to the inverted-V may play an important role for the formation of the inverted-V structure.　In addition, the relation between the peak energy of the inverted-V accompanying the downward FAC and its upward FAC density will be discussed in terms of the linearized Knight relation.

Inverted-V 構造は、衛星が観測する降下電子フラックスのスペクトログラムの中に見られる逆 V 字型の電子分布構造で、明るいオーロラを発生させる。Inverted-V 構造は上向きの沿磁力線電流に相当するが、衛星観測の先行研究から、Inverted-V 構造の中には、それに隣接して下向きの沿磁力線電流を伴うものがあることが報告されている[Marklund et al., 1997, 2004, 2011; Baddeley et al., 2017]。
Marklund et al. [2011]は、Cluster 衛星を用いたオーロラ加速領域の電場の直接観測によって、Inverted-V を発生させるような電場が、少なくとも 5 分存在していることを示している。しかし、この downward FAC を伴う Inverted-V 構造の性質の詳細は、未だ明確になっていない。　本研究では、2015 年から 2016 年の DMSP 衛星(F16, F17, F18)の降下電子フラックスおよび磁場のデータを解析し、downward FAC を伴う Inverted-V 構造の性質を明らかにする。また、Svalbard 諸島 Longyearbyen に設置されている地上全天イメージャーのオーロラ画像（557.7 nm と 630 nm）と DMSP 衛星の同時観測から、この電流系に付随するオーロラの時間発展を追う。　これらの解析の結果より、Inverted-V に相当する upward FAC の電流密度と、Inverted-V の赤道側に流れる downward FAC の電流密度の間には非常に良い相関があることが分かった。さらに、地上全天イメージャーとの同時観測から、Inverted-V に対応するオーロラアークの赤道側において、発光強度の低い black structure が発生するイベントを見出した。これらの観測結果から、Inverted-V を含む電流系において、Inverted-V に隣接する downward FAC はオーロラ電流回路の一端を担い、Inverted-V の形成に重要な役割を果たしていると考えられる。以上に加え、downward FAC を伴う Inverted-V について、Inverted-V 構造のピークエネルギーと upward FAC の電流密度の関係についても Knight-relation の観点から議論する。

R006-07
Zoom meeting B ：11/1　AM2　(10:45-12:30)
11:00-11:15

国際宇宙ステーションからのリム方向デジカメ観測を用いたオーロラ電子のエネルギー推定

#南條　壮汰[1)],佐藤　夏雄[2)],穂積　裕太[1)],細川　敬祐[1)],片岡　龍峰[2)3)],三好　由純[4)],大山　伸一郎[2)4)5)],尾崎　光紀[6)],塩川　和夫[4)],栗田　怜[7)]
[1)]電通大,[2)]極地研,[3)]総研大,[4)]名大 ISEE,[5)]オウル大,[6)]金沢大,[7)]京都大学 生存研

Estimating the energy of auroral electrons using color digital camera observations from the International Space Station

#Sota Nanjo[1)], Natsuo Sato[2)], Yuta Hozumi[1)], Keisuke Hosokawa[1)], Ryuho Kataoka[2),3)], Yoshizumi Miyoshi[4)], Shin-ichiro Oyama[2),4),5)], Mitsunori Ozaki[6)], Kazuo Shiokawa[4)], Satoshi Kurita[7)]
[1)]UEC,[2)]NIPR,[3)]SOKENDAI,[4)]ISEE, Nagoya Univ.,[5)]Univ. of Oulu,[6)]Kanazawa Univ.,[7)]RISH, Kyoto Univ.

Astronauts have been taking a large number of auroral photographs of the Earth from the International Space Station (ISS) using digital single lens reflex (DSLR) cameras. We have introduced a method for projecting the photographs of aurora from ISS onto the geographic coordinate system using night city lights in the images as markers [Nanjo et al., 2020]. The temporal resolution of the ISS photography is mostly shorter than 1 sec with a wide field-of-view (FOV) coverage (as wide as the FOVs of multiple ground-based all-sky imagers). Besides, the FOV of the ISS photography sweeps through a long distance (4-5 hours in local time) in a short time interval (~10 min). In addition, because the images are taken in the rim direction of the Earth, they allow us to visualize the height structure of the aurora, which is difficult to be revealed by optical observations from the ground and space.

The purpose of this study is to estimate the energy of the precipitating electrons from the color of auroras in the ISS digital images. For pulsating auroras which are known to have a narrow range of emission altitude, we tried to infer the average energy from the B/G (blue to green) ratios of the digital images. This idea is based on the fact that the 557.7 nm emission of oxygen atoms should contribute to the G channel and the band emission of molecular nitrogen ions should contribute to the B channel. During the two cases of pulsating aurora, the B/G ratio tended to be higher on the morning sector than on the midnight sector. This tendency has always been reported in a number of studies, indicating that the B/G ratio from the ISS images can be a qualitative proxy for the energy of precipitating electrons.

We also investigated the colors of aurora during so-called omega bands and identified unique wall-like aurorae in the western boundary of torches of omega bands. There wall-like aurorae are tall in altitude and thin in the longitudinal direction; thus, we call them "Great Walls". To quantitatively validate the energy of the electrons precipitating into the Great Wall, we compared the field-aligned altitude profiles of luminosities of the RGB channels with those of the 557.7 nm and 630.0 nm obtained from the GLOW model. The Great Walls were found to extend for more than 200 km in altitude and contain greenish and reddish colors respectively at the bottom and top of the structures, which is inconsistent the previous study showing only 2-5 keV electron precipitations on the western flank of the torches [Amm et al., 2005]. In the presentation, we will discuss the detail of the analysis and introduce a future plan aiming at the quantitative use of B/G ratios from the ISS images.

国際宇宙ステーション（International Space Station: ISS）から、デジタル一眼レフカメラ（デジカメ）を用いてオーロラの連続カラー画像が撮影され、NASA のウェブサイトで公開されている。我々は、それらの画像を背景に写っている街明かりをマーカーにすることで地理座標上に投影する手法を提案した［Nanjo et al., 2020］。この ISS からのデジカメ観測は 1 秒以下の時間分解能と、地上全天カメラ 3-4 台分の広い視野を持ち、約 10 分の間にローカルタイム方向に 4-5 時間分に相当する領域を俯瞰的に撮像することができる。さらに、撮影は地球の縁を捉える向き（斜め）に行われているため、従来の典型的な光学観測では捉えることのできないオーロラの高さ構造を可視化することができる。本研究では、カラー画像であるという特徴を生かし、オーロラの色から降り込み電子のエネルギーを推定することを目標とした。発光高度の幅が小さい脈動オーロラに対しては、酸素原子の 557.7 nm の発行が緑色のチャネルに寄与し、427.8 nm を代表とする窒素分子イオンのバンド発光が青色のチャネルに寄与すると考え、B/G の値からエネルギーを推定できるかを検討した。また、ISS のデジカメ観測により初めて観測されたオメガバンド中に現れる壁状オーロラ“Great Wall" に対しては、沿磁力線方向の RGB チャネルの輝度値の変化と、GLOW モデルから得た 557.7 nm と 630.0 nm の発光強度の高度分布を比較することにより、降り込み電子のエネルギー帯を定量的に推定することを目指した。脈動オーロラについては、B/G の値に真夜中に比べ朝側で高くなる傾向が見られたことから、B/G の値が電子のエネルギーを表す指標として少なくとも定性的に有効であることが示された。また、"Great Wall" は高さ方向のスケールが 200 km 以上になることがわかり、先行研究のオメガバンドの西側に 2-5 keV のみの降り込みが存在するとの報告［Amm et al., 2005］とは異なる結果となった。発表では、B/G の値を定量的に用いるための今後の研究方針や“Great Wall" のより詳細なエネルギー帯についても報告を行う。

R006-08
Zoom meeting B ：11/1　AM2　(10:45-12:30)
11:15-11:30

しらせ搭載の全天多波長姿勢安定イメージャーによるオーロラ・大気光観測

#坂野井　健[1)],津田　卓雄[2)],穂積　裕太[2)],青木　猛[2)],齊藤　昭則[3)],直井　隆浩[4)],永原　政人[4)],江尻　省[5)],西山　尚典[5)]
[1)]東北大・理,[2)]電通大,[3)]京都大・理・地球物理,[4)]情報通信研究機構,[5)]国立極地研究所

Aurora and airglow observations with the multi-wavelength all-sky attitude-stabilized imagers on Shirase

#Takeshi Sakanoi[1)], Takuo Tsuda[2)], Yuta Hozumi[2)], Takeshi Aoki[2)], Akinori Saito[3)], Takahiro Naoi[4)], Masato Nagahara[4)], Mitsumu K. Ejiri[5)], Takanori Nishiyama[5)]
[1)]Grad. School of Science, Tohoku Univ.,[2)]UEC,[3)]Dept. of Geophysics, Kyoto Univ.,[4)]NICT,[5)]NIPR

In this presentation, we give the results on the all-sky imaging observation on Shirase at 630 nm during the period of 2019-2020, and the status for improved imaging system for the operation in 2020-2021. To cover the auroral and airglow observation gap in the Southern Ocean, we developed an all-sky imaging system (Shirase ASI) with a 3-axis attitude stabilized gimbal installed on the icebreaker Shirase. The route of Shirase from February to March is preferable to observe aurora in the aurora region at the south of Australia. This region is also important to understand the height and zonal variations of mesospheric atmospheric gravity waves (AGWs). This all-sky image data on Shirase is useful in collaboration with ground-based imager networks, such as ANGWINS, UAO and AGO. In addition to auroral observation, Shirase ASi can observe airglow variations caused by plasma bubbles and MSTID when Shirase is located at the mid- and low-latitudes between Japan and Antarctica.
We developed a monochromatic all-sky imager at 630 nm in 2019, and carried out continuous observation on Shirase from November 2019 to March 2020 as a part of 61th Japanese Antarctic Research Expedition (JARE) conducted by NIPR. In 2020, we are additionally developing an all-sky imager for the measurement of auroral and airglow emissions at N2 1PG/OH at 650-690 nm, and going to perform similar operation in the 62th JARE period. A compact and high-sensitivity all-sky imager consits of the low-noise CMOS camera (ZWO ASI183MM Pro), the fisheye lens (Fujinon FE185C086HA, f=2.7 mm, F/1.8), and the bandpass interference filter (Andover, center wavelength 630nm, FWHM 4.4nm). The sensitivity at a wavelength of 630nm was calibrated by the integrated sphere in NIPR on June 26 and 27, 2019, and confirmed dynamic range is 80-20000R with a resolution of 5R with an exposure time of 19s. This optical system was mounted on a 3-axis attitude stabilized gimbal (DJI Ronin-S), and installed in the water-proof observation box on the 06 deck of Shirase. The controlling laptop PC obtained the current location from GPS signal, and calculated the appropriate start and end timings of observation every day. The exposure time and interval were changeable, and set to be 19s and 20s, respectively. All data were stored in NAS via PC, and analyzed after April 2020 when Shirase returned to Japan. Thumbnail images and housekeeping data were sent to Japan via e-mail everyday to monitor the operation status. The temperature of observation box on the Shirase deck worked sufficiently using heater, and cooler throughout the operation period. We confirmed the performance of attitude stabilization by the gimbal of which vibration was attenuated by 1/14, and the resolution of obtained image is sufficient for auroral and airglow measurements.
On several nights from February to March in 2020, we observed 630nm auroral emission with intensity of several kR in the northward direction when Shirase existed in the polar cap region. We also observed the enhancement of 630nm airglow emission with intensity of a few hundreds R at the equatorial ionospheric anormaly (EIA) on November 22 and 23, 2019. On the other hand, the gimbal stopped on March 21 due to the DC-DC regulator of power supply was broken. In addition, the controlling PC had been stopped on the return route from Australia to Japan.
In 2020-2021 (JARE62), we adopt more reliable power supply and controlling PC, and develop the two-imager system to observe auroral and airglow emissions at OI 630 nm and N2 1PG/OH at 650-690nm. We also install a GNSS receiver to monitor ionospheric total electron content. Our system can be applied to automatic and independent observation system for other ships and ocean buoys.

本講演では、南極観測船「しらせ」に搭載された姿勢安定全天イメージャーの 2019-2020 年の成果と、2020-2021 年観測に向けた装置改良と運用計画を報告する。本研究は、しらせに搭載する全天イメージングシステム(Shirase ASI)を開発し、オーロラと大気光の南極海上の観測欠落を解消することを目的とする。南極海におけるしらせの航路は、例年 2-3 月にオーストラリア南側のオーロラオーバル直下を通過するため、オーロラ観測に最適である。また、この領域は中間圏大気重力波（AGW）変動の理解にも重要である。 この海上データは、ANGWINS、UAO、AGO などの南極陸域のネットワーク観測との連携に役立つ。さらに、本観測はしらせ航海中に継続して行われるため、中低緯度における大気光発光を観測からプラズマバブルや MSTID 現象解明にも貢献できる。
我々は、2019 年に第 61 次南極地域観測（JARE61）の公開利用研究として OI630nm 単色全天イメージャーを開発し、しらせ上で 2019 年 11 月から翌年 3 月まで連続観測を実施して装置性能を実証した。 2020 年はこれを発展さ

せ、第 62 次南極地域観測（JARE61）の萌芽研究として、新たに N2 1PG / OH 650-690 nm 観測イメージャーを追加し、2020-21 年に船上観測を行う計画である。
装置について、低ノイズ冷却 CMOS カメラ（ZWO 社 ASI183MM Pro）に魚眼レンズ（フジノン社 FE185C086HA, f = 2.7 mm, F/1.8）と干渉フィルター（アンドーバ社, 中心波長 630 nm、FWHM 4.4 nm）を取り付けた軽量コンパクトな高感度全天イメージャーを 2019 年に開発した。このイメージャーの波長 630nm における感度は、2019 年 6 月 26-27 日に極地研究所積分球によって校正され、ダイナミックレンジが 80 - 20000 R、分解能が~5 R（露出時間 19 秒）であることが確認された。光学系は 3 軸姿勢安定ジンバル（DJI Ronin-S）に搭載され、しらせ 06 甲板上に設置された防水観測箱内に格納された。露出時間と間隔はそれぞれ 19 秒と 20 秒に設定した。全期間の観測データは NAS に保存され、2020 年 4 月にしらせが日本に戻った後に解析に用いられた。航海期間を通じてサムネイル画像や温度・湿度等は毎日メールで日本に送信され、稼働状況の監視に用いられた。また、ジンバルにより船の振動が 1/14 に減衰されることがわかり、オーロラと大気光の長時間露出観測でも十分な空間分解を達成することを実証した。
2019 年の観測成果として、11 月 12 日のしらせ出航以来約 4 ヶ月間の自動連続観測に成功した。 特に 2020 年の 2 月下旬から 3 月上旬の数夜において、しらせが極冠域にいた際に、北側（低緯度側）に数 kR の 630 nm のオーロラ発光を観測した。また、2019 年 11 月 22 日と 23 日には、低緯度域において赤道電離層異常（EIA）と考えられる数 100R の増光を捉えた。一方、帰途の 3 月 21 日にジンバルへの電源供給が故障したため、ジンバルによる姿勢制御が停止した。さらに、オーストラリアから日本への帰路で制御 PC がフリーズしたため、データ記録がなされなかった。
2020-2021 年（JARE62）の観測では、より信頼性の高いジンバル要電源と制御 PC を採用し、OI 630 nm 発光と N2 1PG / OH650-690 nm 発光を同時撮像する 2 台の全天イメージャーシステムを開発している。加えて、電離圏全電子量を監視するために GNSS 受信機を設置する。本システムは、他の船舶や海洋ブイを用いた自動独立観測システムに適用可能である。

R006-09
Zoom meeting B ：11/1　AM2　(10:45-12:30)
11:30-11:45

超高高度からの加速電子降下で励起される活動的オーロラアーク

#今城　　峻[1)],三好　由純[2)],風間　洋一[3)],浅村　和史[4)],篠原　育[5)],塩川　和夫[6)],笠原　禎也[7)],笠羽　康正[8)],松岡　彩子[9)],Wang　Shiang-Yu[10)],Tam　Sunny W. Y.[11)],Chang　Tzu-Fang[11)],Wang　B.-J.[12)],Angelopoulos　Vassilis[13)],田　采祐[14)],小路　真史[2)],中村　紗都子[15)],北原　理弘[2)],寺本　万里子[16)],栗田　怜[17)],堀　智昭[2)]
[1)]名大・ISEE,[2)]名大 ISEE,[3)]中央研究院天文・宇宙物理学研究所,[4)]宇宙研,[5)]宇宙研／宇宙機構,[6)]名大宇地研,[7)]金沢大,[8)]東北大・理,[9)]京都大学,[10)]Academia Sinica,[11)]国立成功大学宇宙・プラズマ科学研究所,[12)]ASIAA, Taiwan,[13)]UCLA,[14)]名大 ISEE 研,[15)]ISEE,[16)]九工大,[17)]京都大学 生存研

Active auroral arc powered by accelerated electrons from very high altitude

#Shun Imajo[1)], Yoshizumi Miyoshi[2)], Yoichi Kazama[3)], Kazushi Asamura[4)], Iku Shinohara[5)], Kazuo Shiokawa[6)], Yoshiya Kasahara[7)], Yasumasa Kasaba[8)], Ayako Matsuoka[9)], Shiang-Yu Wang[10)], Sunny W. Y. Tam[11)], Tzu-Fang Chang[11)], B.-J. Wang[12)], Vassilis Angelopoulos[13)], ChaeWoo Jun[14)], Masafumi Shoji[2)], Satoko Nakamura[15)], Masahiro Kitahara[2)], Mariko Teramoto[16)], Satoshi Kurita[17)], Tomoaki Hori[2)]
[1)]ISEE, Nagoya Univ.,[2)]ISEE, Nagoya Univ.,[3)]Institute of Astronomy and Astrophysics, Academia Sinica, Taiwan,[4)]ISAS/JAXA,[5)]ISAS/JAXA,[6)]ISEE, Nagoya Univ.,[7)]Kanazawa Univ.,[8)]Tohoku Univ.,[9)]Kyoto University,[10)]Academia Sinica,[11)]Institute of Space and Plasma Sciences, National Cheng Kung University, Taiwan,[12)]ASIAA, Taiwan,[13)]UCLA,[14)]ISEE, Nagoya Univ.,[15)]ISEE,[16)]Kyutech,[17)]RISH, Kyoto Univ.

We show that active auroral arcs are powered by electrons accelerated at altitudes reaching greater than 30,000 kilometers. We employ high-angular-resolution electron observations achieved by the Arase satellite in the magnetosphere and optical observations of the aurora from a THEMIS ground-based all-sky imager. Our observations of electron properties and dynamics at ~02:37 UT on September 15, 2017 resemble those of electron potential acceleration reported from low-altitude satellites except that the acceleration region is much higher than previously assumed. Downgoing monoenergetic electrons, whose flux often forms the inverted-V shape in an energy-time spectrogram, indicate that these electrons are accelerated above the satellite prior to precipitating to auroral altitudes. These precipitating electrons can be the main carrier of the upward field-aligned current, which is observed as an azimuthal magnetic field deflection. In the region of those accelerated current carriers, the plasma number density is expected to be small, also known as plasma cavity. The upgoing proton and converging electric field indicate a U-shape potential drop below the satellite. The lack of upgoing electrons within the loss cone is consistent with accelerated electrons that are lost to the atmosphere while exciting auroral emissions. Since the parallel acceleration makes a pitch angle more field-aligned, in contrast to the mirror force, the electron loss cone width depends on the potential drop below. These observations show that the dominant auroral acceleration region can extend far above a few thousand kilometers, well within the magnetospheric plasma proper, suggesting the formation of the acceleration region by some unknown magnetospheric mechanisms. Similar features of the acceleration and precipitation from very high altitudes are also found in other periods, and these events are investigated in detail.

R006-10
Zoom meeting B ：11/1 AM2 (10:45-12:30)
11:45-12:00

Modeling of SEP induced auroral emission at Mars: Different behaviors of electron and proton in the presence of crustal fields

#Yuki Nakamura[1)], Naoki Terada[2)], Hiromu Nakagawa[3)], Shotaro Sakai[4)], Sayano Hiruba[5)], Francois Leblanc[6)]
[1)]Dept. Geophys., Science, Tohoku Univ.,[2)]Dept. Geophys., Science, Tohoku Univ.,[3)]Dept. Geophys., Science, Tohoku Univ.,[4)]Dept. Geophys., Science, Tohoku Univ.,[5)]Dept. Geophys., Science, Tohoku Univ.,[6)]LATMOS-IPSL, CNRS

Since Mars lacks a global intrinsic magnetic field, Solar Energetic Particles (SEPs) can directly precipitate into its atmosphere, causing increased ionization, dissociation and excitation of the atmospheric molecules. Simultaneous observations with Solar Energetic Particle (SEP) and the Imaging UltraViolet Spectrograph (IUVS) instruments on board the Mars Atmosphere and Volatile EvolutioN (MAVEN) spacecraft have revealed the existence of SEP induced diffuse auroral emission spanning across nightside Mars [Schneider et al., 2015, 2018]. Several model studies showed that about 100 keV monoenergetic electron precipitation was preferable for the low altitude (~60 km) peak of the limb emission of CO2+ ultraviolet doublet [Schneider et al., 2015; Gerard et al., 2017; Haider et al., 2019]. However, no models were able to reproduce the low altitude emission peak using the observed electron energy population ranging from few keV to 200 keV. Previous auroral emission models did not take into account the contribution of MeV proton precipitation, although few MeV proton can penetrate into ~60 km altitude as well [e.g., Jolitz et al., 2017]. This study aims to model the SEP induced diffuse auroral emission by both electrons and protons to explain the observed diffuse auroral emission profiles. In order to constrain the possible source of the diffuse auroral emission, we focus on the different behaviors of electrons and protons in the presence of crustal fields due to a large difference in their gyro radii. Crustal fields on Mars largely change over an altitude range of precipitation, whereas Earth's global magnetic field did not change at all over the altitude range. Hence, the magnetic mirror plays a major role in altering the pitch angle of incident charged particles in the atmosphere of Mars, which is expected to affects the auroral emission profiles in the presence of crustal field.

In order to take into account the effects of crustal fields on the transport of electrons and protons, we have newly developed a Monte-Carlo collision and transport model of SEP electrons and protons with magnetic fields on Mars. We calculated following three modes: (1) a trace-only mode which solves equation of motion in the presence of three-dimensional inhomogeneous electromagnetic field without collision, (2) a collision-only mode which tracks all collisions in the absence of electromagnetic field and (3) a collision-trace mode which solves equation of motion in the presence of electromagnetic field and tracks all collisions. We focus on the SEP electrons with energy below 100 keV and protons with energy below 5 MeV due to the available energy range of the cross sections.

In a collision-only mode, we confirmed that 100 keV electrons and 5 MeV protons can penetrate into 60 km altitude, which is consistent with stopping height obtained by the previous models [e.g., Gerard et al., 2017; Jolitz et al., 2017]. We performed a case study of September 2017 event, using the energy population of electrons and protons observed by MAVEN/SEP. The ionization rate by protons is one order of magnitude larger than that by electrons, which suggests the auroral emission by protons can largely contribute to the total auroral emission.

Insights into the effects of crustal fields on the auroral emission by both electrons and protons will be shown at the presentation.

R006-11
Zoom meeting B ：11/1　AM2　(10:45-12:30)
12:00-12:15

第 24 太陽周期中のオーロラ活動：南極昭和基地における観測

#門倉　昭
ROIS-DS/極地研

Auroral activity during the solar cycle 24: Observations at Syowa Station, Antarctica

#Akira Kadokura
ROIS-DS/NIPR

Auroral activities observed at Antarctic Syowa Station during the solar cycle 24, from 2009 to 2020, are analyzed. In this presentation, characteristics of auroral substorm observed with the Scanning Photometer (SPM) will be focused.

第 24 太陽周期中（2009 年～2020 年）に南極昭和基地で観測されたオーロラ活動について、特に掃天フォートメータにより観測されたオーロラサブストームの特徴について紹介する。

R006-12
Zoom meeting B ：11/1　PM1　(13:45-15:30)
13:45-14:00

朝側 Pc-3 の出現を決める太陽風磁場の方向について

#小原　隆博[1)],吉川　顕正[2)],魚住　禎司[2)],阿部　修司[2)]
[1)]東北大・惑星プラズマ大気研究センター,[2)]九州大・国際宇宙天気科学研究教育センター

IMF control of Pc-3 occurrence in the morning sector

#Takahiro Obara[1)], Akimasa Yoshikawa[2)], Teiji Uozumi[2)], Shuji Abe[2)]
[1)]PPARC, Tohoku University,[2)]ICSWSE, Kyushu University

It has been recognized that there are two major candidates for the origin of daytime low-latitude Pc-3 magnetic pulsations; i.e. upstream waves in the solar wind and surface waves at the magnetopause boundary. In order to have a solid proof, we have surveyed MAGDAS magnetic field data obtained at Kyushu University and found following things. Pc-3 pulsations in the day time likely occur during low cone angle of inter planetary magnetic field (IMF). However, morning time (6~9 LT) Pc-3 pulsation tends to have a strong dependence on the IMF orientation. That is, these morning time Pc-3 pulsations mostly appear during Parker spiral situation of IMF. During parker spiral condition, surface of the magnetopause boundary becomes unstable due to the Kelvin-Helmhortz (KH) instability, causing large surface waves, which penetrate into the magnetosphere and to the ground. The evidence, we identified, is likely to be a proof of significant contribution of the surface waves to the Pc-3 pulsation in the morning side magnetosphere.

R006-13
Zoom meeting B ：11/1　PM1　(13:45-15:30)
14:00-14:15

昼側脈動オーロラの周期性に関する統計解析

#安倍　峻平[1)],細川　敬祐[1)],小川　泰信[2)]
[1)]電通大,[2)]極地研

Periodicity of dayside pulsating aurora: A statistical analysis in Longyearbyen

#Shumpei Abe[1)], Keisuke Hosokawa[1)], Yasunobu Ogawa[2)]
[1)]UEC,[2)]NIPR

Pulsating aurora (PsA) is a type of diffuse aurora which shows quasi-periodic modulation of luminosity. It has been known that PsA is usually observed during the late recovery phase of substorms in a magnetic local time (MLT) sector extending from the post-midnight to dawn. Previous studies indicated that PsA originates from quasi-periodic precipitation of electrons, which are scattered by whistler mode chorus waves near the equatorial plane of the magnetosphere.
Most of the previous studies of PsA are focused on observations on the nightside and dawnside. However, recent studies, for example Han et al. (2015), indicated that PsA is observed even on the dayside (from the morning to the noon sector) at high-latitudes slightly below the cusp region. In addition, Motoba et al. (2017) showed that intensity modulation of whistler mode chorus waves which is considered to drive the dayside PsA (DPA) was associated with magnetic pulsations in the Pc3 range (22-100mHz). This result suggests that the pulsating period of DPA should be within the Pc3 range. However, it has not yet been clarified what factors determine the periodicity of DPA. To reveal such properties of DPA, we have used optical data obtained from the all-sky WATEC imagers (AWIs, Ogawa et al., 2019) in Longyearbyen, Norway (78.1N,16.04E), whose temporal resolution is 1 Hz for the green-line (557.7 nm) observations.
To clarify the distribution of pulsating period of DPA, we performed automatic extraction of the pulsation period from AWI images by applying the Stockwell transform to Several events of DPA seen in Longyearbyen. In addition, we investigated the dependence of the periodicity of DPAs on the background parameters such as solar wind parameters (e.g., solar wind dynamic pressure) and geomagnetic activity (Kp, AE and Dst indices). From this statistical analysis, we found that several parameters such as MLT are associated with the pulsation period. This association suggests that these parameters may contribute to the period of DPA thorough that of Pc3 geomagnetic pulsation.

ディフューズオーロラのうち，準周期的な発光を伴うものを脈動オーロラ（Pulsating Aurora : PsA）と呼ぶ． PsA は主にサブストームの回復期に発生することが知られており，磁気的地方時（Magnetic Local Time : MLT）の真夜中から朝方にかけて多く観測される．先行研究では， PsA の発生は準周期的な電子降下に起因し，その電子降下は磁気圏赤道面付近でのホイッスラーモードコーラス波動によるピッチ角散乱によって引き起こされることが示されている．PsA に関する先行研究は真夜中から朝にかけての観測に関するものが大半である．しかし，近年は昼側での PsA (Dayside PsA : DPA)の観測に関する研究も行われている． Han et al . (2015) は，カスプ領域よりわずかに低緯度側の高緯度地域において，朝から正午にかけての時間帯にも PsA が存在することを示した．更に、Motoba et al.(2017)において、脈動オーロラを駆動すると考えられているホイッスラーモードコーラス波動の強度変調が、Pc3 レンジ(22-100 mHz)の地磁気脈動と関連することが示されている。しかし、DPA の周期性を決定づける要素が何であるかはまだ知られていない。これらの DPA に関する性質を調査するために、我々はノルウェーのロングイェールビン(78.1N°,16.04° E)における all-sky WATEC imagers (AWIs, Ogawa et al., 2019)による地上観測データを用いた解析を行った。
DPA の周期分布を明らかにするために、ロングイェールビンで観測された複数の DPA イベントにおいて、AWI の各画素に対する S 変換から脈動周期の自動抽出を行った。これに加え、本研究では、太陽風パラメータ(太陽風動圧等)や地磁気活動(Kp,AE,Dst 指数)などのバックグラウンドパラメータに対する DPA の周期性の依存性を調べた。この統計解析の結果、MLT などのいくつかのパラメータが脈動周期と関連していることがわかった。このことは、これらのパラメータが Pc3 地磁気脈動の周期と同様に DPA の周期に寄与している可能性を示唆している。

R006-14
Zoom meeting B ：11/1　PM1　(13:45-15:30)
14:15-14:30

安定した北向き IMF 時におけるカスプへのイオン降下フラックス：制御パラメータ

#小池　春人[1)],田口　聡[1)]
[1)]京大理

The flux of the ion precipitation in the cusp for stably northward IMF: Control parameters

#Haruto Koike[1)], Satoshi Taguchi[1)]
[1)]Grad school of Science, Kyoto Univ.

When IMF is northward, reconnection occurs poleward of the cusp, and magnetosheath plasmas can enter the cusp via this lobe reconnection. Previous studies on the proton aurora in the low-altitude cusp have suggested that the ion precipitation flux in the low-altitude cusp tends to increase roughly in proportion to the solar wind dynamic pressure under the northward IMF condition. Since the flux of the reconnection outflow is associated with the plasma density in the inflow regions, one of which is the high-latitude magnetosheath, it is reasonable that the number density of the solar wind plasma is associated with the flux of the ion precipitation in the cusp. However, how the dynamic pressure, which includes the contribution from the solar wind speed, is related to this process is unclear. In this study, in order to clarify how the solar wind parameters including the dynamic pressure control the ion precipitation in the cusp for northward IMF, we examined particle data obtained by DMSP F16 and F17 during more than three years. We took more than 300 events of the cusp ion precipitation using an automated method for the event identification. The result of the analysis has shown that the correlation of the total flux of the ion precipitation with the solar wind dynamic pressure is higher than that with the solar wind number density, suggesting the importance of the dynamic pressure, while there is little correlation with the solar wind speed itself. The result has also shown that the ion precipitation flux tends to increase as the solar zenith angles decreases, implying that the ionospheric conductivity could control the ion precipitation into the cusp as a secondary parameter. We will discuss possible mechanisms for explaining these tendencies.

惑星間空間磁場(IMF)が北向き時においては、マグネトシースの下流側へと速い速度でプラズマが流れている高緯度マグネトポーズにおいてローブリコネクションが起こる。それを介してマグネトシースのプラズマがカスプに入り込み、電離圏の高度まで降下してくる。電離圏カスプに降下したプロトンが光らせるプロトンオーロラの先行研究からは、その発光強度は太陽風の動圧と正の相関があることが知られている。電離圏高度へのプロトンの降下が、ローブリコネクションからのアウトフローの結果であるとすると、そのプロトンの降下フラックスが、ローブリコネクションに流入するマグネトシースプラズマの起源である太陽風プラズマの数密度と正の相関をもつことは自然である。しかし、数密度とともに動圧に関わる量である太陽風速度がどのような関わりをしているのかはまだはっきりわかっていない。また、IMF が南向きの時のカスプ域へのイオンの降下には、地球のダイポール角の関わりを報告する先行研究もあり、IMF が北向き時のカスプのイオンの降下のフラックスの大小がどのようなパラメータで決まっているのかについては、まだ十分な理解が得られていない。

本研究では、IMF が北向き時に電離圏カスプに降下してくるイオンのフラックスの量が、太陽風の数密度以外にどのようなパラメータによって決まっているのかを、DMSP F16 と F17 衛星で得られた大量の粒子のデータをもとに明らかにする。導入するカスプイオンの自動同定方法については、過去の研究と矛盾のないものとし、さらに、北向き IMF 時でも閉じた磁力線上のマグネトポーズでリコネクションが起こりうるため、沿磁力線電流を表す DMSP 衛星の磁場変動データも用いて、ローブリコネクション起源のイベントを厳選した。300 例以上のイベントに基づく統計解析の結果、カスプに降下するイオンのフラックスは、確かに太陽風動圧と高い正の相関を示すことが明らかになった。太陽風密度との相関も見られたが、太陽風速度自体との相関はほとんど同定できなかった。一方、ダイポール軸の傾きとの関係については、軸が北半球で太陽側に傾くことで、北半球のマグネトシースにおいて数密度が相対的に高い領域でローブリコネクションが生じていることを示す傾向が見出された。その効果を除いた上でイオン降下のフラックスとその観測位置での太陽天頂角の関係を調べると、太陽天頂角が小さいほどイオンの降下フラックスが大きくなる緩やかな傾向も見出された。太陽風動圧の関わりと電離圏の電気伝導度の関わりの原因について議論する。

R006-15
Zoom meeting B ：11/1 PM1 (13:45-15:30)
14:30-14:45

Importance of the northward IMF for the quasi-static mesoscale FACs embedded in the diminished large-scale Region 1 current

#Yoshihiro Yokoyama[1)], Satoshi taguchi[1)], Toshihiko Iyemori[2)]
[1)]Grad school of Science, Kyoto Univ.,[2)]Kyoto Univ.

Irregular mesoscale magnetic perturbations embedded in the diminished large-scale Region 1 current are observed almost all MLT except for the near-noon region during prolonged northward IMF conditions. The results of our recent event study have shown these irregular magnetic perturbations in the dusk sector are not simple remnants of the large-scale Region 1 current but a result of spatial structures of quasi-static field-aligned currents (FACs), which are persistently generated in the low-latitude boundary layer (LLBL) during northward IMF. To clarify the key parameters for the generation of these mesoscale field-aligned currents, we analyzed magnetic field data obtained by SWARM satellites during more than 3 years (from May 2014 to May 2017), and investigated the dependence of the occurrence on the solar zenith angle, IMF, and solar wind plasma parameters. Our statistical results have shown the FAC event can occur in a wide range of the solar zenith angles, indicating that whether the ionosphere is sunlit or dark is not crucial for the appearance of the event. The ionospheric conductivity appears to be less important for the generation of the event. The occurrence ratio clearly increases as IMF Bz increases. For positive IMF Bz, the event can be detected in the dusk sector at a ratio of more than 30%. Considering the possible longitudinal size, we can infer from this ratio that the events are almost always present in the dusk auroral oval when IMF has a northward component. This suggests that the duskside mesoscale FACs are generated in the LLBL through a mechanism related to physical processes that can be more easily attained as the northward component of IMF increases. We will show the result from the data in the dawn sector, and discuss the difference between the features in the dawn and dusk sectors in terms of the dawn-dusk asymmetry of the solar wind entry in the LLBL.

R006-16
Zoom meeting B ：11/1 PM1 (13:45-15:30)
14:45-15:00

The energy flow route from the solar wind to the magnetosphere for infinitesimal northward interplanetary magnetic field

#Tsubasa Hashimoto[1)], Masakazu Watanabe[2)], Ryuho Kataoka[3)], Shigeru Fujita[4)], Takashi Tanaka[5)]
[1)]Earth and Planetary Sciences,Kyushu Univ.,[2)]Earth & planetary Sci., Kyushu Univ.,[3)]NIPR,[4)]Meteorological College,[5)]REPPU code Institute

The environment of near-Earth space, including the magnetosphere and ionosphere, is affected greatly by the solar activity. In particular, the interplanetary magnetic field (IMF) has a large effect on the solar wind-magnetosphere interaction. If the magnetosphere is totally closed in terms of magnetic field topology, in ideal magnetohydrodynamics, there is no solar wind energy flowing into the magnetosphere. One important element determining the energy inflow rate is the connectivity of the geomagnetic field and the IMF, namely, magnetic reconnection between the two fields. For southward IMF, reconnection occurs on the nose of the magnetosphere. The solar wind energy enters the magnetosphere effectively, producing magnetic storms, auroral substorms, and so forth. Meanwhile, for northward IMF, reconnection occurs on the high-latitude magnetopause. Though not so effective as for southward IMF, the solar wind energy also enters the magnetosphere, producing phenomena specific to northward IMF periods such as theta auroras. Thus, it is expected in the real magnetosphere that the energy inflow is minimized when the IMF is northward and extremely small (say B=0.1nT). However, prolonged periods of such IMF are of very rare occurrence, and consequently observational studies are virtually impossible. I this study, therefore, we performed a numerical simulation using the Reproduce Plasma Universe (REPPU) code (Tanaka, 2015) and reproduced a magnetosphere under northward and extremely small IMF conditions. We set the IMF magnitude to 0.1 nT and the IMF clock angle (measured from due north) to 30 degrees and made a quasi-steady state magnetosphere in the simulation. We then visualized various physical quantities in the magnetosphere and the ionosphere. We found that the energy flow route from the solar wind to the magnetosphere for northward and extremely small IMF is totally different from that for southward IMF. The major difference is the absence of the dayside “cusp" that is characterized by high pressure plasmas. Although the role of the cusp in magnetospheric dynamo energetics has been being recognized recently, the cusp did not appear for the IMF conditions we simulated. Nevertheless, a dynamo region appeared in the high-latitude boundary layer with the formation of the region 1 current system. This result is totally different from that for southward IMF (Tanaka et al., 2016), indicating the existence of another energy supply mechanism(s) and route(s) dissociated from the cusp. In the presentation, we report the results of the simulation analysis and discuss the energy supply mechanism(s) and route(s) in detail.

R006-17
Zoom meeting B ：11/1 PM2 (15:45-17:30)
15:45-16:00

Plasma flow burst in the cusp: Relationship to the large-scale poleward motion of the electron precipitation region

#Satoshi Taguchi[1)], Yunosuke Nagafusa[1)], Yasunobu Ogawa[2)], Keisuke Hosokawa[3)], Tomokazu Oigawa[1)], Morio Tanaka[1)], Hiroyuki Shinagawa[4)]
[1)]Grad school of Science, Kyoto Univ.,[2)]NIPR,[3)]UEC,[4)]NICT

Previous studies on the plasma flow in the cusp have shown that the fast flow regions can exist in the vicinity of the mesoscale moving cusp aurora. For the large-scale motion of the electron precipitation region in the cusp, it is understood that fast ion flow often occurs nearly simultaneously with the intensification of the electron precipitation, but the detailed spatial relations between the fast ion flow and the large-scale motion of the electron precipitation region require clarification. In this study, we examined auroral image data obtained by an all-sky imager at Longyearbyen, Svalbard, plasma data from field-aligned fixed EISCAT Svalbard Radar (ESR), and the line-of-sight velocity data from the Hankasalmi SuperDARN radar to clarify this issue. We first identified approximately 84 hours as the period of the simultaneous observation of the all-sky imager and the field-aligned fixed ESR from the observation in the daytime sector during six winter seasons (December 2012 to January 2018). Examination of the ESR ion temperature at F region altitudes during those periods of time has shown that ion temperatures exceeding 2000 K are very limited, while the ion temperatures up to 2000 K are often observed. Since high ion temperatures at F region altitudes reflect how fast the ions convect through the slower moving neutral gas, these high ion temperatures can be regarded as events of very fast flow, which have speed faster than 2 km/s. Multiple flow burst events occurred in the cusp on 8 December 2016. One flow burst occurred at the time of the equatorward shift of the large-scale cusp aurora belt responding to the southward turning of the IMF, and then several flow bursts occurred repeatedly. With the help of a high-resolution two-dimensional local model representing the time-dependent interaction between the ions and neutrals in the high-latitudes (Oigawa et al.), we show the spatial relationship of the flow burst to the large-scale motion of the electron precipitation using the aforementioned data obtained simultaneously, and discuss the intrinsic difference between the large-scale poleward motion of the aurora and mesoscale poleward motion of the aurora in the cusp.

R006-18
Zoom meeting B ：11/1　PM2　(15:45-17:30)
16:00-16:15

地球磁気圏 X 線撮像計画 GEO-X の現状

#江副　祐一郎[1)],船瀬　龍[2)],永田　晴紀[3)],三好　由純[4)],中嶋　大[5)],三石　郁之[3)],石川　久美[2)],山崎　敦[2)],長谷川　洋[2)],藤本　正樹[2)],上野　宗孝[2)]
[1)]都立大,[2)]JAXA 宇宙研,[3)]北海道大,[4)]名古屋大学,[5)]関東学院大学

Status of GEO-X (GEOspace X-ray imager) mission

#Yuichiro Ezoe[1)]
[1)]Tokyo Metropolitan University,[2)]ISAS/JAXA,[3)]Hokkaido University,[4)]Nagoya University,[5)]Kanto Gakuin University

GEO-X (GEOspace X-ray imager) aims first observations of the dayside boundaries of the Earth's magnetosphere from the vicinity of the Moon around the next solar maximum. Soft X-ray emission below 2 keV is generated via charge exchange between high charge state solar wind ions (O7+, C5+, …) and neutrals in geocorona. Past observations and simulations predict that this emission will allow us to image dayside structures of the Earth's magnetosphere such as magnetosheaths, cusps and bow shock. To demonstrate the X-ray global imaging of the Earth's magnetosphere, we plan a 50-kg class small satellite mission GEO-X which will carry a miniaturized X-ray imaging spectrometer composed of a ultra light-weight X-ray telescope and a high speed readout X-ray detector combined with a thin optical blocking filter. In this paper, we describe the status of GEO-X mission.

GEO-X（GEOspace X-ray imager）は世界初の地球磁気圏の X 線撮像を目指す衛星計画であり、太陽活動極大が期待される 2022-25 年頃の打ち上げを目指している。太陽から吹く高速のプラズマ流である太陽風には酸素や窒素などの多価イオンが含まれ、地球周辺の超高層大気である外圏と衝突して電荷交換反応による X 線を生じる。イオンの空間分布は、地球磁気圏の太陽側境界面の構造を反映するため、X 線は目には見えない磁気圏構造を可視化する全く新しい手段になる。
地球磁気圏からの電荷交換 X 線放射は月付近から見た場合、約 10x20 度に大きく広がっていると考えられ、多くの X 線天文衛星が投入されてきた近地球軌道よりも遠くから俯瞰的に観測する必要がある。我々は本目的に特化した GEO-X 衛星計画を発案し、2018 年度より JAXA 宇宙理学委員会の Working Group として活動している。12 U CubeSat 約 30 kg に月付近までの高度に投入するための推進系 約 20 kg を加え、約 50 kg の衛星とする予定である。搭載機器は、広がった天体への高感度と高い放射線・可視光耐性を両立するため、マイクロマシン技術を用いた超軽量 X 線望遠鏡と pixel 毎に読み出しが可能な X 線 CMOS に可視光防護フィルタを組み合わせた新しい超小型 X 線撮像分光装置を実現する。本講演では開発現状と将来の展望について紹介する。

R006-19
Zoom meeting B ：11/1　PM2　(15:45-17:30)
16:15-16:30

電離圏でのプラズマシート孤立化を引き起こす磁気圏尾部「乗り換え」リコネクション

#渡辺　正和[1)],田中　高史[2)],藤田　茂[3)]
[1)]九大・理・地惑,[2)]九大・国際宇宙天気科学教育センター,[3)]気象大

Magnetotail "crossover" reconnection producing plasma sheet isolation in the ionosphere

#Masakazu Watanabe[1)], Takashi Tanaka[2)], Shigeru Fujita[3)]
[1)]Earth & planetary Sci., Kyushu Univ.,[2)]REPPU code Institute,[3)]Meteorological College

Plasma sheet isolation in the ionosphere was first proposed by Newell & Meng (1995) as a formation process of so-called theta auroras for northward interplanetary magnetic field (IMF). During periods of northward IMF, it often occurs in the ionosphere that open magnetic flux intrudes into the flankside plasma sheet (presumed to be a closed flux region), with the poleward-most portion of the plasma sheet detached from the main body. Following Newell & Meng, we call this phenomenon “plasma sheet isolation." The isolated plasma sheet may be related to optical phenomena called sun-aligned arcs or oval-aligned arcs. Unintentionally, we could reproduce plasma sheet isolation in a simulated magnetosphere using the REPPU (Reproduce Plasma Universe) code (Tanaka, 2015). We first made a quasi-steady state magnetosphere with parameters of a total IMF intensity of B=6nT and a clock angle of $\theta = -45$? (By<0), and then changed the parameters stepwise to B=13nT and $\theta = -70$?. The clock angle is defined as θ=Arg(Bz+iBy). The plasma sheet isolation stared about 50 min after the IMF change and lasted about 40 min. Detailed analysis of the simulation results revealed that the plasma sheet isolation was a consequence of Dungey-type “crossover reconnection" in the magnetotail. This reconnection is prohibited in the normal global magnetic field topology consisting of 2 nulls and 2 separators. In the presentation, we will discuss in detail how crossover reconnection locally breaks the global structure and how it produces the plasma sheet isolation in the ionosphere. At the moment, the relevance to real sun-aligned arcs or oval-aligned arcs is unclear.

電離圏におけるプラズマシートの孤立化は、惑星間空間磁場（IMF）北向き時に発生するシータオーロラの形成過程として、Newell & Meng（1995）によって初めて提唱された。北向き IMF 時の電離圏では、開磁束が朝側夕側のプラズマシート（閉磁束領域と仮定）に侵入し、最も高緯度側の部分が本体から切り離されることがよく起こる。Newell & Meng に従い、この現象を我々は「プラズマシートの孤立化」と呼ぶ。孤立化したプラズマシートは、サンアラインドアークあるいはオーバルアラインドアークと呼ばれる光学現象と関連があるかもしれない。我々は意図せずして、REPPU（Reproduce Plasma Universe）コード（Tanaka, 2015）を用いてシミュレーションした磁気圏の中に、孤立化プラズマシートを再現することができた。まず IMF の強度を B=6nT、時計角を $\theta = -45^\circ$（By<0）にして準定常磁気圏を作り、続いてそれらの IMF パラメータを階段的に B=13nT かつ $\theta = -70^\circ$ に変えた。ここで IMF 時計角は θ=Arg(Bz+iBy)で定義される。プラズマシートの孤立化は IMF を変化させてから約 50 分後から始まり、その後約 40 分間続いた。シミュレーション結果を詳細に解析したところ、プラズマシートの孤立化は磁気圏尾部におけるダンジー型「乗り換え」リコネクションの結果であると判明した。このリコネクションは、零点 2 個、セパレータ 2 本から成る通常の大域磁場トポロジーでは禁止されている。発表では、乗り換えリコネクションがいかに大域構造を局所的に壊し、いかに電離圏でのプラズマシート孤立化を引き起こすかを詳細に議論する。現時点では、現実のサンアラインドアークやオーバルアラインドアークとの関係は不明である。

R006-20
Zoom meeting B ：11/1 PM2 (15:45-17:30)
16:30-16:45

On the origin of cold-dense plasmas in the dusk magnetotail plasma sheet: MMS observations

#Masaki N Nishino[1)], Yoshifumi Saito[1)], Hiroshi Hasegawa[1)], Yukinaga Miyashita[2)], Tsugunobu Nagai[1)], Barbara L. Giles[3)], Christopher Russell[4)], Daniel J. Gershman[3)]
[1)]JAXA/ISAS,[2)]KASI,[3)]NASA/GSFC,[4)]UCLA

The near-Earth plasma sheet becomes cold and dense under northward interplanetary magnetic field (IMF) condition, which suggests entry of solar wind plasma into the magnetosphere across the magnetopause. The cold and dense trend of the plasma sheet is more apparent in the magnetotail flank regions that are interface between cold solar wind plasma and hot magnetospheric plasma. Several physical mechanisms have been proposed to explain the solar wind plasma entry across the magnetopause and resultant formation of the cold-dense plasma sheet (CDPS) in the tail flank regions. However, transport path of the cold-dense plasma inside the magnetotail has not been understood yet. Here we report a case study of CDPS in the dusk magnetotail by MMS (Magnetospheric Multiscale) spacecraft under strongly northward IMF and high-density solar wind conditions. The ion distribution function consists of high-energy and low-energy components, and the low-energy one intermittently shows energy dispersion in the directions parallel and anti-parallel to the local magnetic field. Considering the time-of-flight effect of the energy-dispersed ions, we infer that the low-energy ions have their origin in the region down the tail, and move along the magnetic field toward the ionosphere and then come back to the magnetotail by the mirror reflection. The longer energy dispersion observed in the developed CDPS shows a longer path length and suggests a change of the injection source to the regions further down the tail.

R006-21
Zoom meeting B ：11/1 PM2 (15:45-17:30)
16:45-17:00

Field-aligned low-energy O+ ion flux variations in the inner magnetosphere observed by Arase

#Masahito Nose[1)], Ayako Matsuoka[2)], Yoshizumi Miyoshi[1)], Kazushi Asamura[3)], Tomoaki Hori[1)], Mariko Teramoto[4)], Iku Shinohara[3)], Masafumi Hirahara[1)]
[1)]ISEE, Nagoya Univ.,[2)]Graduate School of Science, Kyoto University,[3)]ISAS/JAXA,[4)]Kyutech

Recent studies employing the Van Allen Probes [Chaston et al., 2015; Kistler et al., 2016; Nose et al., 2016; Gkioulidou et al., 2019] have shown that unidirectional/bidirectional energy-dispersed O+ flux appears a few minutes after substorms in the inner magnetosphere and lasts for ~10 min with a decrease in its energy from ~5 keV to 10?100 eV. Nose et al. [2016] found that the unidirectional energy-dispersed O+ flux is observed in 80% of the total events and that its direction is parallel (antiparallel) to the magnetic field when the Van Allen Probes are located below (above) the geomagnetic equator. This strongly implies that these O+ ions are extracted from the ionosphere at the onset of substorms and flow along the magnetic field toward the geomagnetic equator. Low-energy O+ ions may be scattered near the geomagnetic equator and remain there, although the scattering mechanism is yet unknown. They will contribute to the O+ content of the inner magnetospheric plasma, and the resultant increase in the O+ density may provide a precondition for the O+-rich ring current.
In the present study, we examine the low-energy O+ ion flux variations observed by the Arase satellite in the inner magnetosphere. Magnetic field dipolarization is selected from the magnetic field data obtained by the fluxgate magnetometer (MGF) [Matsuoka et al., 2018] in the period of April 1?October 31, 2017 and July 1, 2018?January 31, 2019, and we find 192 events. Data from the low-energy particle experiments?ion mass analyzer (LEPi) [Asamura et al., 2018] are examined to check if the selected dipolarization events are accompanied by low-energy O+ ion flux variations in the direction along the local magnetic field. There are some events of the low-energy O+ ion flux enhancement, which (1) starts a few minutes after the dipolarization onset, (2) has energy-dispersed signatures with decreasing energy down to ~10 eV, (3) can be observed in both storm and non-storm periods, (4) has a field-aligned distribution (pitch angle is ~ 0 degree below the equator and ~ 180 degrees above the equator), and (5) causes increases of the O+ density and the O+/H+ density ratio by ~8 times and ~3 times, respectively. In the presentation, we will show the analysis results in more detail and discuss their contribution to the O+ content of the inner magnetospheric plasma, such as the warm plasma cloak and the oxygen torus.

R006-22
Zoom meeting B ：11/2 AM1 (9:00-10:30)
09:00-09:15

IMF dependence of multi-harmonic toroidal ULF waves: A Statistical study of the Arase satellite observations

#Kazuhiro Yamamoto[1)], Kanako Seki[2)], Ayako Matsuoka[3)], Shun Imajo[4)], Mariko Teramoto[5)], Yoshiya Kasahara[6)], Atsushi Kumamoto[7)], Fuminori Tsuchiya[8)], Masafumi Shoji[9)], Yoshizumi Miyoshi[9)]
[1)]UTokyo,[2)]Dept. Earth & Planetary Sci., Science, Univ. Tokyo,[3)]Kyoto University,[4)]ISEE, Nagoya Univ.,[5)]Kyutech,[6)]Kanazawa Univ.,[7)]Dept. Geophys, Tohoku Univ.,[8)]Planet. Plasma Atmos. Res. Cent., Tohoku Univ.,[9)]ISEE, Nagoya Univ.

Multi-harmonic toroidal ultra-low frequency (ULF) waves have been reported by several event studies (e.g., Takahashi & McPherron, 1984; Engebretson et al., 1986; Takahashi et al., 2014, 2020). These waves are the standing Alfven waves and their excitation is related to small cone angle, and hence the ion foreshock is a possible energy source of them (Takahashi & McPherron, 1984). The characteristics of wave frequencies of the multi-harmonic toroidal waves may reflect the frequency spectrum of the wave source around the magnetopause, that is, fast mode perturbation which is coupled with toroidal mode oscillations in the magnetosphere as suggested by Hasegawa et al. (1983). Therefore, the characteristics of the multi-harmonic toroidal waves can be connected to the frequency dependence of energy transmission from the magnetopause to the earth's magnetosphere. However, why they have the harmonic frequency structure and what determines a frequency range of the harmonic spectrum is not fully understood from previous event studies.
In this study, we conducted a statistical study of the occurrence distributions and the characteristics of wave frequencies to understand the excitation mechanism of the multi-harmonic toroidal waves. We used the magnetic field and electron density data obtained from the Arase satellite. The Arase satellite has an inclined orbit with an apogee of ~6.1 R_E and covers a wide range of L-shell up to 10-11 (Miyoshi et al., 2018). This enable us to investigate global distributions of ULF waves beyond the geosynchronous orbit.
From the Arase observations, we found that the MLT distributions of toroidal waves with a single wave frequency (category a) and multiple frequencies (category b) show different response to the interplanetary magnetic field (IMF). At L = 7-10, the multi-harmonic waves (category b) are frequently detected on the dusk and dawn flanks and the occurrence rate on the dawn side is slightly higher than the dusk side for the Parker spiral IMF orientation. For the ortho-Parker spiral IMF orientation, the multi-harmonic waves are frequently detected on the dusk side. This IMF dependence of the MLT distributions of the occurrence rate implies that the multi-harmonic waves are related to the location of a quasi-parallel shock or ion foreshock. We also found that multi-harmonic waves more strongly depend on the cone angle and solar wind speed than the waves with a single frequency. This result suggests that the excitation mechanism of the waves in categories a and b is different.
We examined the wave frequency for categories a and b in detail. The wave frequency for category a is ~ 5 mHz at L = 7-10 and corresponds to the fundamental mode frequency predicted by Singer et al. (1981). The median values of wave frequencies for category b range from 15 to 25 mHz, and they are close to the third harmonic toroidal wave frequency at L = 7-10. Therefore, the wave frequency of category a is close to that of the waves excited by the KH instability, while the wave frequency of category b is close to that of the upstream waves. The central frequency of the frequency band of the multi-harmonic waves is positively correlated with the theoretical frequency of the upstream waves calculated from Takahashi et al. (1984) during a small cone angle. Therefore, we consider that fast mode perturbations with broadband frequencies around the upstream frequency propagate in the magnetosphere and are coupled with toroidal mode oscillations, resulting in the field line resonance.

R006-23
Zoom meeting B ：11/2 AM1 (9:00-10:30)
09:15-09:30

Study of internally driven ULF waves by ring current ions based on the Magnetosphere-Ionosphere coupled model

#Tomotsugu Yamakawa[1)], Kanako Seki[2)], Takanobu Amano[1)], Naoko Takahashi[3)], Yoshizumi Miyoshi[4)], Aoi Nakamizo[5)]
[1)]University of Tokyo,[2)]Dept. Earth & Planetary Sci., Science, Univ. Tokyo,[3)]The University of Tokyo,[4)]ISEE, Nagoya Univ.,[5)]NICT

Internally driven ULF waves are electromagnetic fluctuations in the inner magnetosphere, and can be generated by ring current ions associated with the injection from the magnetotail during substorms. The excitation mechanism and global distribution of ULF waves are keys to understand dynamic variation of the outer radiation belt, since ULF waves in the Pc5 range (1.67-6.67 mHz) are considered to contribute to the radial diffusion of radiation belt electrons [e.g. Elkington et al., 2003]. Promising candidates of excitation mechanism of internally driven ULF waves is drift-bounce resonance [Southwood, 1976]. Although previous spacecraft observations suggest the resonant excitation [e.g., Dai et al., 2013], there are other possibilities such as periodic pressure inhomogeneity formed by time-dependent injections. Recently, by using a global drift kinetic model (GEMSIS-RC), Yamakawa et al. [2019] confirmed the drift resonance excitation of storm-time Pc5 waves under the initial PSD with north-south symmetry. Also, Yamakawa et al. [submitted, 2020] reproduced the drift-bounce resonance excitation of Pc3 waves by including the asymmetry in pitch angle direction of the initial PSD. However, GEMSIS-RC model does not contain some important physical processes such as the feedback from the ionosphere and the dynamics of cold particles. In order to discuss the excitation of ULF waves more quantitatively, we will need to include these processes.
In order to simulate magnetosphere-ionosphere coupling, we use GEMSIS-RC model [Amano et al., 2011] for the inner magnetosphere and GEMSIS-POT model [Nakamizo et al., 2012] for the ionosphere. GEMSIS-RC solves 5-D drift-kinetic equation for PSD of ring current ions and Maxwell equations are solved self-consistently under the assumption that the first adiabatic invariant is conserved. GEMSIS-POT is a thin-shell model, which solves a 2-D ionospheric electric potential, and this model can include both Region 1 and Region 2 field aligned current. Since GEMSIS-RC model is capable of reproducing the Region 2 current, we use FAC from GEMSIS-RC as an input to GEMSIS-POT for the Region 2 current. In addition, the Region 1 current is exerted based on empirical models. The resultant electric field potential is then used as inner boundary condition of GEMSIS-RC. The coupled model enables us to simulate the ion injection from the plasma sheet into the inner magnetosphere. We will report on the details of effects of the M-I coupling on the excitation of ULF waves.
References:
Amano et al., J. Geophys. Res., vol.116, No.A2, 216, 2011.
Dai et al., Geophys. Res. Lett., vol.40, No.16, 4127-4132, 2013.
Elkington et al., J. Geophys. Res., vol.108, No.A3, 1116, 2003.
Nakamizo et al., J. Geophys. Res., vol.117, A09231, 2012.
Southwood, J. Geophys. Res., vol.81, No.19, 3340-3348, 1976.
Yamakawa et al., Geophys. Res. Lett., vol.46, No.4, 1911-1918, 2019.
Yamakawa et al., J. Geophys. Res., submitted, 2020.

R006-25
Zoom meeting B ：11/2 AM1 (9:00-10:30)
09:45-10:00

Toward automatic identification of FLR simultaneously observed by multiple SuperDARN radars

#Hideaki Kawano[1)], Akira Sessai Yukimatu[2)], Nozomu Nishitani[3)], Yoshimasa Tanaka[2)], Satoko Saita[4)], Tomoaki Hori[3)]
[1)]Dept. Earth Planet. Sci., and ICSWSE, Kyushu Univ.,[2)]NIPR/SOKENDAI,[3)]ISEE, Nagoya Univ.,[4)]NITkit

The FLR (field-line resonance) can take place where the frequency of waves coming into the magnetosphere matches the eigenfrequency of a geomagnetic field line, which runs through the ground, the ionosphere, and the magnetosphere. The FLR causes field-line eigen-oscillations having the maximum in power and the largest changing rate in phase (as functions of L or the latitude) at the resonance point. From the FLR frequency one can estimate the density along the corresponding magnetic field line, because, in a simplified expression, 'heavier' field line oscillates more slowly.
Since the FLR oscillates the ionospheric plasma, too, the SuperDARN radars could monitor the two-dimensional (2D) instantaneous distribution of the FLR frequency, from which one could estimate the 2D plasma-density distribution on the magnetospheric equatorial plane, including the location of the plasmapause. However, visual identification of the FLR in the SuperDARN VLOS (Velocity along the Line of Sight) data is time-consuming, and the visual identification could miss FLR events superposed by non-FLR oscillations of VLOS (which could be called 'hidden' FLR events). In addition, there are lots of VLOS data to be analyzed.
Thus, we have been developing a computer code to automatically identify the FLR by using the Gradient method (a general name referring to both the amplitude-ratio and the cross-phase methods). This method cancels out the superposed perturbations by dividing the data from a Range Gate (RG) by the data from a nearby RG along the same beam, since the FLR frequency tends to depend on the latitude more strongly than the superposed perturbations. Another advantage of applying the Gradient method to the SuperDARN VLOS data is that we can choose any pair of RGs (along the same beam) with different distances, and thus can identify what distance is the best to identify the FLR. This distance reflects the resonance width, which is an important quantity reflecting the diffusion and dissipation of the FLR energy.
We have been developing a computer code to do the above. So far we have developed a subroutine to be applied to one beam, and tested it: The code successfully identifised all the visually identified FLR events in a few tens of beams of a few radars. The subroutine has also identified FLR events which were missed by the visual identification. In addition, the subroutine has identified possible 'hidden' FLR events.
We are now developing a code to automatically apply the subroutine to all the beam-aligned RG pairs (with all the RG-RG distances) of all the beams of a SuperDARN radar. By using the code we expect to identify much more FLR events than by visual identification; the automatically identified FLR events would include events simultaneously observed at several locations by several radars, enabling to monitor the 2D distributions of the plasma density. We will present such a case.

R006-26
Zoom meeting B ：11/2 AM1 (9:00-10:30)
10:00-10:15

Ultra low frequency wave index in the inner magnetosphere derived from Arase and RBSP satellites

#Mariko Teramoto[1)], Yoshizumi Miyoshi[2)], Ayako Matsuoka[3)], Nana Higashio[4)], Craig A. Kletzing[5)], Takeshi Takashima[4)], Reiko Nomura[4)], Satoshi Kurita[6)], Shun Imajo[3)], Iku Shinohara[4)]
[1)]Kyutech,[2)]ISEE, Nagoya Univ.,[3)]Kyoto University,[4)]ISAS/JAXA,[5)]Department of Physics and Astronomy, UoI,[6)]RISH, Kyoto Univ.

Ultra-low frequency (ULF) wave indices characterize the level of the geomagnetic fields. They are derived from the amplitude of the magnetic field distributions with time periods of 2?8 min, using either ground-based measurements at high latitudes or data from satellites in geosynchronous orbits. The ULF wave indices thus formulated are correlated with the energetic electron flux enhancements in the radiation belt [Kozyeva et al., 2007; Romanova et al., 2007; Romanova and Pilipenko, 2009].
In this study, we derived the ULF wave indices for different L-shells in the inner magnetosphere (where, $L < 8$), using the magnetic field data obtained from the Arase and RBSP satellites, in the toroidal as well as poloidal modes. We then compared them with the energetic electron flux in the radiation belts, the solar wind parameters, and the geomagnetic indices, which is followed by a discussion on the possible applications of the index.

R006-27
Zoom meeting B ：11/2 AM2 (10:45-12:30)
10:45-11:00

A study of longitudinal extent of Pc1 pulsations using six PWING ground stations at subauroral latitudes

#Jie Liu[1)], Kazuo Shiokawa[1)], Shin-ichiro Oyama[1)], Yuichi Otsuka[1)], Chae-Woo Jun[1)], Masahito Nose[1)], Tsutomu Nagatsuma[2)], Kaori Sakaguchi[2)], Akira Kadokura[3)], Mitsunori Ozaki[4)], Martin Connors[5)], Dmitry Baishev[6)], Nozomu Nishitani[1)], Alexander Pashinin[7)], Ravil Rakhmatulin[7)]
[1)]ISEE,[2)]NICT,[3)]ROIS-DS/NIPR,[4)]Kanazawa Univ.,[5)]Centre for Science, Athabasca Univ.,[6)]IKFIA, SB, RAS,[7)]ISTP SB RAS

The ultra-low-frequency (ULF) Pc1 geomagnetic pulsations correspond to the electromagnetic ion cyclotron (EMIC) waves in the magnetosphere, and are excited sporadically in the magnetospheric equatorial plane with the frequency range of 0.2-5 Hz. Pc1/EMIC waves occur as a result of the ion-cyclotron instability. These waves may contribute to loss of the radiation belt electrons in the inner magnetosphere through wave-particle interactions. The previous research on the spatial extent of EMIC waves mainly used only a specific ground station or several ground stations. There are also some researches in global distribution using single satellite rather than through ground stations. However, the instantaneous longitudinal extent of the Pc1 waves has not been fully understood yet. In order to investigate this instantaneous longitudinal extent of the Pc1 waves, in this study, we analyze the magnetic field data obtained at the six stations at Athabasca (54.6N, 246.36E), Kapuskasing (49.39N, 277.81E), Gakona (62.39N, 214.78E), Husafell (64.67N, 338.97E), Zhigansk (66.78N, 123.37E) and Istok (70.03N, 88.01E) for one year from July 2018 to June 2019. The magnetometers at these stations have been deployed and operated by “the study of dynamical variation of Particles and Waves in the Inner magnetosphere using Ground-based network observations (PWING)" project. We will report the occurrence rates and average frequencies of the Pc1/EMIC waves at these stations and discuss the characteristics of the wave appearance including their instantaneous longitudinal extent.

R006-28
Zoom meeting B ：11/2 AM2 (10:45-12:30)
11:00-11:15

A comprehensive study of EMIC (ElectroMagnetic Ion Cyclotron) waves observed by the Van Allen Probes and Arase satellites.

#ChaeWoo Jun[1)], Yoshizumi Miyoshi[1)], Satoko Nakamura[1)], Shun Imajo[1)], Chao Yue[2)], Jacob Bortnik[3)], Larry Lyons[3)], C. Kletzing[4)], Yoshiya Kasahara[6)], Yasumasa Kasaba[7)], Shoya Matsuda[8)], Masafumi Shoji[1)], Fuminori Tsuchiya[6)], Atsushi Kumamoto[6)], Ayako Matsuoka[9)], Iku Shinohara[8)], Yukitoshi Nishimura[3),5]
[1)]ISEE, Nagoya Univ., Japan,[2)]Peking University, China,[3)]University of California Los Angeles, USA,[4)]University of Iowa,USA,[5)]Boston University, USA,[6)]Kanazawa Univ., Japan,[7)]Tohoku Univ., Japan,[8)]ISAS/JAXA, Japan,[9)]Kyoto University, Japan

To understand possible generation processes of electromagnetic ion cyclotron (EMIC) waves in the magnetosphere, we performed a comprehensive study of EMIC waves observed by the Van Allen Probes (RBSP) and Exploration of energization and Radiation in Geospace (Arase) satellite. From 2017 to 2018, we identified EMIC wave events observed by both satellite missions and categorized them with respect to wave bands (H- and He- EMIC waves) and relative locations from the plasmasphere (inside and outside the plasmasphere). We found that EMIC waves show significant characteristics at the four different peak occurrence regions depending on geomagnetic conditions. In the morning sector (5-8 MLT) at L>8 with quiet geomagnetic conditions, H-band EMIC waves are predominantly observed in a higher normalized frequency with very narrow bandwidth, a mixture of linear and right-handed polarity and oblique wave normal angle. In the noon sector (10-14 MLT) at L~4-6, both H- and He-band EMIC waves are frequently observed with strong solar wind dynamic pressure during the recovery phase of the magnetic storm. They mainly have left-handed polarity and higher center frequency with broad bandwidth. In the afternoon sector (12-17 MLT), He-band EMIC waves are dominantly observed with the strongest wave power at L~6-8 during the storm main phase, while they have another peak occurrence region at L>8 in the higher magnetic latitudes during geomagnetic quiet conditions. From these observational facts, we suggest that the major driver of EMIC waves depends on geomagnetic conditions and environments. In this presentation, we will discuss possible free energy sources causing EMIC waves, such as energetic particle input in the afternoon sector during the disturbed conditions, adiabatic heating in the noon sector due to the magnetospheric compressions, suprathermal proton heating by magnetospheric waves in the morning sector, and generation of EMIC waves at off-equator source regions in the afternoon sector.

R006-29
Zoom meeting B ：11/2　AM2　(10:45-12:30)
11:15-11:30

2017年3月15日にアラスカで観測されたサブオーロラ帯における孤立プロトンオーロラとIPDP型Pc1地磁気脈動の関連

#中村　幸暉[1)],塩川　和夫[1)],大山　伸一郎[1)],長妻　努[2)],坂口　歌織[2)],Spence　Harlan[3)],Reeves　Geoff[4)],Macdowall　Robert J.[5)],Smith　Charles W.[3)],Funsten　Herbert O.[4)],Kletzing　Craig A.[6)],Wygant　John[7)],Bonnell　John[7)]
[1)]名古屋大学宇宙地球環境研究所,[2)]情報通信研究機構,[3)]ニューハンプシャー大学,[4)]ロスアラモス国立研究所,[5)]NASAゴダード宇宙航空センター,[6)]アイオワ大学,[7)]ミネソタ大学

Relationship between the isolated proton aurora and the IPDP type Pc1 pulsation observed at subauroral latitudes on March 15, 2017

#Kohki Nakamura[1)], Kazuo Shiokawa[1)], Shin-ichiro Oyama[1)], Tsutomu Nagatsuma[2)], Kaori Sakaguchi[2)], Harlan Spence[3)], Geoff Reeves[4)], Robert J. Macdowall[5)], Charles W. Smith[3)], Herbert O. Funsten[4)], Craig A. Kletzing[6)], John Wygant[7)], John Bonnell[7)]
[1)]ISEE, Nagoya Univ.,[2)]NICT,[3)]New Hampshire Univ.,[4)]Los Alamos National Laboratory,[5)]NASA's Goddard Space Flight Center,[6)]Iowa Univ.,[7)]Minnesota Univ.

Isolated Proton Aurora (IPA) is the spot-like aurora extending east and west at subauroral latitudes and is produced by energetic proton precipitation. From previous studies, the one-to-one correspondence between IPAs and Pc1 geomagnetic pulsations which corresponds to the electromagnetic ion cyclotron (EMIC) waves in the magnetosphere, have been reported. However, studies which show the relationship between IPAs and intervals of pulsations of diminishing periods (IPDP) type Pc1 pulsations have not been well investigated except for that using satellite IPA images by Yahnin et al. (JGR, 2009). Because EMIC waves are a key component contributing to the rapid loss of radiation-belt particles into the atmosphere, it is important to understand the mechanisms of EMIC wave-particle interaction. In the present study, we studied an IPA event associated with the IPDP-type Pc1 pulsation by using a ground-based all-sky imager and an induction magnetometer at Gakona, Alaska. An IPDP type Pc1 pulsations at a frequency range of 0.2-0.4 Hz was observed at 06:20-06:40 UT on March 15, 2017. This IPA moved from east to west associated increase of the frequency of the IPDP-type Pc1 pulsation. The magnetic local time of Gakona was at ~20 MLT in this event. We considered that this westward motion of the IPA is consistent with the westward ion drift. The Van Allen Probes satellite (Probe B) was near the conjugate magnetosphere to Gakona. The enhancement of 20-40 keV ion flux was observed by the HOPE instrument onboard the satellite. We will discuss these observations in relation to the characteristics of IPAs and IPDP-type Pc1 pulsations.

孤立プロトンオーロラ（IPA）は、オーロラオーバルより低緯度のサブオーロラ帯に現れるオーロラの一種で、高エネルギープロトンの降りこみによって引き起こされる東西方向に薄く伸びたスポット状のオーロラである。過去の研究では、Pc1地磁気脈動（磁気圏の電磁イオンサイクロトロン（EMIC）波動に対応）と孤立プロトンオーロラの関連が報告されてきたが、時間の経過とともに周波数が上昇するIPDP型のPc1地磁気脈動と孤立プロトンオーロラの関連を示した研究は、Yahnin et al. (2009)による人工衛星からのプロトンオーロラの観測以外にない。EMIC波は放射線帯粒子の大気中への急速な損失を引き起こす原因の一つであると考えられているため、波動粒子相互作用の仕組みを理解することは重要である。本研究では、アラスカのガコナに設置された全天カメラと誘導磁力計を用いて、IPDP型のPc1地磁気脈動に伴って発生した孤立プロトンオーロラについて詳細な解析を行った。その結果、2017年3月15日06:20-06:40 UTに、0.2-0.4 HzのIPDP型Pc1地磁気脈動を観測し、この周波数の上昇に伴って東から西へ移動する孤立プロトンオーロラを観測した。ガコナの磁気地方時は~20 MLTであり、IPAの西向きの動きは西向きのイオンドリフトに対応していると考えられる。また、このときVan Allen Probes衛星（Probe B）がガコナの磁気共役点付近におり、衛星に搭載されているHOPE観測器で20-40 keVのイオンフラックスの上昇が観測された。講演では、これらの観測事実をこれまで提案されてきた孤立プロトンオーロラやIPDP型のPc1地磁気脈動の特徴と照らし合わせて議論する。

R006-30
Zoom meeting B ：11/2 AM2 (10:45-12:30)
11:30-11:45

Swarm measurement of ionospheric plasma density oscillation associated with Pc1 geomagnetic pulsations

#Hyangpyo Kim, Kazuo Shiokawa, Jaeheung Park[2)], Yoshizumi Miyoshi, Yukinaga Miyashita[2)], Claudia Stolle[3)], Khan-Hyuk Kim[4)], Jurgen Matzka[3)], Stephan Buchert[5)], Tanja Fromm[6)]
ISEE, Nagoya University,[2)]Korea Astronomy and Space Science Institute,[3)]GFZ, German Research Centre for Geosciences,[4)]School of Space Research, Kyung Hee University,[5)]Swedish Institute of Space Physics,[6)]Alfred-Wegener-Institut fur Polar- und Meeresforschung

Electromagnetic ion cyclotron (EMIC) waves propagate along the magnetic field as shear Alfven mode from the magnetospheric source region toward the ionosphere and observed as Pc1 geomagnetic pulsations on the ground. On arriving at ionospheric altitudes, they undergo mode conversion to the compressional mode due to the Hall conductivity and then they propagate across the magnetic field. According to the ideal magnetohydrodynamic (MHD) wave theory, EMIC Pc1 waves can be accompanied by density perturbation when they propagate in compressional mode. This expectation, however, has not yet been confirmed observationally due to the lack of in situ data with sufficient time resolution. In this presentation, we show the first observation of ionospheric plasma density oscillations driven by EMIC Pc1 waves based on the observation by the Swarm satellites. Swarm satellites observed compressional Pc1 wave activity in the 0.5-3 Hz band, which was coherent with in-situ plasma density oscillations. Around the Pc1 event location, the Antarctic Neumayer station (L ~ 4.2) recorded similar Pc1 pulsations in the horizontal component while NOAA-15 observed isolated proton precipitations at energies above 30 keV. All these observations support that the compressional Pc1 waves at Swarm were oscillations converted from EMIC waves coming from the magnetosphere. Cross-spectral analyses between the plasma density and EMIC Pc1 waves showed high coherence, but the amplitude ratio and phase change exhibited characteristics deviating from the ideal MHD wave theory: e.g., significant larger amplitudes than predicted were observed in electron density. This difference cannot be explained by a simple MHD model, although steep horizontal/vertical gradients of background ionospheric density can partly explain the discrepancy.

R006-31
Zoom meeting B ：11/2 AM2 (10:45-12:30)
11:45-12:00

Observations of drifting hole structures in radiation belt electrons induced by EMIC waves

#Satoko Nakamura[1)], Yoshizumi Miyoshi[1)], Kazuo Shiokawa[1)], Yoshiharu Omura[3)], Takefumi Mitani[2)], Takeshi Takashima[2)], Tomoaki Hori[1)], Ayako Matsuoka[4)], Shun Imajo[1)], Iku Shinohara[2)]
[1)]ISEE, Nagoya Univ.,[2)]ISAS/JAXA,[3)]RISH, Kyoto Univ.,[4)]Kyoto University

We present observations of drifting hole structures in radiation belt electrons. The Arase satellite and Van Allen Probes often detect fine structures in energy spectra of particle fluxes. We examined time variations of energetic electron fluxes normalized by their averaged fluxes over the previous 10 minutes. The flux variation shows 1-min scale depressions with clear energy dispersion, which appear only in the relativistic energy ranges (500 keV - a few MeV) and small pitch angles. We find that these “drifting hole structures" are frequently observed with EMIC waves in space or around the ionospheric footprint of a satellite. The energy range and the pitch-angle dependency of drifting hole is consistent with nonlinear cyclotron resonances with EMIC waves. These observational characteristics suggest that EMIC waves cause a strong pitch-angle scattering, leading to a sharp loss of small pitch-angle electrons. We show some examples of simultaneous observations of drifting hole structures and EMIC waves observed by the Arase satellite and Van Allen Probes, and compare the results with nonlinear resonance theory and drift periods of relativistic electrons.

R006-32
Zoom meeting B ：11/2 AM2 (10:45-12:30)
12:00-12:15

Estimation of inhomogeneity factor for the interaction between the protons and EMIC wave

#Naritoshi Kitamura[1)], Yoshiharu Omura[2)], Takanobu Amano[3)], Satoko Nakamura[4)], Masafumi Shoji[5)], Masahiro Kitahara[5)], Yoshizumi Miyoshi[5)], Yuto Katoh[6)], Scott Boardsen[7)], Yoshifumi Saito[8)], Shoichiro Yokota[9)], Daniel J. Gershman[7)], Barbara L. Giles[7)], Craig J. Pollock[10)], Christopher Russell[11)], Robert J. Strangeway[12)], James L. Burch[13)]
[1)]University of Tokyo,[2)]RISH, Kyoto Univ.,[3)]Univ. Tokyo,[4)]ISEE,[5)]ISEE, Nagoya Univ.,[6)]Dept. Geophys., Grad. Sch. Sci., Tohoku Univ.,[7)]NASA/GSFC,[8)]ISAS,[9)]Osaka Univ.,[10)]Denali Scientific,[11)]IGPP, UCLA,[12)]Inst. of Geophys. and Planet. Phys., Univ. of California, Los Angeles,[13)]Southwest Research Institute

Nonlinear theory for wave-particle interactions (e.g., Omura et al., 2010) indicate that the magnitude of inhomogeneity factor (S) is the important factor for particle trapping in the nonlinear wave-particle interactions. If the magnitude of S is smaller than 1, particles can be trapped, and efficient interaction can occur due to the formation of a hole (or hill) in the phase space distribution of the particle. We applied the Wave-Particle Interaction Analyzer (WPIA) method to the data obtained by the MMS spacecraft for one of the EMIC wave events. The energy transfer rate by cyclotron resonance was calculated as the dot product of the wave component of the perpendicular electric fields and ion current perpendicular to the magnetic field around the resonance velocity which is called the resonant current. The distribution of the energy transfer rate indicates that the energy transfer from hot protons (about 18-30 keV) to the EMIC wave occurred around the cyclotron resonance velocity. Temporal variations of the wave frequency and the gradient of the magnetic field intensity along the field line are the important factor for S. In the event, there were no clear temporal variation of wave frequency and the effect of temporal variations of wave frequency is negligible. Taking advantage of the fact that the gradient of the magnetic field intensity can be calculated from the four spacecraft measurements by MMS, we show that S can become smaller than 1 for the hot resonant protons within the limit of accuracy of the measurements of the magnetic field intensity.

R006-33
Zoom meeting B ：11/2 AM2 (10:45-12:30)
12:15-12:30

Statistical analyses of low energy ion heating by EMIC waves via WPIA: Arase observations

#Masafumi Shoji[1)], Yoshizumi Miyoshi[1)], Lynn Kistler[1),2)], Kazushi Asamura[3)], Yasumasa Kasaba[4)], Ayako Matsuoka[5)], Yoshiya Kasahara[6)], Shoya Matsuda[3)], Fuminori Tsuchiya[4)], Atsushi Kumamoto[4)], Satoko Nakamura[1)], Masahiro Kitahara[1)], Shun Imajo[1)], ChaeWoo Jun[1)], Iku Shinohara[1)]
[1)]ISEE, Nagoya Univ.,[2)]University of New Hampshire,[3)]ISAS/JAXA,[4)]Tohoku Univ.,[5)]Kyoto University,[6)]Kanazawa Univ.

Electromagnetic ion cyclotron (EMIC) waves are generated through the cyclotron wave-particle interaction, affecting the plasma environment in the magnetosphere. Heating of ions by EMIC waves in the inner magnetosphere has been investigated using spacecraft observations by comparing the pitch angle distribution of the ions and the wave emissions. We can directly detect the energy transfer between the plasma waves and the ions via the wave-particle interaction analysis (WPIA) method which calculates the inner product between the wave electric fields and the ion velocities. We adapt the WPIA method to the Arase spacecraft data and investigate the spatial distribution of the positive qV?E region in the inner magnetosphere. From March 21st 2017 to September 27th 2019, we select 60 EMIC wave events with associated proton flux enhancement between 10 eV to 100 eV which are a suitable dataset for the WPIA method observed by PWE/EFD, MGF, and LEP-i onboard the Arase satellite. The peak of the proton heating occurrence appears in the dayside and post noon regions. Typical EMIC waves inside the plasma plume contribute to the peak in the afternoon sector in both geomagnetically quiet and active times. On the other hand, in the dayside region, the proton heating takes place predominantly during quiet times. It suggests that the protons in the region are energized by the EMIC waves generated through compression of the ambient magnetic field. We also discuss the species dependence of the ion heating.

R006-34
Zoom meeting B ：11/2　PM1　(13:45-15:30)
13:45-14:00

オーロラ電子加速過程に関わる電磁圏プラズマの沿磁力線分布についての研究

#齋藤　幸碩[1)],加藤　雄人[1)],熊本　篤志[1)],木村　智樹[1)],川面　洋平[1)]
[1)]東北大・理・地球物理

Study of the field-aligned distribution of ionospheric/magnetospheric plasma related to the auroral electron acceleration process

#Koseki Saito[1)], Yuto Katoh[1)], Atsushi Kumamoto[1)], Tomoki Kimura[1)], Yohei Kawazura[1)]
[1)]Dept. Geophys., Grad. Sch. Sci., Tohoku Univ.

Observation NASA's spacecraft Juno revealed the downward electrons in the energy range from a few tens keV to hundreds keV in the Jupiter's auroral regions. The observed energy and pitch angle distributions suggested that Alfvenic acceleration process plays significant roles in the formation of Jupiter's aurora [Mauk et al., 2017; Saur et al., 2018]. Alfvenic acceleration is expected to occur at the Earth [Chaston et al., 2002]. Despite the increasing attention to the Alfvenic acceleration process in considering the aurora formation of magnetized planets, physical processes controlling the characteristic energy and pitch angle distributions have been still unclear.

For the discussion of Alfvenic acceleration, the spatial distribution of multispecies ions and electrons along a field line is necessary to understand property of Alfven waves. In the present study, based on the model used in Ergun et al. (2000) and Matsuda et al. (2010), we developed a Plasma Distribution Solver for the plasma distribution along a magnetic field line between the ionosphere and magnetic equator. The developed Plasma Distribution Solver iteratively computes both the spatial distribution of multispecies plasma and the electrostatic potential so as to satisfy Poisson's equation, as shown in Fig.(a) and (b). We obtain the number density of each species by integrating the distribution function in the velocity space. We assume bi-Maxwellian distributions for the initial velocity distributions of both ions and electrons at the ionospheric end and at the magnetic equator. By referring to both energy conservation law and adiabatic invariant, we determine the interval of integration in the velocity space for a certain location, and then integrate the distribution function at the boundary in the determined interval of the velocity space in order to obtain the number density there.

Using the developed Plasma Distribution Solver, we study the effects of the assumed boundary condition and the initial condition of the electrostatic potential. We found that the plasma distribution changes according to the assumed boundary condition. Higher plasma temperature at the boundary results in broader distribution of plasmas along a field line. This confirms that the convergence cannot be obtained in this case. It is also confirmed that there can be multiple solutions under the same boundary condition and different initial gap position of the electrostatic potential.

In this presentation, we show results of the Plasma Distribution Solver and discuss the variations of the solution under different initial settings. We also compare the results of the Plasma Distribution Solver with those obtained by the conventional plasma distribution model considering the diffusive equilibrium of plasmas along a field line.

木星探査機 Juno の観測により、数十 keV から数百 keV に至る幅広いエネルギー帯におけるオーロラ電子降下が確認された。観測された電子のエネルギー分布ならびにピッチ角分布から、「Alfv?nic acceleration」が木星におけるオーロラ電子加速過程において重要な役割を果たしていることが示唆された[Mauk et al., 2017; Saur et al., 2018]。Alfv?nic acceleration は地球極域で観測されるオーロラ電子の生成過程としても議論されている[Chaston et al., 2002]。磁化惑星におけるオーロラ電子加速過程での Alfv?nic acceleration の重要性が高まる一方で、被加速電子の特徴的なエネルギー分布やピッチ角分布を決定づける要因については未解明の問題が残されている。

Alfv?nic acceleration が効率的に生じる領域を考察するためには、磁気圏内での Alfv?n 波の伝播と波動特性の変化を調べる必要がある。Alfv?n 波の伝播媒質であるプラズマの分布を明らかにすることにより、Alfv?n 速度の空間分布の考察が可能となる。そこで本研究では、Ergun et al.(2000)や Matsuda et al.(2010)で用いられた手法に基づいて、磁化惑星の磁力線に沿ったプラズマ分布を求める「Plasma Distribution Solver」を開発した。Plasma Distribution Solver は、Poisson 方程式を満たすことを収束条件に用いて、複数の粒子種の電荷密度分布と静電ポテンシャルの空間分布を反復法により求める手法である。磁気赤道及び電離圏側の境界におけるイオンと電子の初期速度分布を bi-Maxwellian 分布として与えて、任意の地点における速度分布についてはエネルギー保存則及び断熱不変量から境界での速度空間にトレースすることにより求める。得られた分布関数を速度空間で積分することにより、磁力線上の各位置における各粒子種の数密度を計算する。

本研究では開発したコードを用いて、電離圏・磁気圏側での境界条件がプラズマ分布に及ぼす影響、ならびに、初期条件として与える静電ポテンシャルの空間構造の影響についてそれぞれ調べた。その結果、Plasma Distribution Solver の特性として、境界条件がプラズマ分布に大きな影響を及ぼすことが示された。境界における電離圏・磁気圏プラズマの温度が高いほど、各粒子種の数密度の空間勾配が緩やかとなる様相が再現された。また、初期条件として与える静電ポテンシャルが不連続となる位置を変化させた場合には、境界条件を同一とした場合でも異なる解に収束し得ることが示された。本発表では Plasma Distribution Solver により得られた結果の詳細を報告するとともに、

境界条件の影響に関する考察ならびに拡散平衡モデルなど沿磁力線方向のプラズマ密度分布に関する既存のモデルとの比較した結果について議論する。

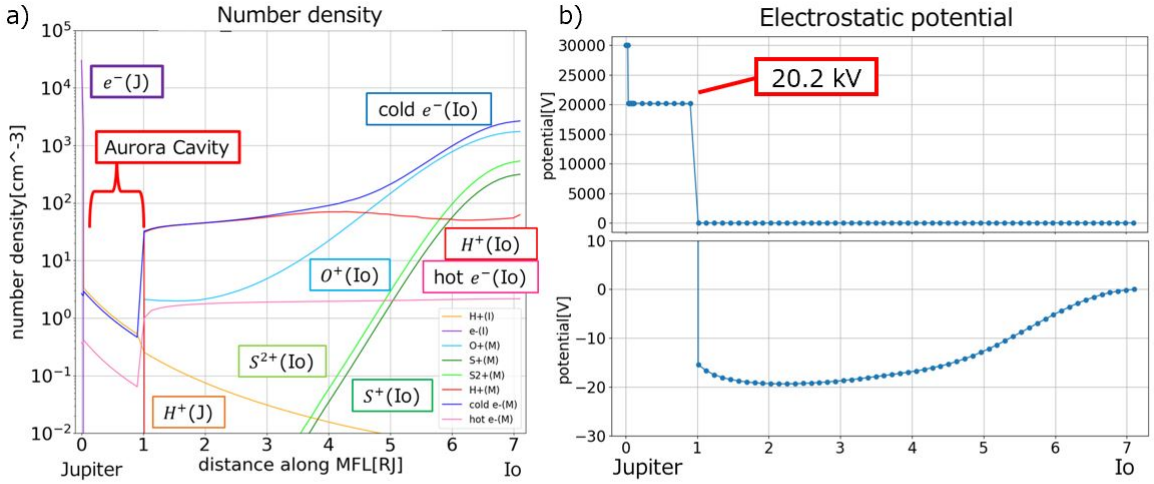

Fig. a) Number density of Jupiter-Io case. (J) is the mark of particles from Jovian ionospheric end. (Io) is the mark of particles from Io. From $0.0352R_J$ to $0.902R_J$, number densities sharply decrease, and Aurora Cavity where only H^+(J) & e^-(Io) exist is generated.
b) Electrostatic potential profile consistent with a). The profile is formed stepwise.

R006-35
Zoom meeting B ：11/2　PM1　(13:45-15:30)
14:00-14:15

あらせ衛星で観測された孤立静電ポテンシャル構造の解析

#滝　朋恵[1)],小嶋　浩嗣[2)],栗田　怜[3)],笠原　禎也[4)],三好　由純[5)],篠原　育[6)],臼井　英之[7)],風間　洋一[8)],松田　昇也[9)],Wang　S.-Y.[10)],Tam　Sunny W. Y.[11)],松岡　彩子[12)]
[1)]京大・工・電気,[2)]京大・生存圏,[3)]京都大学 生存研,[4)]金沢大,[5)]名大 ISEE,[6)]宇宙研／宇宙機構,[7)]神戸大・システム情報,[8)]ASIAA,[9)]ISAS/JAXA,[10)]台湾・中央研究院,[11)]国立成功大学宇宙・プラズマ科学研究所,[12)]京都大学

Isolated electrostatic potential structures observed by the Arase satellite

#Tomoe Taki[1)], Hirotsugu Kojima[2)], Satoshi Kurita[3)], Yoshiya Kasahara[4)], Yoshizumi Miyoshi[5)], Iku Shinohara[6)], Hideyuki Usui[7)], Yoichi Kazama[8)], Shoya Matsuda[9)], S.-Y. Wang[10)], Sunny W. Y. Tam[11)], Ayako Matsuoka[12)]
[1)]Engineering, Kyoto Univ.,[2)]RISH, Kyoto Univ.,[3)]RISH, Kyoto Univ.,[4)]Kanazawa Univ.,[5)]ISEE, Nagoya Univ.,[6)]ISAS/JAXA,[7)]System informatics, Kobe Univ,[8)]ASIAA,[9)]ISAS/JAXA,[10)]ASIAA, Taiwan,[11)]Institute of Space and Plasma Sciences, National Cheng Kung University, Taiwan,[12)]Kyoto University

In this study, we analyze the isolated potential structure observed by the Arase satellite.
It is well-known that there are isolated potential structures in the magnetosphere through the different satellites such as VIKING, FAST, POLAR, GEOTAIL and RBSP. Some of them are thought to correspond to electron or ion holes in phase space. Double layers are also the candidate to the structure. Once such spatially isolated potential structures pass through a satellite, these isolated potential structures can be observed as time-varying electric field waveforms by an onboard plasma wave receiver. For example, the GEOTAIL satellite found electrostatic solitary waves (ESW) in the magnetotail region in 1994. The ESW are bipolar pulses indicating that positive potentials pass through the satellite. In addition to the positive potentials like ESW, the RBSP satellite also observed double layer structures. The Arase satellite investigates the terrestrial inner magnetosphere along the similar orbit with the RBSP except the magnetic latitude. The Arase satellite covers higher latitude than the RBSP and its unique orbits allow us to examine differences in properties of isolated potentials observed in wider magnetic latitude regions.
In this study, we decompose the electric field solitary waveforms observed by the Arase satellite into parallel and perpendicular waveforms relative to the background magnetic field and construct the corresponding isolated potential structure models. The electric field waveforms in both horizontal and vertical directions have dipole-type pulses similar to those of ESW, which are different from those observed only in the parallel direction by GEOTAIL satellite and RBSP satellite. In some cases, there are phase differences between the parallel and perpendicular waveforms with respect to the background magnetic field.
In the present study, we classify the solitary waveforms observed by the Arase satellite and discuss their plausible potential structures referring to electric field directions relative to the background magnetic field. We also discuss differences between isolated potential structures observed by the Arase satellite and those by the RBSP.

本研究ではあらせ衛星によって観測された孤立静電ポテンシャル構造の解析を行う。
宇宙プラズマ中には、孤立した静電ポテンシャル構造が存在することが知られている。地球磁気圏においても、VIKING、FAST、GEOTAIL、POLAR、RBSP 衛星などにより、同様なポテンシャル構造が観測されている。それらは、位相空間におけるイオンや電子の局所的な欠如によるイオンホール、電子ホールなどで、説明できるものの他、イオンと電子のレイヤーから形成されるダブルレイヤーで説明されるものまで様々である。これらのポテンシャル構造は、電子、イオンの加速・減速への寄与の他、その生成メカニズムについても議論が行われている。
空間的に広がる孤立ポテンシャル構造が観測衛星に対して相対速度をもつと、この孤立ポテンシャル構造は時間的に変化する電界波形としてプラズマ波動観測器で観測可能である。例えば、1994 年に磁気圏尾部領域で GEOTAIL 衛星が静電孤立波（ESW）を発見した。ESW は bipolar 型の孤立したパルス波形をしており、その孤立波形は、正のポテンシャル構造が衛星を通過することで観測されることが示された。また、RBSP 衛星によっても多くの孤立ポテンシャルが同様の波形として観測されている。RBSP 衛星による観測では ESW と同様の正のポテンシャルに加えて、ダブルレイヤーの観測も報告されている。あらせ衛星は RBSP 衛星と同様に地球の内部磁気圏を観測しているが、RBSP の軌道が磁気緯度 20 度以内にフォーカスしているのに対し、あらせ衛星は低緯度から磁気緯度 40 度程度までを観測しており、あらせ衛星による孤立ポテンシャル構造の観測から、磁気緯度のより高い領域までを包括して観測し、そのポテンシャル構造とその磁気緯度による属性の違いを明らかにすることができると考えられる。
本研究では、まずあらせ衛星によって観測された電界波形から孤立ポテンシャルが観測されていることを確認した。ESW などの孤立ポテンシャルを観測したパルス波形は広帯域のスペクトルを持つことを利用し、観測された電界波形が広帯域のスペクトルを持つ時間帯を調査することで多くの静電的な孤立波を見出した。いずれの波形も磁場のチャンネルには現れておらず、これらの波形は静電的な孤立ポテンシャル構造を観測したものであると考えられる。さらに、これらの電界波形を背景磁場に対する平行方向と垂直方向に分解し、それぞれの静電的な孤立波に対応する孤立ポテンシャル構造を考察した。あらせ衛星は、スピン面内に展開された 2 成分の電界センサーしかもたないため、3 次元で観測される背景磁場を二次元で観測される電界センサー面内に射影し、観測平面内で背景磁場に対して垂直および平行な二成分に分解した。解析の結果、あらせ衛星で観測された電界波形は、平行方向、垂直方向共に ESW と似た bipolar 型のパルス波形となっていることが判明した。また、背景磁場に対して平行方向と垂直方向の

bipolar 型のパルス波形に位相差が存在するものも多く存在した。さらに、平行方向と垂直方向のどちらか一方が bipolar 型のパルス波形を持ち、もう一方が正負非対称の凸型になった波形も見られた。これらの結果から、それぞれの場合について通過した孤立ポテンシャルの構造として、背景磁場に対して斜めのシート状構造をしたポテンシャルや、すり鉢状の構造をしたポテンシャルが考えられた。これまでの GEOTAIL 衛星や RBSP 衛星による観測から導かれる孤立ポテンシャル構造は、背景磁場に対して平行なシート状構造や、正と負のシート状構造が隣り合った構造であった。しかし、今回導かれた孤立ポテンシャル構造はこれまでの観測から導かれた構造と異なるものがみつかった。
本発表では、あらせ衛星によって観測した電界の孤立波形について、その形状による分類を行ったのち、外部磁場に平行、垂直方向の電界ベクトルの時間変化から、それぞれの波形に相当するポテンシャル構造を推定し、同じ内部磁気圏の低緯度領域において RBSP 衛星で観測された結果と比較し、そのポテンシャル構造の相違について議論を行う。

R006-36
Zoom meeting B ：11/2 PM1 (13:45-15:30)
14:15-14:30

Occurrence characteristics of large amplitude whistler-mode chorus waves observed by the Arase satellite

#Satoshi Kurita[1)], Yoshizumi Miyoshi[2)], Yoshiya Kasahara[3)], Hirotsugu Kojima[4)], Shoya Matsuda[5)], Satoshi Kasahara[6)], Shoichiro Yokota[7)], Ayako Matsuoka[8)], Iku Shinohara[9)]
[1)]RISH, Kyoto Univ.,[2)]ISEE, Nagoya Univ.,[3)]Kanazawa Univ.,[4)]RISH, Kyoto Univ.,[5)]ISAS/JAXA,[6)]The University of Tokyo,[7)]Osaka Univ.,[8)]Kyoto University,[9)]ISAS/JAXA

Whistler-mode chorus is electromagnetic waves in nature observed in the frequency range from 0.1 to 0.8 times of electron gyrofrequency, fce, and they frequently appear in the dawn and noon side magnetosphere. Chorus waves often have a gap of wave power at 0.5 fce, and the waves below and above 0.5 fce are called lower-band (LBC) and upper-band chorus (UBC), respectively. These waves have been considered as the primary driver of the electron dynamics in the Earth's inner magnetosphere, since they can resonate with electrons in the wide energy range and cause the acceleration and loss of these electrons.
Characteristics of the waves such as the wave normal angle, wave power, and their spatial distributions have been investigated using the data processed by Onboard Frequency Analyzer (OFA), which is one of the receivers of the Plasma Wave Experiment (PWE) onboard the Arase satellite. We have found that there are large amplitude (> 100 pT) tails in the occurrence frequency distributions of the wave magnetic field power of nightside LBC and UBC with wave vector close to the local magnetic field. The large amplitude tails appear near the magnetic equator, and the large amplitude waves are less frequently observed above the magnetic latitude of 10 degrees. The tails are not present in the occurrence frequency distributions of the wave power of the dayside LBC and UBC. The wave power occurrence frequency distributions of nightside LBC and UBC can be fitted well by a bimodal distribution.
To understand the cause of the bimodal occurrence frequency distributions, we first consider the occurrence characteristics of large amplitude waves. We have investigated when large amplitude LBC and UBC waves are observed by using the data from Medium Energy Particle experiment-electron analyzer (MEP-e) and PWE. We have found that the large amplitude waves are accompanied by electron injections observed by MEP-e near the equator. Even though electron injections are observed by MEP-e at the off-equatorial region, large amplitude waves are not observed by PWE. Within the electron injection event near the equator, the amplitudes of LBC and UBC are highly fluctuated in the amplitude range from 1 pT to > 100 pT. Thus it is speculated that microscopic rather than macroscopic views may be important to understand the generation of large amplitude chorus waves.

R006-37
Zoom meeting B ：11/2　PM1　(13:45-15:30)
14:30-14:45

プラズマ圏磁気赤道付近におけるホイッスラーモード・ヒス放射の非線形生成機構

#大村　善治[1)],疋島　充[2)],サマーズ　ダニ―[3)]
[1)]京大・生存圏,[2)]宇宙科学研究所,[3)]ニューファウンドランド・メモリアル大学

Nonlinear generation mechanism of whistler-mode hiss emissions near the equatorial plasmasphere

#Yoshiharu Omura[1)], Mitsuru Hikishima[2)], Danny Summers[3)]
[1)]RISH, Kyoto Univ.,[2)]ISAS/JAXA,[3)]Memorial University of Newfoundland

We have conducted a one-dimensional electromagnetic particle simulation with a parabolic magnetic field to reproduce whistler-mode hiss emissions in the plasmasphere [1]. We assume a bi-Maxwellian distribution with temperature anisotropy for energetic electrons injected into the plasmasphere, and find that hiss emissions are generated locally as an absolute instability with spectrum characteristics typical of those observed by spacecraft near the magnetic equator. The hiss emissions contain fine structures involving rising tone and falling tone elements with variation in frequencies. The amplitude profile of the spectra agrees with the optimum wave amplitude derived from the nonlinear wave growth theory [2]. The simulation demonstrates that hiss emissions are generated locally near the magnetic equator through linear and nonlinear interactions with energetic electrons with temperature anisotropy. The coherent hiss emissions efficiently scatter resonant electrons of 2.5keV - 80keV into the loss cone.
References:
[1] Hikishima, M., Omura, Y., & Summers, D. (2020). Particle simulation of the generation of plasmaspheric hiss. J. Geophys. Res. Space Physics, 125, e2020JA027973, doi:10.1029/2020JA027973
[2] Omura, Y., S. Nakamura, C. A. Kletzing, D. Summers, and M. Hikishima (2015), Nonlinear wave growth theory of coherent hiss emissions in the plasmasphere, J. Geophys. Res. Space Physics, 120, 7642?7657, doi:10.1002/2015JA021520.

R006-38
Zoom meeting B ：11/2 PM1 (13:45-15:30)
14:45-15:00

Green's function of electron flux in the outer radiation belt interacting with localized oblique whistler mode chorus emissions

#Yikai Hsieh[1)], Yoshiharu Omura[2)], Yuko Kubota[3)]
[1)]RISH, Kyoto Univ.,[2)]RISH, Kyoto Univ.,[3)]RISH, Electric engineering, Kyoto Univ.

Oblique whistler mode waves are observed frequently in dayside and dawnside of the Earth's magnetosphere around the outer radiation belt. Through the nonlinear trapping, by coherent chorus waves, energetic resonant electrons (tens keV) can be accelerated rapidly and become relativistic electrons (a few MeV). Electron acceleration of velocity perpendicular to the background magnetic field of resonant electrons plays an important role in both cyclotron and Landau resonances. Green's functions are treated as the results of wave-particle interactions between the target waves and the given electrons. We build up a database of Green's functions for a large number of electrons interacting with oblique whistler mode chorus emissions. The formation processes of the outer radiation belt electron fluxes interacting with consecutive chorus emissions are traced by applying the convolution integrals for the Green's functions. We trace the evolution of the radiation belt electron fluxes for a few minutes and find that MeV electrons are generated promptly due to the combination of cyclotron resonance and Landau resonance with oblique chorus waves. We compare the formation processes among waves with different wave normal angles, and the results show that chorus waves with larger wave normal angles can accelerate 10-30 keV electrons to MeV faster. We further trace the formation processes of MeV electron fluxes for oblique chorus emissions localized in longitude for an hour, and then compare the results among several different longitudinal ranges. The acceleration rate of electrons is highly related to the longitudinal range of chorus occurrence.

R006-39
Zoom meeting B ：11/2 PM2 (15:45-17:30)
15:45-16:00

Energetic electron precipitation associated with pulsating aurora: Statistical analysis

#Fuminori Tsuchiya[1)], Asuka Hirai[2)], Takahiro Obara[3)], Hiroaki Misawa[4)], Yoshizumi Miyoshi[5)], Kazuo Shiokawa[6)], Hiroyo Ohya[7)], Martin Connors[8)], Yoshiya Kasahara[9)], Atsushi Kumamoto[1)], Masafumi Shoji[5)], Iku Shinohara[10)]
[1)]Tohoku Univ.,[2)]Tohoku Univ.,[3)]Tohoku Univ.,[4)]Tohoku Univ.,[5)]ISEE, Nagoya Univ.,[6)]ISEE, Nagoya Univ.,[7)]Engineering, Chiba Univ.,[8)]Centre for Science, Athabasca Univ.,[9)]Kanazawa Univ.,[10)]ISAS/JAXA

Whistler mode chorus wave is one of candidate plasma waves which causes pitch angle scattering of relativistic electron trapped in the radiation belt and precipitation of the electrons into the atmosphere [1,2,3]. The energetic electron precipitation (EEP) caused by the chorus wave could influence significantly on chemistry in the mesosphere and lower thermosphere [4,5]. Observational evidences of the EEP associated with pulsating aurora (PsA) which is also caused by the chorus wave have been reported [6,7,8]. However, these results were based on case studies. Here, we used a long-term data set of VLF subionospheric propagation in subauroral latitude to investigate statistical property of the EEP. The subionospheric propagation is sensitive to EEP with energy >100keV [9]. We used 25.2 kHz VLF radio signal which is transmitted at North Dakota (L=3.0) and received at Athabasca University GeoSpace Observatory (L=4.3) to identify occurrence of EEP in the subauroral latitude. We identified quasi-periodic change in the VLF amplitude whose time scales are similar with PsA and assumed that power spectrum density of the amplitude changes integrated from 4 to 20 sec range reflects occurrence of EEP associated with PsA. We surveyed the EEP from October 2016 to December 2017 and found occurrence distribution of the EEP with respect to magnetic local time (MLT) and its dependence on AE and Dst indices. The result shows that the EEP occurrence show strong dependences on MLT and geomagnetic activities. The EEP preferentially occurs in the post-midnight sector during high AE period (the occurrence rate reaches 7% around 2 MLT for AE>300nT). EEP does not occur when AE<100nT (below 1%). These are similar with occurrence characteristics of PsA and the chorus wave. It is worth to note that the occurrence rate reaches 20% around 1-2MLT for Dst<-40nT while the occurrences are smaller than 3% for -40nT<Dst<0nT and almost zero % for Dst>0nT. This means that occurrences of the EEP in subauroral latitude is significant during magnetic storms. We also found 24 EEP events which had good conjunction between all sky imager at The PAS and POES /NOAA 19 satellite during the period of the statistical analysis. NOAA 19 satellite observed short lived spikes of EEP when the satellite passed over PsA regions or closed to the VLF radio propagation which was detecting the EEP. Among them, 22 and 12 events accountancies >100keV and >300keV EEP, respectively, and 6 events include >800 keV EEP. These results suggest that the chorus wave is responsible for EEP with energy >100keV and the energy of EEP extents up to relativistic energy.

[1] Horne, R. B., & Thorne, R. M. (2003). Geophys. Res. Lett., https://doi.org/10.1029/2003GL01697
[2] Miyoshi, Y. et al. (2010). Journal of Geophysical Research, https://doi.org/10.1029/2009JA015127
[3] Saito, S. et al. (2012). Journal of Geophysical Research, https://doi.org/10.1029/2012JA018020
[4] Miyoshi, Y. et al. (2015). Journal of Geophysical Research. https://doi.org/10.1002/2014JA020690
[5] Grandin, M.et al. (2017). Geophysical Research Letters, https://doi.org/10.1002/2017GL073901
[6] Tsuchiya, F. et al. (2018). Geophysical Research Letters, https://doi.org/10.1029/2018GL080222
[7] Turunen, E.et al. (2016). Journal of Geophysical Research. https://doi.org/10.1002/2016JD025015
[8] Tesema, F.et al. (2020). Journal of Geophysical Research, https://doi.org/10.1029/2019JA027713
[9] Rodger, C. J. et al. (2012). Radio Science, https://doi.org/10.1029/2011RS004971

R006-40
Zoom meeting B ：11/2 PM2 (15:45-17:30)
16:00-16:15

Spatio-temporal characteristics of the precipitating electron energy of pulsating aurora estimated by optical observation

#Kohei Toyama[1)], Satoshi Kurita[2)], Yoshizumi Miyoshi[1)], Keisuke Hosokawa[4)], Yasunobu Ogawa[5)], Shin-ichiro Oyama[3)], Satonori Nozawa[6)], Tetsuya Kawabata[6)]
[1)]ISEE, Nagoya Univ.,[2)]RISH, Kyoto Univ.,[3)]ISEE, Nagoya Univ.,[4)]UEC,[5)]NIPR,[6)]ISEE, Nagoya Univ.

Pulsating aurora (PsA) is characterized by quasi-periodic intensity modulation with ~2 -20 s intervals as a main modulation. Electrostatic Cyclotron Harmonic waves and whistler-mode waves cause the pitch angle scattering of energetic electrons in the magnetosphere, and PsA is generated by the precipitating electrons with energies of several to 100 keV. In particular, whistler-mode chorus waves play a crucial role in the pitch angle scattering of the electrons. The lower-band chorus causes precipitation of electrons more than several keV, and the upper-band chorus causes steady precipitation of less than 1 keV [Miyoshi et al., 2015]. Previous studies have estimated the precipitating electron energy of pulsating auroras from the ground-based optical observations. Ono et al.[1993] observed the emission intensities of pulsating auroras at wavelength of 427.8 and 844.6 nm using photometers, and estimated the energy of the precipitating electron by combining the ratio of the two emission intensities and the model calculation. However, Ono et al.[1993] conducted observations using the instrument with narrow field-of-view, and the energy estimation using all-sky imagers has not been performed. In Tromsoe, Norway, several high-sensitivity EMCCD cameras have been operated, which have simultaneously observed the all-sky image of the emission intensity of the two-wavelength at a sampling frequency of 10 Hz. In addition, a five-wavelength photometer has been also operated. In this study, we investigate spatio-temporal variations of precipitating electron energy using these EMCCD cameras. The optical data taken from EMCCD cameras have been calibrated simultaneous measurements of the photometer. We estimated the precipitating electron energy of the pulsating aurora by comparing the emission intensity ratio of the two emission lines using the all-sky image and the emission intensity calculation results obtained by the GLOW model [Solomon, 2017]. In this presentation, we show the spatio-temporal characteristics of the precipitating electron energy of the pulsating aurora.

R006-41
Zoom meeting B ：11/2 PM2 (15:45-17:30)
16:15-16:30

Fine scale structures of chorus elements characterizing internal modulation of pulsating aurora

#Satoshi Ebukuro[1)], Keisuke Hosokawa[1)], Yoshizumi Miyoshi[2)], Shin-ichiro Oyama[2)], Yasunobu Ogawa[3)], Satoshi Kurita[14)], Yoshiya Kasahara[4)], Satoshi Kasahara[5)], Ayako Matsuoka[6)], Kunihiro Keika[7)], Tomoaki Hori[2)], Shoichiro Yokota[8)], Shoya Matsuda[9)], Masafumi Shoji[2)], Masahiro Kitahara[2)], Satoko Nakamura[10)], Shun Imajo[11)], Iku Shinohara[12)], Ryoichi Fujii[13)]
[1)]UEC,[2)]ISEE, Nagoya Univ.,[3)]NIPR,[4)]Kanazawa Univ.,[5)]The University of Tokyo,[6)]Kyoto University,[7)]University of Tokyo,[8)]Osaka Univ.,[9)]ISAS/JAXA,[10)]ISEE,[11)]ISEE, Nagoya Univ.,[12)]ISAS/JAXA,[13)]ROIS,[14)]RISH, Kyoto Univ.

Pulsating aurora (PsA) is known to show two periodic variations: main pulsation and internal modulation. The main pulsation is a slower modulation whose period ranges from a few to a few tens of seconds. The internal modulation is a scintillating luminosity change, whose period is around 3Hz, only seen during the ON phase of the main pulsation. Previous ground-satellite conjunction studies demonstrated a clear relationship between the periodicities of PsA and temporal variations of magnetospheric chorus waves. The previous studies also confirmed one-to-one correspondence between the “internal modulation" of PsA and “discrete elements" of chorus. However, the internal modulations are not always observed when chorus elements exist; thus, it is still unrevealed that how the presence/absence of internal modulation is controlled by the properties of chorus waves. This was partly because the analysis of precipitating electrons corresponding to the observation of chorus elements and internal modulation was insufficient. To overcome this problem, in this study, we investigated the relationship between the properties of chorus elements and the characteristics of internal modulation of PsA by analyzing the 64 kHz waveform data from PWE/WFC(Plasma Wave Experiment/Waveform Capture) and energetic electron data from MEP-e (Medium-Energy Particle Experiments - Electron Analyzer) onboard the Arase satellite in combination with 100 Hz ground-based optical data from a network of EMCCD cameras operated in Sodankyla in Finland and Tjautjas in Sweden.
We studied a time interval of simultaneous observation on September 28, 2019 (01:00-02:40 UT). During this event, Arase was located near the magnetic equator with a distance of around 6 Re at ~04 MLT, and its footprint was within the field of view of the two EMCCD cameras. In this time interval, two signatures of injections were detected by the Arase satellite. During an ~50 min interval from the first injection which happened at around 01:00 UT, weak amplitude and short duration chorus elements were observed. In this period of less structured chorus waves, the EMCCD cameras at the ionospheric side observed PsA without internal modulation (i.e., main pulsation only). On the other hand, after the occurrence of the second injection at 01:50 UT, large-amplitude and distinct rising tone elements became obvious. An interesting point is that after this injection and associated change in the property of chorus, PsA measured on the ground suddenly started showing signatures of internal modulation superimposed on the main pulsation. That is, there was a sharp change of properties in both PsA and chorus waves at around 01:50 UT. Our previous case study on March 28, 2017 (23:30-24:10 UT) showed a similar sharp change in the presence/absence of internal modulation, but it was a spatial boundary. At that time, the position of the Arase satellite was off the magnetic equator; thus, we employed numerical simulation to suggest that both the frequency band, the repetition period of chorus elements and the energy distribution of electrons control the presence/absence of internal modulation. In this presentation, we will discuss how the electron injection modifies the temporal variation of chorus waves and eventually determines the periodicities of PsA seen from the ground.

R006-42
Zoom meeting B ：11/2 PM2 (15:45-17:30)
16:30-16:45

Spatial distribution of pulsating aurora with/without internal modulation

#Yuki Kawamura[1)], Keisuke Hosokawa[1)], Shin-ichiro Oyama[2),3),6)], Yoshizumi Miyoshi[2)], Yasunobu Ogawa[3)], Satoshi Kurita[4)], Satoshi Ebukuro[1)], Ryoichi Fujii[5)]
[1)]UEC,[2)]ISEE, Nagoya Univ.,[3)]NIPR,[4)]RISH, Kyoto Univ.,[5)]ROIS,[6)]Univ. of Oulu

Pulsating aurora (PsA) is a kind of diffuse aurora which almost always appears in the morning side during the recovery phase of auroral substorm. PsA typically has two distinct temporal variations. One is so-called main pulsation whose period ranges from a few to a few tens of seconds. The other is a few Hz modulation (internal modulation), which is occasionally seen during the ON phase of the main pulsation. Previous studies have suggested that the temporal variation of PsA is characterized by wave-particle interaction between whistler-mode chorus waves and energetic electrons in the magnetosphere. Especially, it has been indicated that there is a one-to-one correspondence between the amplitude variation of chorus waves and the luminosity modulation of PsA. However, there have been no studies which analyzed the spatial distribution of PsA with/without internal modulation, especially the percentage of PsA having internal modulation and its dependence on latitude are still unknown.
To reveal the spatial distribution of PsA with internal modulation, we have performed frequency analyses of multi-scale temporal variations of PsA by using data from high speed optical cameras capable of providing a wide spatial coverage and categorized PsA into ones with/without internal modulation. In this study, we make use of highly sensitive EMCCD cameras, which have been in operation in Sodankyla and Kevo, Finland, Tromsoe, Norway, and Tjautjas, Sweden. All-sky aurora images are taken with a temporal resolution of 0.01 sec. The temporal resolution of these cameras is sufficient to identify the multi-scale temporal variation of PsA. Note that in this study, to make the analysis easily, the images have been down-sampled to 25 Hz.
In the frequency analysis, we have examined all-sky images taken on March 14, 15, and 23, 2018. We detected PsA with/without internal modulation automatically and computed the average frequency of internal modulation from each pixel of the EMCCD cameras. Regardless of latitude, the luminosity of pulsating patches was fluctuating with a periodicity of ~3 Hz. We also computed a percentage of existence of internal modulation and found that the percentage of PsA with internal modulation increases at higher latitudes. These results indicate that the frequency of internal modulation is concentrated around 3 Hz and PsA with internal modulation has the dependence on latitude. In the presentation, we will discuss what factor controls the existence/absence of internal modulation using a TOF simulation in Miyoshi et al. [2010].

R006-43
Zoom meeting B ：11/2 PM2 (15:45-17:30)
16:45-17:00

Resolving the evolution of pulsating aurora: High-speed Tjornes-Arase-Syowa conjugate observation

#Herbert Akihito Uchida[1)], Ryuho Kataoka[2)], Kiyoka Murase[1)], Shoya Matsuda[3)], Yoshiya Kasahara[4)], Masafumi Shoji[5)], Yoshizumi Miyoshi[5)], Iku Shinohara[3)], Ayako Matsuoka[6)], Satoshi Kurita[7)], Keisuke Hosokawa[8)], Shun Imajo[5)]
[1)]SOKENDAI,[2)]NIPR,[3)]ISAS/JAXA,[4)]Kanazawa Univ.,[5)]ISEE, Nagoya Univ.,[6)]Kyoto University,[7)]RISH, Kyoto Univ.,[8)]UEC

Pulsating auroras were observed by ground-based high-speed imagers after an auroral breakup at Tjornes in Iceland and at its magnetic conjugate station, Syowa station in Antarctica simultaneously on 22 September 2018. Two identical all-sky imagers at both stations and a narrow field-of-view imager at Syowa station were used to elucidate the hierarchical structure of the modulation in the auroral luminosity and the evolution of pulsating patches at different time scales. A few minutes before the main pulsation start, a fast intensity modulation of ~20 Hz was identified by the narrow field-of-view imager with ~3 Hz modulation in a small aurora patch. The Arase satellite was located on the magnetic field line connecting these two stations at that time. Although the foot-print of Arase satellite was out of the narrow field-of-view, the Plasma Wave Experiment onboard Arase satellite observed chorus emissions whose intensity was modulated at the same period of the auroral fast intensity modulation. The patch size and the pulsation period evolved in time at both hemispheres and the period settled in the period of main pulsation. The variation of chorus emission intensity of main-pulsation time scale shows a good correlation with the intensity variation of pulsating aurora. The pulsating patches differ in its shape and period between both hemispheres although several synchronized patches were also observed when the pulsating aurora drifted away from the all-sky field-of-view. We show the evidence of the fast modulation of the auroral luminosity and the chorus wave intensity, and the evolution of pulsating aurora in terms of the transition of on and off of the pulsating patch, patch size, and pulsating period in both hemispheres in different timescales.

R006-44
Zoom meeting B ：11/3 AM1 (9:00-10:30)
09:00-09:15

Simulation on rapid flux change of energetic electrons in the upper-band whistler burst event observed by Arase

#Shinji Saito[1)], Yoshizumi Miyoshi[2)], Satoshi Kurita[2)], Yoshiya Kasahara[3)], Shoya Matsuda[4)], Fuminori Tsuchiya[5)], Atsushi Kumamoto[5)], Masafumi Shoji[2)], Satoshi Kasahara[6)], Shoichiro Yokota[7)], Kunihiro Keika[8)], Tomoaki Hori[2)], Ayako Matsuoka[9)], Iku Shinohara[10)]
[1)]NICT,[2)]ISEE, Nagoya Univ.,[3)]Kanazawa Univ.,[4)]ISAS/JAXA,[5)]Planet. Plasma Atmos. Res. Cent., Tohoku Univ.,[6)]The University of Tokyo,[7)]Osaka Univ.,[8)]University of Tokyo,[9)]Kyoto University,[10)]ISAS/JAXA

The Medium Energy Particle Experiment-electron analyzer (MEP-e) onboard The Arase satellite detected a rapid flux change of a few tens keV electrons close to the magnetic equator. At the same time, an upper-band whistler chorus burst was also detected by the Onboard Frequency Analyzer (OFA) of the Plasma Wave Experiment (PWE) instrument in about 30 seconds. Kurita et al. (2018) studied the event and concluded that quasi-linear diffusion processes do not explain such a rapid flux enhancement of electrons. In order to verify the electron scattering observed in the event, we have performed a test-particle simulation to calculate electron scattering by whistler mode waves propagating along a magnetic field line. The simulation imported the wave spectrum observed by OFA/PWE and the initial electron flux distribution observed by MEP-e. The simulation results show that the flux of electrons with an energy of 24.5 keV and pitch angles of 70-80 degrees noticeably increases in 30 seconds, which is consistent with the Arase observations during the event. The simulation also shows that the electrons contributing to the flux enhancement are transported from those with pitch angles less than 50 degree and energies lower than 15 keV. We confirm that a quasi-linear diffusion theory cannot reproduce such a rapid change of pitch angle and energy. Our simulation concludes that the rapid flux enhancement observed by Arase is due to electron transport driven by electron cyclotron resonance lasting for over a few tens milli-seconds rather than quasi-linear diffusion.

R006-45
Zoom meeting B ：11/3 AM1 (9:00-10:30)
09:15-09:30

ULF modulation of energetic electron precipitations observed by using VLF/LF transmitter signals

#Hiroyo Ohya[1)], Takuya Miyashita[2)], Fuminori Tsuchiya[3)], Mitsunori Ozaki[4)], Kazuo Shiokawa[5)], Yoshizumi Miyoshi[6)], Nozomu Nishitani[6)], Tomoaki Hori[6)], Mariko Teramoto[7)], Martin Connors[8)], Simon G. Shepherd[9)]
[1)]Engineering, Chiba Univ.,[2)]Core Engineering, Chiba Univ.,[3)]Planet. Plasma Atmos. Res. Cent., Tohoku Univ.,[4)]Kanazawa Univ.,[5)]ISEE, Nagoya Univ.,[6)]ISEE, Nagoya Univ.,[7)]Kyutech,[8)]Centre for Science, Athabasca Univ.,[9)]Dartmouth College

It has been expected that ULF (ultra low frequency, 1 mHz ? 1 Hz) magnetic pulsations modulate the precipitation of electrons in the magnetosphere [Coroniti and Kennell, 1970]. In this process, periodic change in the local magnetic field strength due to the ULF pulsations modulates the growth rate of whistler mode chorus waves and resultant pitch angle scattering rate. That is, flux of the precipitating electrons may depend on the strength of pitch angle diffusion coefficient at the same frequency as the ULF pulsations. There have been several studies of Pc5 (1.67?6.67 mHz, the periods: 150?600 s) ULF modulation of energetic electron precipitations (EEP) in the D-region ionosphere based on ground-based riometers and X-ray observations [e.g., Brito et al., 2012]. The EEPs associated with Pi2 pulsations (40-150 s) were reported [Asnes et al., 2004]. Auroral precipitations and energetic particle flux near the equator in nightside magnetosphere occur due to Pi2 modulation [Saka et al., 1999]. Precipitation of low energy electrons below 300 eV was reported when a Pi2 pulsation with short periods (less than 40 s) occurred [Tsunomura et al., 1990]. However, there have been few reports for the ULF modulation of high energy electrons that modulate the D-region ionosphere. In this study, we investigate the D-region signatures of the modulation due to the ULF waves using a network of VLF/LF transmitter signals in North America. The transmitter signals from NLK (USA, 24.8 kHz, L = 2.88), NDK (USA, 25.2 kHz, L = 2.98) and WWVB (USA, 60.0 kHz, L = 2.26) were observed by a receiver at ATHA (Athabasca, Canada, L = 4.31). We show the first observations of oscillations in intensities and phases on the NDK-ATH and WWVB-ATH paths with periods of 3-4 minutes during a small substorm at 05:25-05:50 UT on 4 June, 2017 (AE index = 140 nT). Based on ground-based magnetic observations, there were pulsations with the same periods with the VLF/LF oscillations both at high- and low-latitudes. The ground-based H-component magnetic field variations and Doppler velocity observed by the SuperDARN (Super Dual Auroral Radar Network) HF (high frequency, 8-20 MHz here) radars showed the same periodic changes as seen in the VLF/LF oscillations, suggesting that energetic electron precipitation over the WWVB-ATHA and NDK-ATHA paths was modulated by the ULF waves. Based on the ground-based magnetic field data, we conclude that the ULF wave was the Pi2 pulsations associated with the substorm, because propagation direction of the wave was westward (66.4 km/s) from the pre-midnight sector, the magnetic variations at low latitudes were in-phase over wide longitudes, and the magnetic variations at ATHA slightly preceded those at low latitudes. The VLF/LF oscillations preceded magnetic variations at ATHA by several tens of seconds, which may be caused by time difference between the EEPs and ULF wave propagation. In this presentation, we will discuss possible causes of these VLF/LF oscillations.

R006-46
Zoom meeting B ：11/3 AM1 (9:00-10:30)
09:30-09:45

Computer simulations of precipitating electrons through chorus-wave particle interactions

#YOSHIKI ITO[1)], Shinji Saito[2)], Yoshizumi Miyoshi[3)]
[1)]ISEE, Nagoya Univ.,[2)]NICT,[3)]ISEE, Nagoya Univ.

Whistler mode chorus waves cause scattering and acceleration of energetic electrons in the inner magnetosphere, and recent studies identified that chorus waves cause the pulsating aurora. The interaction processes have been modeled as diffusions in the velocity space, and the scattering rate increases with increasing the wave amplitude. However, the wave-particle interactions with chorus waves are non-linear process, so that it is expected that the scattering rate does not show a simple correlation with wave amplitude. In this study, we investigate chorus wave amplitude dependence of electron scattering using the GEMSIS-RBW simulation code. The GEMSIS-RBW simulation calculates variations of local pitch angle and energy by the imposed chorus waves. In this simulation, chorus bursts that consist of multiple rising tone elements are imposed at the equatorial plane, and these bursts propagate along the field line with L= 4. We calculate the trajectory of a number of electrons with initial energy of 50 keV. We calculated the number of precipitating electrons with various wave amplitudes. The number of precipitating electrons increase when the wave amplitude increases from 10 pT to ~200 pT. However, as the wave amplitude increases more than 200 pT, the number of precipitating electrons decreases. From this simulation, the simple relationship between the wave amplitudes and precipitating flux is not always satisfied due to the non-linear wave particle interactions, and the depression of the precipitating flux is expected with the wave amplitude of more than a few hundred pT. From the analysis on the electron motion in the phase space as well as the parameter ρ that is a proxy of the ratio of the wave-induced and the background inhomogeneity effects for the momentum change of the resonant electron, the phase trapping effect suppress the precipitating flux in the large amplitudes. During the multiple interactions with chorus elements, subsequent interactions with chorus waves changes electron motions from diffusive interactions and diffusive interactions, i.e., non-linear phase trapping and dislocation occur for electrons whose initial ρ are small enough to be diffusion. As a result, the number of precipitating electrons decrease even though the initial conditions for interactions between electrons and chorus waves are categorized in the diffusion.

R006-47
Zoom meeting B ：11/3 AM1 (9:00-10:30)
09:45-10:00

Relative contribution of ULF waves and whistler-mode chorus to the radiation belt variation during May 2017 storm

#Naoko Takahashi[1)], Kanako Seki[1)], Mei-Ching Fok[2)], Yihua Zheng[2)], Yoshizumi Miyoshi[3)], Satoshi Kasahara[1)], Kunihiro Keika[1)], David Hartley[4)], Yoshiya Kasahara[5)], Yasumasa Kasaba[6)], Nana Higashio[7)], Ayako Matsuoka[8)], Shoichiro Yokota[9)], Tomoaki Hori[3)], Masafumi Shoji[3)], Satoko Nakamura[3)], Shun Imajo[3)], Iku Shinohara[10)]
[1)]The University of Tokyo,[2)]NASA/GSFC,[3)]ISEE, Nagoya Univ.,[4)]Univ. of Iowa,[5)]Kanazawa Univ.,[6)]Tohoku Univ.,[7)]JAXA,[8)]Kyoto University,[9)]Osaka Univ.,[10)]ISAS/JAXA

The purpose of the present study is to understand when, where, and how ultra-low frequency (ULF) waves and whistler-mode chorus contribute to the Earth's radiation belt dynamics. We first investigate the temporal contribution of ULF waves and whistler-mode chorus to the relativistic electron flux enhancement during 27 May 2017 storm. Both Arase (post-midnight) and Van Allen Probe (RBSP)-B (dusk) show the global enhancement of ULF waves during the early recovery phase, which corresponds to the global increase of relativistic electron fluxes. On the other hand, whistler-mode chorus is mainly enhanced during the late recovery phase even RBSP-B locates at the dusk sector where is far from the ordinary location of wave generation. Relativistic electron fluxes significantly increase around L~4 during the late recovery phase. We also investigate the spatial contribution of waves using Comprehensive Ring Current Model (CRCM) coupled with Block-Adaptive-Tree Solar-Wind Roe-Type Upwind Scheme (BATS-R-US) simulation. The simulation qualitatively reproduces the global evolution of externally-driven ULF waves. The estimated region where the thermal energy anisotropy of electrons (~20-60 keV) is large shifts toward dusk during the recovery phase. We also find the large magnetic field curvature at noon and dusk sectors during the recovery phase. Estimated spatial distributions of thermal energy anisotropy and magnetic field curvature give explanation of the observational result that enhanced whistler-mode chorus exists at the dusk sector.

R006-48
Zoom meeting B ：11/3 AM1 (9:00-10:30)
10:00-10:15

PINO (Particle Instrument for Nano-Satellite) onboard the BIRDS-5 satellite

#Iku Shinohara[1)], Takefumi Mitani[1)], Mariko Teramoto[2)], Kazushi Asamura[1)], Onogi Ryota[1)], Takeshi Takashima[1)]
[1)]JAXA/ISAS,[2)]Kyushu Institute of Technology/Graduate School of Engineering

Recently, the use of CubeSats has become more familiar, and researches in space science by using CubeSats are no longer unusual. We expect that CubeSats could be applied to full-scale observations in the space environment research. However, our experience of CubeSat usage is still lacking, and more opportunities to install instruments onboard CubeSats are desired for future planning and the development of new instruments.
Fortunately, we are provided a chance to install a high-energy electron measurement onboard the BIRDS-5 satellite, which is the fifth satellite in Joint Global Multi-Nation Birds Satellite (BIRDS) Program of Kyushu Institute of Technology. The BIRDS-5 project was kicked off in July 2020, and, thanks to the JSPS KAKENHI support, we have started to develop the high-energy electron analyzer, PINO: Particle Instrument for Nano-Satellite. In this presentation, we will present the outline of the science plan and the latest status of PINO development.

R006-49
Zoom meeting B ：11/4 AM1 (9:00-10:30)
09:00-09:15

Spatial evolution of injected energetic electrons as observed by Arase and Van Allen Probes

#Tomoaki Hori[1)], Yoshizumi Miyoshi[1)], Takefumi Mitani[2)], Satoshi Kurita[3)], Mariko Teramoto[4)], Takeshi Takashima[5)], Iku Shinohara[6)], Ayako Matsuoka[7)], S. G. Claudepierre[8)], J. F. Fennell[8)], J. B. Blake[8)], Craig A. Kletzing[9)]
[1)]ISEE, Nagoya Univ.,[2)]ISAS/JAXA,[3)]RISH, Kyoto Univ.,[4)]Kyutech,[5)]ISAS, JAXA,[6)]ISAS/JAXA,[7)]Kyoto University,[8)]Space Sciences Department, The Aerospace Corporation,[9)]Department of Physics and Astronomy, Univ. of Iowa

In this study, we investigate how drifting energetic electron populations evolve in the inner magnetosphere, using the Arase and Van Allen Probes (RBSP) satellites. Electrons and ions of the plasma sheet origin are energized up to tens to hundreds of keV and abruptly transported on the night side into geosynchronous distance and even further inward during substorms, which is referred to as substorm injection. Then injected electrons drift eastward and disperse along their drift path with azimuthal drift velocities depending on their energies. Extensive observations with geosynchronous satellites have shown that energy dispersion signatures can be quantitatively explained by magnetic drift velocities, while its two-dimensional evolution, particularly the radial structure of a drifting electron population has not been well examined except for a few case studies where many satellites were available simultaneously at different radial distances and local times. In this regard, we make a statistical study on simultaneous observations of Arase and RBSPs to examine how injected energetic electrons spread radially in the course of their eastward drift. Our preliminary analysis on one of the events where the three satellites were located on the dusk side shows that Arase (L ~ 7.7, MLT ~ 10h) and RBSP-B (L ~ 5.8, MLT ~ 4h) observed an energy-dispersed electron population nearly at the same time (within a few minutes), despite the large difference in MLT sector. This result strongly suggests that the “drift front" of energetic electrons goes significantly ahead at farther radial distances even if they have started drifting at the same MLT. On the basis of statistics with many simultaneous observations, we address how the spatial shape of drifting populations looks like and how it evolves as drifts eastward from night to the dayside.

R006-51
Zoom meeting B ：11/4　AM1　(9:00-10:30)
09:30-09:45

あらせ衛星と SuperDARN による SAPS 電場の同時観測

#高田　知弥[1)],西谷　望[2)],堀　智昭[2)],Shepherd　Simon G.[3)],笠羽　康正[4)],熊本　篤志[4)],加藤　雄人[4)],笠原　禎也[5)],小路　真史[2)],中村　紗都子[2)],北原　理弘[2)],土屋　史紀[4)],浅村　和志[6)],三好　由純[2)],風間　洋一[7)],Wang　S.-Y.[7)],Jun　C.-W.[2)],横田　勝一郎[8)],笠原　慧[9)],桂華　邦裕[9)],松岡　彩子[9)],今城　峻[2)],篠原　育[6)]
[1)]ISEE,[2)]名大 ISEE,[3)]Thayer School of Engineering, Dartmouth College,[4)]東北大学,[5)]金沢大学,[6)]宇宙航空研究開発機構 宇宙科学研究所,[7)]Academia Sinica, Taiwan,[8)]大阪大学,[9)]東京大学

Simultaneous observations of SAPS electric field with the Arase satellite and SuperDARN radars

#Tomoya Takada[1)], Nozomu Nishitani[2)], Tomoaki Hori[2)], Simon G. Shepherd[3)], Yasumasa Kasaba[4)], Atsushi Kumamoto[4)], Yuto Katoh[4)], Yoshiya Kasahara[5)], Masafumi Syoji[2)], Satoko Nakamura[2)], Masahiro Kitahara[2)], Fuminori Tsuchiya[4)], Kazushi Asamura[6)], Yoshizumi Miyoshi[2)], Yoichi Kazama[7)], S.-Y. Wang[7)], C.-W. Jun[2)], Shoichiro Yokota[8)], Satoshi Kasahara[9)], Kunihiro Keika[9)], Ayako Matsuoka[9)], Shun Imajo[2)], Iku Shinohara[6)]
[1)]ISEE,[2)]ISEE, Nagoya Univ.,[3)]Thayer School of Engineering, Dartmouth College,[4)]Tohoku University,[5)]Kanazawa University,[6)]JAXA,[7)]Academia Sinica, Taiwan,[8)]Osaka University,[9)]The University of Tokyo

The comparison between the ionospheric convection and magnetospheric electric field is important for understanding the magnetosphere-ionosphere coupling. However, there have been few studies of the comparison between the SuperDARN convection and satellite electric field data (e.g., Baker et al., 2003) and almost no studies on the Sub-Auroral Polarization Streams (SAPS) related electric field so far. In this study, simultaneous observation of the SAPS electric field was carried out by SuperDARN radar and Arase satellite. In the event of June 22, 2017, SAPS was observed by the SuperDARN radar near the calculated footprint of the Arase satellite and almost concurrently the satellite detected electric field enhancements. Nearly simultaneously, the satellite observed the plasmapause crossing and increase of low energy (< 1 keV) ions. On the other hand, it is also suggested that the real ionospheric footprint of the Arase satellite deviates from the calculated point. Details of the relationship between these low-energy ion characteristics and the electric field distribution, as well as the deviation of the ionospheric footprint of the satellite, will be discussed.

磁気圏-電離圏結合を理解する上で電離圏対流と磁気圏電場の比較は極めて重要であるが、SuperDARN と人工衛星データの比較は Baker et al. (2003)他数えるほどしかなく、さらには SAPS に代表されるサブオーロラ帯現象に関連した比較観測はほとんど存在しなかった。本研究においては SuperDARN レーダーとあらせ衛星による、SAPS 電場の同時観測及びに、あらせ衛星による粒子観測を行った。2017 年 6 月 22 日のイベント解析結果においては、SuperDARN で SAPS が観測された時間帯で、あらせ衛星の footprint が SAPS 構造付近を通過した際に局在化した強い電場の構造を観測することができた。加えて上記イベントでは、SAPS 電場の存在する領域に対応して、あらせ衛星の粒子データではプラズマ圏の境界領域および低エネルギーイオンフラックスの増大が見られた。一方、あらせ衛星の電離圏への真の footprint は計算上の点からずれがあることも示唆された。この特徴的な粒子分布と電場・対流分布との対応関係、ならびに人工衛星の footprint のずれの詳細について講演で報告・議論する。

R006-52
Zoom meeting B ：11/4　AM1　(9:00-10:30)
09:45-10:00

あらせ衛星・SuperDARN でサブストーム中に観測された SAPSWS の事例解析

#深見　岳弘[1)],熊本　篤志[1)],加藤　雄人[1)],西谷　望[2)],堀　智昭[2)],笠羽　康正[1)],土屋　史紀[1)],寺本　万里子[3)],木村　智樹[1)],川面　洋平[1)],笠原　禎也[4)],小路　真史[2)],中村　紗都子[2)],北原　理弘[2)],松岡　彩子[5)],今城　　峻[2)],笠原　慧[6)],横田　勝一郎[7)],桂華　邦裕[6)],風間　洋一[8)],Wang　S.-Y.[8)],田　采祐[2)],浅村　和史[9)],三好　由純[2)],篠原　育[9)],Shepherd Simon G.[10)]
[1)]東北大学,[2)]名大 ISEE,[3)]九州工業大学,[4)]金沢大学,[5)]京都大学,[6)]東京大学,[7)]大阪大学,[8)]台湾・中央研究院,[9)]宇宙研,[10)]Dartmouth College

Case analysis of SAPS Wave Structure (SAPSWS) event during a substorm observed by Arase and SuperDARN

#Takehiro Fukami[1)], Atsushi Kumamoto[1)], Yuto Katoh[1)], Nozomu Nishitani[2)], Tomoaki Hori[2)], Yasumasa Kasaba[1)], Fuminori Tsuchiya[1)], Mariko Teramoto[3)], Tomoki Kimura[1)], yohei kaswazura[1)], Yoshiya Kasahara[4)], Masafumi Shoji[2)], Satoko Nakamura[2)], Masahiro Kitahara[2)], Ayako Matsuoka[5)], Shun Imajo[2)], Satoshi Kasahara[6)], Shoichiro Yokota[7)], Kunihiro Keika[6)], Yoichi Kazama[8)], S.-Y. Wang[8)], ChaeWoo Jun[2)], Kazushi Asamura[9)], Yoshizumi Miyoshi[2)], Iku Shinohara[9)], Simon G. Shepherd[10)]
[1)]Dept. Geophys., Grad. Sch. Sci., Tohoku Univ.,[2)]ISEE, Nagoya Univ.,[3)]Kyutech,[4)]Kanazawa Univ.,[5)]Kyoto University,[6)]The University of Tokyo,[7)]Osaka Univ.,[8)]ASIAA, Taiwan,[9)]ISAS/JAXA,[10)]Dartmouth College

Subauroral Polarization Stream (SAPS) and Subauroral Ion Drift (SAID) are westward high-speed flows that occur in the subauroral region of the ionosphere, and found frequently during geomagnetic disturbances such as magnetic storms and substorms [Anderson et al., 1993; Foster and Vo, 2002]. Recently, SAPS wave structure (SAPSWS) has been reported [Mishin et al., 2005], and it is implied that SAPSWS influences fluctuations in the trough region from Ionospheric satellite and GNSS-TEC observations [Mishin et al., 2004; Horvath and Lovell, 2016].
In this study, we analyzed a SAPS event observed during the conjugate observation of the Arase satellite, which measures the electromagnetic field and the flux of particles in the ring current, and the SuperDARN radar, which can observe two-dimensional plasma flow in the ionosphere. The analysis was performed on the data obtained in the period from 2:00 to 3:00 UT on July 9, 2017. In this event, 10 minutes after substorm onset, Christmas Valley East radar of SuperDARN in the sub-auroral region detected an increase in westward flow velocity of ~1,000 m/s, which is considered to be SAPS, and with temporal fluctuations. At that time, the magnetic field footprint of Arase satellite was located on the westward flow in the ionosphere, we found a radial outward electric field of ~5 mV/m at an L value of 4 to 5 around 20:00 MLT. The electric field shows fluctuations with a frequency of 2.5 to 3.5 mHz with an amplitude of 1.5 to 2 mV/m in the radial direction. The amplitude and frequency of the fluctuations of the ionospheric flow, and magnetospheric electric field are consistent with those of the SAPSWS reported in previous studies. Therefore we consider that SuperDARN radar and Arase satellite observed the same SAPSWS both in the ionosphere and magnetosphere, simultaneously. In this presentation, we will show details of ionospheric flows and magnetospheric electric fields, and discuss the mode and generation mechanisms of electromagnetic field fluctuations measured in the magnetosphere.

Subauroral Polarization Stream (SAPS)や Subauroral Ion Drift(SAID)は，地球電離圏サブオーロラ帯に発生する西向きの高速フローであり，磁気嵐やサブストームといった擾乱時によく発生することが知られている[Anderson et al., 1993; Foster and Vo, 2002]．近年、SAPS の波状構造(SAPS wave structure: SAPSWS)が報告され[Mishin et al., 2005]，低高度衛星と GNSS-TEC の観測から SAPSWS が電離圏トラフ領域の変動にも影響を与えていることが示唆されている[Mishin et al., 2004; Horvath and Lovell, 2016].
そこで本研究では，磁気圏で電磁場や環電流粒子のフラックスを計測するあらせ衛星と，2 次元的に電離圏のフローを観測できる SuperDARN レーダーの共役観測が行われた際に観測された SAPS イベントに対して解析を行った．イベントの観測日時は 2017/7/9 の 2:00-3:00UT である．このイベントでは，サブストームオンセットから 10 分後，SuperDARN の Christmas Valley East レーダーではサブオーロラ帯で SAPS とみられる~1,000 m/s の西向きフロー速度の増大が確認され，かつフロー速度が時間的に変動する様子が観測された．一方，あらせ衛星では，footprint が西向きフロー上にある時間帯に，L 値 4~5，MLT 20 時付近で~5 mV/m の動径方向外向きの電場を確認しており，実際にあらせ衛星が SAPS 領域を通過していると考えられる．また，電場は変動を伴っており，振幅は動径方向に 1.5~2 mV/m，周波数は 2.5~3.5 mHz だった。これらの電離圏フローと磁気圏電場の振幅，変動周期は従来報告されている SAPSWS のものと一致しており．SuperDARN レーダーとあらせ衛星で，同じ SAPSWS イベントをとらえていたと考えられる．本発表ではこれらの電離圏フロー・磁気圏電場の観測の詳細を示すとともに，観測された電磁場変動のモードや成因についても議論する．

R006-53
Zoom meeting B ：11/4 AM1 (9:00-10:30)
10:00-10:15

Study of the seasonal dependence of SAPS occurrence using the SuperDARN radars

#Kento Oya[1)], Nozomu Nishitani[1)], Tomoaki Hori[1)]
[1)]ISEE, Nagoya Univ.

We make a statistical study on occurrence characteristics of Sub-Auroral Polarization Streams (SAPS), using the Super Dual Auroral Radar Network (SuperDARN) data. We use several years of SuperDARN data and study the seasonal dependence of SAPS type flows. We identify the equatorward aurora oval boundary using the precipitating energy fluxes data of the NOAA POES satellites and use only the SuperDARN echoes equatorward of this boundary. We set criteria to identify SAPS events, i.e., the flow speed exceeds 150 m/s [Nagano et al., 2015] and has a westward component (-45 deg $< \Delta\theta <$ +45 deg). Some past studies suggested existence of the seasonal dependence of SAPS, e.g., SAPS-like high velocity flow occurs over a larger MLT extent during winter months [Koustov et al., 2006], lower velocity flows are observed more often in the summer Northern Hemisphere than in the winter Southern Hemisphere [Kunduri et al., 2012], but these results are in slight disagreement with another interhemispheric study [Parkinson et al., 2005], who showed that summer Southern Hemisphere velocities are slightly higher than in the winter Northern Hemisphere. Yet complementary study on statistics of the seasonal dependence has not been made very much. To the best of our knowledge, the present study is the first comprehensive statistical study focusing on the seasonal dependence of SAPS using the mid-latitude SuperDARN radars. Our results show the clear seasonal dependence of SAPS; SAPS occur over a larger MLT extent in winter months than other months and rarely occur at lower latitude in summer months. In addition, the SAPS speed distribution obtained by the present study is consistent with those of Koustov et al. [2006] and Kunduri et al. [2012].

R006-54
Zoom meeting B ：11/4 AM2 (10:45-12:30)
10:45-11:00

Statistical investigation of cross energy coupling during magnetic storms

#Yoshizumi Miyoshi[1)], Satoshi Kurita[2)], Inchun Park[3)], Takefumi Mitani[4)], Iku Shinohara[5)], Satoshi Kasahara[6)], Shoichiro Yokota[7)], Kunihiro Keika[8)], Tomoaki Hori[1)], Nana Higashio[9)], Shun Imajo[10)], ChaeWoo Jun[11)], Ayako Matsuoka[12)], Yoshiya Kasahara[13)], Shoya Matsuda[14)], Fuminori Tsuchiya[15)], Atsushi Kumamoto[15)], Masafumi Shoji[1)]
[1)]ISEE, Nagoya Univ.,[2)]RISH, Kyoto Univ.,[3)]ISEE,Nagoya univ.,[4)]ISAS/JAXA,[5)]ISAS/JAXA,[6)]The University of Tokyo,[7)]Osaka Univ.,[8)]University of Tokyo,[9)]JAXA,[10)]ISEE, Nagoya Univ.,[11)]ISEE, Nagoya Univ.,[12)]Kyoto University,[13)]Kanazawa Univ.,[14)]ISAS/JAXA,[15)]Planet. Plasma Atmos. Res. Cent., Tohoku Univ.

The Arase satellite has observed a number of magnetic storms since March 2017, which corresponds to the declining phase of the solar cycle 24. We performed the superposed epoch analysis of energetic electrons and related parameters in the inner magnetosphere using data obtained by Arase satellite. The electron measurements in the wide energy range are utilized to clarify the cross energy coupling process during storms. The energetic electron flux variations strongly depend on the storm phase and L-shell as well as the electron energy. Electrons with energies ranging from tens of keV to ~200 keV largely increase their fluxes in the outer radiation belt during the main phase, and the electron fluxes gradually decrease during the recovery phase. The sub-relativistic/relativistic electrons show different flux variations. The electron fluxes decrease at the outer part of the outer belt during the main phase, and the fluxes gradually increase from the inner part of the outer belt during the recovery phase. The variations in the energy spectrum and phase space density indicate that the local accelerations mainly contribute to enhancements of MeV electrons in the outer belt. The thermal plasma density derived from the Arase observations shows the significant shrinkage of the plasmapause during the main phase and subsequent, gradual refilling of the plasmasphere during the recovery phase. The whistler mode chorus wave intensity estimated from the POES satellite observations shows continuous enhancement of chorus waves during the main phase and early recovery phase. In this study, we discuss variations in the energy spectrum by considering different roles of each energy range in the cross energy coupling process, i.e., source population for generating waves, seed population for subsequent acceleration, and relativistic electrons.

R006-55
Zoom meeting B ：11/4 AM2 (10:45-12:30)
11:00-11:15

Comparative study of flux and pressure variations in inner magnetosphere using Arase and RAM-SCB simulations

#Sandeep Kumar[1)], Yoshizumi Miyoshi[1)], Vania Jordanova[2)], M Engel[2)], Ayako Matsuoka[3)], Kazushi Asamura[3)], Shoichiro Yokota[4)], Satoshi Kasahara[5)], Kunihiro Keika[5)], Tomoaki Hori[1)], Takefumi Mitani[3)], Takeshi Takashima[3)], Yoichi Kazama[6)], S.-Y. Wang[6)], ChaeWoo Jun[1)], Fuminori Tsuchiya[7)], Atsushi Kumamoto[7)], Yoshiya Kasahara[8)], Masafumi Shoji[1)], Satoko Nakamura[1)], Masahiro Kitahara[1)], Ayako Matsuoka[9)], Shun Imajo[1)], Iku Shinohara[3)]
[1)]ISEE,Nagoya University,[2)]LANL,USA,[3)]ISAS/JAXA,[4)]Osaka University,[5)]University of Tokyo,[6)]ASIAA, Taiwan,[7)]Tohoku University,[8)]Kanazawa University,[9)]Kyoto University

Understanding the physical processes that control the dynamics of energetic particles in the inner magnetosphere is important for both space-borne and ground-based assets essential to the modern society. The storm time distribution of ring current ions in the inner magnetosphere depend strongly on their transport in evolutions of electric and magnetic fields along with acceleration and loss. In this study, we compare the ion flux (H+, He+, and O+) and electron flux variations during geomagnetic storms using Arase observations with the self-consistent inner magnetosphere model: Ring current Atmosphere interactions Model with Self Consistent magnetic field (RAM-SCB). We compare pressure distributions of H+, He+, O+ and electrons from the Arase LEPi/MEPi, LEPe/MEPe/HEP-L as well as the thermal electron density from PWE/HFA measurements and the RAM-SCB simulation to investigate the contribution of the different species (ions and electrons) to the magnetic field deformation observed at ground magnetic stations. The results show that the ions are the major contributor (~ 90 %) to the total ring current pressure. It is also found that electrons (~ 10 %) also contribute significantly to the ring current pressure at post-midnight and dawn sector where electrons flux is higher compared to ions flux.

R006-56
Zoom meeting B ：11/4　AM2　(10:45-12:30)
11:15-11:30

サブストーム回復相におけるオーロラオーバル低緯度側境界からのオーロラアークの分離

#塩川　和夫[1)],稲葉　裕大[1)],Connors　Martin[2)]
[1)]名大宇地研,[2)]Centre for Science, Athabasca Univ.

Detachment of auroral arcs from the equatorward boundary of the auroral oval during substorm recovery phase

#Kazuo Shiokawa[1)], Yudai Inaba[1)], Sneha Yadav[1)], Martin Connors[2)]
[1)]ISEE, Nagoya Univ.,[2)]Centre for Science, Athabasca Univ.

Formation of auroral arcs and their motion are manifestation of plasma dynamics in the magnetosphere. In this presentation, we show a common feature of auroral arc detachment from the equatorward boundary of the auroral oval, which occurs mainly during substorm recovery phase. After the expansion onset of auroral substorms, the equatorward boundary of the auroral oval can expand to lower latitudes. Around the beginning of the substorm recovery phase, the equatorward boundary of the oval starts to retreat back to higher latitudes. At this time, equatorward detachments of weak auroral arcs are often seen in both 630.0-nm and 557.7-nm images and north-south keograms at subauroral latitudes. The detached arcs can later become Stable Auroral Red (SAR) arcs [e.g., Shiokawa et al., AIP, 2009; EPS, 2017; Takagi et al., GRL, 2018] and/or STEVE [e.g., Gallardo-Lacourt et al., JGR, 2018]. We will discuss possible mechanisms that can create this auroral arc detachment from the auroral oval in the context of magnetospheric plasma processes.

Gallardo-Lacourt et al. (JGR, 2018) https://doi.org/10.1029/2018JA025368
Shiokawa et al. (AIP Conf. Proc., 2009) https://doi.org/10.1063/1.3169292
Shiokawa et al. (EPS, 2017) https://doi.org/10.1186/s40623-017-0745-9
Takagi et al. (GRL, 2018) https://doi.org/10.1029/2018GL079615

R006-57
Zoom meeting B ：11/4 AM2 (10:45-12:30)
11:30-11:45

Study of equatorward detachment of auroral arc from the oval using ground-space observations and the BATSRUS+CRCM model

#YADAV SNEHA[1)],塩川 和夫[1)],大山 伸一郎[1)],稲葉 裕大[1)],高橋 直子[2)],関 華奈子[2)],風間 洋一[3)],Wang Shiang-Yu[3)],浅村 和史[4)],笠原 慧[2)],横田 勝一郎[5)],堀 智昭[1)],桂華 邦裕[2)],Kasaba Akimasa[6)],土屋 史紀[6)],熊本 篤志[6)],小路 真史[1)],笠原 禎也[7)],松岡 彩子[4)],田 采祐[1)],今城 峻[1)],三好 由純[1)],篠原 育[4)]
[1)]Nagoya University,[2)]University of Tokyo,[3)]National Cheng Kung University,[4)]Japan Aerospace Exploration Agency,[5)]Osaka University,[6)]Tohoku University,[7)]Kanazawa University

Study of an equatorward detachment of auroral arc from the oval using ground-space observations and the BATSRUS+CRCM model

#SNEHA YADAV[1)], Kazuo Shiokawa[1)], Shin-ichiro Oyama[1)], Yudai Inaba[1)], Naoko Takahashi[2)], Kanako Seki[2)], Yoichi Kazama[3)], Shiang-Yu Wang[3)], Kazushi Asamura[4)], Satoshi Kasahara[2)], Shoichiro Yokota[5)], Tomoaki Hori[1)], Kunihiro Keika[2)], Akimasa Kasaba[6)], Fuminori Tsuchiya[6)], Atsushi Kumamoto[6)], Masafumi Shoji[1)], Yoshiya Kasahara[7)], Ayako Matsuoka[4)], Jun ChaeWoo[1)], Shun Imajo[1)], Yoshizumi Miyoshi[1)], Iku Shinohara[4)]
[1)]ISEE, Nagoya Univ.,[2)]University of Tokyo,[3)]National Cheng Kung University,[4)]Japan Aerospace Exploration Agency,[5)]Osaka University,[6)]Tohoku University,[7)]Kanazawa University

The linkage between equatorward detachment of arc from the auroral oval and magnetospheric processes remains poorly understood mostly due to the lack of satellite measurements in the source magnetosphere at the time of arc detachment. Recently several studies have shown that there is a common features of equatorward arc detachment from the main auroral oval for Stable Auroral Red (SAR) arcs (e.g., Shiokawa et al., AIP, 2009; EPS, 2017; Takagi et al., GRL, 2018) and STEVE (e.g., Gallardo-Lacourt et al., JGR, 2018). In this study, we present observations of an equatorward detachment of auroral arc from the main oval and magnetically conjugate measurements made by the Arase satellite in the inner magnetosphere. The all-sky imager at Gakona (magnetic latitude is 63.6 N), Alaska, shows the presence of auroral arc in both red- and green-line at local midnight (01-02 MLT) on 30 March 2017. The electron density derived from the Arase measurement shows that this arc occurred outside the steep plasmapause. The flux of low to medium energy electrons (10 eV-10 keV) penetrated deeper towards lower L-shells (L equal to 4.2) at the arc crossing as compared to the inner edge (L equal 4.4) of high-energy (greater than10 keV) plasma sheet electrons. We estimated auroral intensities for both red- and green-line by using Arase low-energy electron flux data. The estimated intensities show reasonable correspondence with the observed intensities. Further, we employ the simulation results of the Community Coordinated Modeling Center (CCMC), the BATSRUS+CRCM 3D MHD code to understand the connection between magnetospheric dynamics and detached auroral arc. Simulations show the build-up of higher pressure in the nightside inner magnetosphere and the inward motion of 1-10 keV energy electrons and ions from L equal to 4 to L less than 3 at 1240-1300 UT close to the time interval of the arc detachment. These findings indicate that the observed midnight arc at Gakona was associated with the localized enhancement of 10 eV-10 keV electron flux just inside the inner edge of the electron plasma sheet. We will discuss underlying possible mechanisms that can create such localized enhancement of electrons inside the inner edge of the electron plasma sheet.

The linkage between equatorward detachment of arc from the auroral oval and magnetospheric processes remains poorly understood mostly due to the lack of satellite measurements in the source magnetosphere at the time of arc detachment. Recently several studies have shown that there is a common features of equatorward arc detachment from the main auroral oval for Stable Auroral Red (SAR) arcs (e.g., Shiokawa et al., AIP, 2009; EPS, 2017; Takagi et al., GRL, 2018) and STEVE (e.g., Gallardo-Lacourt et al., JGR, 2018). In this study, we present observations of an equatorward detachment of auroral arc from the main oval and magnetically conjugate measurements made by the Arase satellite in the inner magnetosphere. The all-sky imager at Gakona (magnetic latitude is 63.6 N), Alaska, shows the presence of auroral arc in both red- and green-line at local midnight (01-02 MLT) on 30 March 2017. The electron density derived from the Arase measurement shows that this arc occurred outside the steep plasmapause. The flux of low to medium energy electrons (10 eV-10 keV) penetrated deeper towards lower L-shells (L equal to 4.2) at the arc crossing as compared to the inner edge (L equal 4.4) of high-energy (greater than10 keV) plasma sheet electrons. We estimated auroral intensities for both red- and green-line by using Arase low-energy electron flux data. The estimated intensities show reasonable correspondence with the observed intensities. Further, we employ the simulation results of the Community Coordinated Modeling Center (CCMC), the BATSRUS+CRCM 3D MHD code to understand the connection between magnetospheric dynamics and detached auroral arc. Simulations show the build-up of higher pressure in the nightside inner magnetosphere and the inward motion of 1-10 keV energy electrons and ions from L equal to 4 to L less than 3 at 1240-1300 UT close to the time interval of the arc detachment. These findings indicate that the observed midnight arc at Gakona was associated with the localized enhancement of 10 eV-10 keV electron flux

just inside the inner edge of the electron plasma sheet. We will discuss underlying possible mechanisms that can create such localized enhancement of electrons inside the inner edge of the electron plasma sheet.

R006-58
Zoom meeting B ：11/4 AM2 (10:45-12:30)
11:45-12:00

Plasma and field characteristics observed by the Arase satellite in the source of a substorm brightening aurora at L=6

#LIWEI CHEN[1)], Kazuo Shiokawa[1)], Yoshizumi Miyoshi[1)], Shun Imajo[1)], Shin-ichiro Oyama[1)], Yasunobu Ogawa[2)], Yudai Inaba[1)], Keisuke Hosokawa[3)], Yoichi Kazama[4)], Shiang-Yu Wang[4)], Sunny W. Y. Tam[4)], Tzu-Fang Chang[15)], B.-J. Wang[6)], Kazushi Asamura[7)], Satoshi Kasahara[8)], Shoichiro Yokota[9)], Tomoaki Hori[1)], Kunihiro Keika[8)], Yasumasa Kasaba[10)], Masafumi Shoji[1)], Yoshiya Kasahara[11)], Ayako Matsuoka[12)], Iku Shinohara[7)]
[1)]Institute for Space?Earth Environmental Research, Nagoya University,[2)]National Institute of Polar Research,[3)]The University of Electro-Communications,[4)]National Cheng Kung University,[5)]Institute of Space and Plasma Sciences, National Cheng Kung University,[6)]Institute of Astronomy and Astrophysics, Academia Sinica,[7)]Institute of Space and Astronautical Science, Japan Aerospace Exploration Agency,[8)]University of Tokyo,[9)]Osaka University,[10)]Tohoku University,[11)]Kanazawa University,[12)]Data Analysis Center for Geomagnetism and Space Magnetism, Kyoto University

In this study, we would like to present a unique event in which the Arase satellite crossed the magnetospheric source region of a substorm brightening arc at 1752 UT on 12 October 2017, while a ground-based EMCCD camera at Tromsoe (69.66N, 18.94E) made a conjugate observation at the same time. The L-value of the Arase satellite was 6.9-5.2 at 1700-1830 UT. Magnetograms at Tromsoe and nearby stations in Scandinavia showed a sudden decrease of the H-component magnetic field starting at~1747 UT (1903 LT) with a maximum amplitude of ~180 nT, indicating a major substorm onset. Subsequently at 1750 UT, when the Arase satellite's footprint was moving equatorward in the southern part of the field-of-view of the EMCCD camera, a sudden brightening of auroral arc appeared very close to the footprint of the satellite. In addition to the optical signature, a series of Pi-2 pulsations were recorded at several mid-latitude magnetometers starting at ~1747 UT near the timing of the H-component decrease at Tromsoe, while an auroral kilometric radiation (AKR) starting at ~1749 UT can be seen in the wave data obtained by the Arase satellite. These simultaneous phenomena indicate the occurrence of an onset of a substorm at ~1747 UT. The magnetic and electric field data, as well as the particle data of low energy electrons and medium energy ions, show the characteristic variations and/or energizations around the timing of the Arase crossing over the brightening arc. The cross products of the variation of the electric and magnetic field show a series of field-aligned Poynting flux toward the ionosphere at the timing around the crossing. Field-aligned bi-directional electrons with an energy range between 66-1800 eV can be seen simultaneously with the brightening of auroral arc, which was probably caused by ionospheric electrons from the auroral brightening region. This is a unique conjugate observation that the ground-based optical device was observing the sudden brightening auroral arc during the onset of a substorm while a satellite made an in-situ measurement of the plasma in the auroral source region at the inner magnetosphere. The results of this analysis contribute to the understanding of the mechanism of substorm in the inner magnetosphere.

R006-59
Zoom meeting B ：11/4　AM2　(10:45-12:30)
12:00-12:15

磁気静穏時のサブストーム中に観測された Stable Auroral Red (SAR) arc の地上全天カメラと内部磁気圏衛星による同時観測の複数例解析

#稲葉　裕大[1)],塩川　和夫[1)],大山　伸一郎[1)4)5)],大塚　雄一[1)],Connors　Martin[2)],Schofield　Ian[2)],三好　由純[1)],今城　峻[1)],新堀　淳樹[1)],風間　洋一[3)],Wang　Shiang-Yu[3)]
[1)]名大・宇地研,[2)]Athabasca University Observatories,[3)]Academia Sinica Institute of Astronomy and Astrophysics,[4)]Univ. of Oulu, Finland,[5)]国立極地研究所

Multi-event analysis of Stable Auroral Red (SAR) arcs by all-sky imagers and inner magnetospheric satellites

#Yudai Inaba[1)], Kazuo Shiokawa[1)], Shin-ichiro Oyama[1),4),5)], Yuichi Otsuka[1)], Martin Connors[2)], Ian Schofield[2)], Yoshizumi Miyoshi[1)], Shun Imajo[1)], Atsuki Shinbori[1)], Yoichi Kazama[3)], Shiang-Yu Wang[3)]
[1)]ISEE, Nagoya Univ.,[2)]Athabasca University Observatories,[3)]Academia Sinica Institute of Astronomy and Astrophysics,[4)]Univ. of Oulu, Finland,[5)]National Institute of Polar Research

Stable auroral red (SAR) arcs with 630.0-nm emission are caused by low-energy electron heat flux or precipitation into the topside ionosphere from the inner magnetosphere. SAR arcs are observed at subauroral latitudes equatorward of the auroral oval and often occurs during the recovery phase of magnetic storms and substorms [e.g., Rees and Roble, Rev. Geophys., 1975; Takagi et al., GRL, 2018]. Kozyra et al. [JGR, 1997] has noted that there were three possible mechanisms to generate these low-energy electrons. The first hypothesis is the Coulomb collision between plasmaspheric electrons and ring current ions [e.g., Cole, JGR, 1965; Kozyra et al., JGR, 1987]. The second hypothesis is that the Landau damping of electromagnetic ion cyclotron (EMIC) waves causes heated electrons, resulting in their pitch angle scattering and precipitation into the ionosphere [Cornwall et al., JGR, 1971]. The third is that the kinetic Alfven waves (KAWs) with the electric field parallel to the magnetic field accelerate plasmaspheric electrons into the ionosphere [Hasegawa and Mima, JGR, 1978]. Inaba et al. [submitted to JGR, 2020] has identified that EMIC waves or KAWs associated with the SAR arc were not observed in the magnetospheric source region of a SAR arc and has concluded that the Coulomb collision was likely to be the main cause of the SAR arc. However, the previous study showed only a single event without low-energy ion data, so the Coulomb collision evaluation was not adequate. In this presentation, we show three conjunction events of SAR arcs observed by all-sky imagers and inner magnetospheric satellites (Arase and Van Allen Probes) during non-storm time substorms on 4 November 2019, 17 January 2015, and 19 December 2012. KAWs and EMIC waves were not observed in the source magnetosphere on these three events. We are also evaluating the electron heating rate through the Coulomb collision using full-energy range ion data observed by the satellites. In the presentation, we will discuss the production mechanisms of these SAR arcs based on these detailed analyses.

R006-60
Zoom meeting B ：11/4 AM2 (10:45-12:30)
12:15-12:30

Observational study on preferential energization of low-charge-state heavy ions in the near-Earth magnetotail

#Kunihiro Keika[1)], Satoshi Kasahara[1)], Shoichiro Yokota[2)], Masahiro Hoshino[1)], Kanako Seki[1)], Takanobu Amano[1)], Lynn Kistler[3)], Masahito Nose[4)], Yoshizumi Miyoshi[4)], Tomoaki Hori[4)], Iku Shinohara[5)], Ayako Matsuoka[6)], Mariko Teramoto[7)], Yusuke Ebihara[8)]
[1)]The University of Tokyo,[2)]Osaka Univ.,[3)]University of New Hampshire,[4)]ISEE, Nagoya Univ.,[5)]ISAS/JAXA,[6)]Kyoto University,[7)]Kyushu Institute of Technology,[8)]RISH, Kyoto Univ.

The ion pressure in the Earth's inner magnetosphere is generally dominated by a few to a few 100s keV protons. Oxygen ions of ionospheric origin, O+, can make a significant contribution to the ion pressure during geomagnetically active periods. Our previous study showed clear oxygen-proton differences in energy spectra in the outer part (L>5) of the ring current region. The results indicate the occurrence of mass-dependent acceleration in the inner magnetosphere and/or near-Earth magnetotail. The present study extends analysis toward ions with different mass and/or charge states, for example, He+ and O++ of ionospheric origin and He++ of solar wind origin. We primarily use data from the MEP-i (Medium-Energy Particle experiments - ion mass analyzer), which measures ions with energies of ~10 to 180 keV/q and determines both mass and charge, on board the Arase spacecraft.
We examine characteristics of energy spectra of energetic ions during magnetic storms that occurred when the Arase apogee was positioned on the night side. Energy spectra of singly-charged ions (H+, He+, O+) show mass dependence, with He+ and O+ having harder spectra than H+. The spectral slope of doubly-charged ions (He++, O++) is steeper for He++ than O++. For ions with the same mass, singly-charged ions show harder spectra than doubly-charged ones. The energization occurs more effectively in the direction perpendicular to the magnetic field rather than the parallel direction. The results suggest preferential energization of low-charge-state heavy ions caused by the dawn-dusk electric field in the near-Earth magnetotail. The preferential energization is likely associated with narrow flow channels during magnetic field reconfiguration (dipolarization), which are reportedly generated on the spatial scale comparable to the gyro-radius of low-charge-state heavy ions.

R006-61
Zoom meeting B ：11/4　PM1　(13:45-15:30)
13:45-14:00

あらせ衛星 PWE/EFD によって観測された電場データの波形解析

#中川　朋子[1)],笠羽　康正[2)],小路　真史[3)],中村　紗都子[4)],堀　智昭[3)],三好　由純[3)],北原　理弘[3)],松田　昇也[5)],小嶋　浩嗣[6)],笠原　禎也[7)],篠原　育[8)]
[1)]東北工大・工・情報通信,[2)]東北大・理,[3)]名大 ISEE,[4)]ISEE,[5)]ISAS/JAXA,[6)]京大・生存圏,[7)]金沢大,[8)]宇宙研／宇宙機構

Waveform of DC to low-frequency electric field data obtained by PWE/EFD onboard the Arase satellite

#Tomoko Nakagawa[1)], Yasumasa Kasaba[2)], Masafumi Shoji[3)], Satoko Nakamura[4)], Tomoaki Hori[3)], Yoshizumi Miyoshi[3)], Masahiro Kitahara[3)], Shoya Matsuda[5)], Hirotsugu Kojima[6)], Yoshiya Kasahara[7)], Iku Shinohara[8)]
[1)]Tohoku Inst. Tech.,[2)]Tohoku Univ.,[3)]ISEE, Nagoya Univ.,[4)]ISEE,[5)]ISAS/JAXA,[6)]RISH, Kyoto Univ.,[7)]Kanazawa Univ.,[8)]ISAS/JAXA

Waveform data obtained by the Electric Field Detector (EFD) of the Plasma Wave Experiment (PWE) instrument onboard the Arase spacecraft are examined in detail to assess the quality of the DC to low-frequency electric field and the spacecraft potential. EFD records electric potentials of four metal probes installed at tips of two orthogonal pairs of the wire antennas extending from the satellite body and observes an electric field by measuring an electric potential difference between each pair of two probes. In principle, we expect that the instrument obtains sinusoidal waveforms of the potential difference with a period of the satellite's spin, as the antennas rotate as well in a natural electric field perpendicular to the spin axis. Our detailed analysis, however, has revealed that sometimes the waveforms significantly deviate from a well-defined sinusoidal curve, and the two pairs of antenna yield somewhat inconsistent electric field vectors, particularly in a low plasma density environment such as outside the plasmasphere. We have analyzed and discussed possible causes of the unexpected characteristics of the waveforms in the regular, EFD sub-team meeting, which has been called as “the EFD bootcamp". In this paper, we showcase and review the current issues of the electric field data provided by EFD including data processing pipelines. Detailed behavior of electric potentials of the four probes as well as the spacecraft potential dependent on the spin phase of the spacecraft is also discussed.

磁気圏における静電場観測は、磁気圏内のプラズマの対流、ULF 波動とその伝搬方向、加速電場などを捉えるうえで不可欠な手段である。また 1 Hz 前後の低周波電場変動は、粒子加速と関連して注目される電磁イオンサイクロトロン波の研究にとって不可欠である。
ジオスペース探査衛星「あらせ」では、Plasma Wave Experiment (PWE)によって、4 本のワイヤアンテナ Wire Probe Antenna (WPT, 長さ 15-m, Tip-to-Tip 長 約 32-m）間の電位差計測が、Electric Field Detector (EFD)による「ダブルプローブ法」を用いて、衛星スピン面内の直交 2 系統について行われている。過去の磁気圏探査衛星「あけぼの」では限られたタイミングでしかプローブ電位情報が得られなかったが、「あらせ」PWE/EFD では、1 スピン約 8-sec に対して約 64 点（8 Hz, バーストデータでは 128 Hz）で常時全プローブの電位データを個別に得ており、衛星と各プローブの電位挙動を知るうえで圧倒的に有利な点となっている。
プローブ電位の周辺プラズマ電位への追随性は、電場の観測精度と信頼性に直結する。ダブルプローブ法は、プローブ電位、すなわち「プローブ-衛星間の電位差」の計測を基礎とする。衛星それぞれの電位は、周辺電子（・イオン）の流入電流と光電子の放出電流のバランスで決まる「フローティング電位」を取るため、一般に周辺プラズマの電位からはずれる。プローブに衛星から供給するバイアス電流を加えることで、プローブ電位は周辺プラズマ電位により近づけるものの、周辺プラズマそのものの電位とはまだ若干異なる。この相違量はプローブの表面特性・形状に依存するため、極力これらを揃えたもうひとつのプローブとの電位差によってプラズマ中電場は導出される（この過程で、衛星電位の影響も消されることになっている）。従来の認識では、プローブのシースインピーダンス・シース電圧降下および仕事関数による影響は類似特性のプローブ対ならば相殺ないし少なくとも定数（オフセット）となるであろうとの期待の下、スピン衛星によって計測される自然電場由来のプローブ電位変動は衛星スピン周期の正弦波になるので、プローブ間電位差をスピン周期でサインフィットすれば、正弦波の自然電場とオフセット成分を分離できるはずと考えられてきた。もちろんアンテナ長がデバイ長より長く、衛星ポテンシャルそのものの影響がプローブに及ばないことがその前提である。
現実はより複雑である。「あらせ」PWE/EFD による電場データ（＝プローブ間電位差）および各プローブ電位データにより、オフセット成分にもより複雑なスピン変調があり、プローブ間電位差は歪んだサイン波のような形状を示すとともに、その歪みにはプローブ毎の個性も存在する。このため、サインフィットだけでは信号（自然電場）を正しく分離できない場合がある。高密度域（特にプラズマ圏内）では、衛星電位・プローブ電位とも十分な周辺プラズマ電流に支配されて安定した値をとるため問題なく観測できるものの、プラズマ圏外の低密度域では、歪みが大きく直交 2 系統のワイヤアンテナ対で計測した電場の大きさ・方向が異なったり、磁場と直交しなかったりするように見えるケースが多発している。あらせ衛星はスピン軸を太陽指向とし、プローブに対する太陽光照射のスピン変動を抑制する設計をとったが、これにもかかわらず衛星形状が軸対称ではないためか衛星電位にもスピン変動も見られ、周辺プラズマ電位を乱している可能性が考えられる。これらのため、弱い電場（＜a few mV/m）においては定常的に

磁気圏内で「Dusk-to-Dawn 電場」が見られるといった問題を生んでいる。より大きな非定常の電場・波動については、チーム側の個別確認によるデータ品質保証を行いながらアウトプットにつなげている。
本稿では、PWE チーム内の EFD データ評価・較正・処理サブチーム会合、通称「電場・電位ブートキャンプ」で議論されてきたこれら諸問題の現況と、DC・低周波電場データの精度・信頼性に対する諸注意について紹介する。

R006-62
Zoom meeting B ：11/4 PM1 (13:45-15:30)
14:00-14:15

Characteristics of the magnetic field variations at and above proton cyclotron frequency observed by Arase

#Ayako Matsuoka[1)], Masahito Nose[2)], Yoshizumi Miyoshi[3)], Mariko Teramoto[4)], Reiko Nomura[5)], Akiko Fujimoto[4)], Yoshimasa Tanaka[6)], Manabu Shinohara[7)], Satoshi Kurita[8)], Shun Imajo[9)], Iku Shinohara[10)]
[1)]Kyoto University,[2)]ISEE, Nagoya Univ.,[3)]ISEE, Nagoya Univ.,[4)]Kyutech,[5)]NAOJ,[6)]NIPR/ROIS-DS/SOKENDAI,[7)]Kagoshima National College of Technology,[8)]RISH, Kyoto Univ.,[9)]ISEE, Nagoya Univ.,[10)]ISAS/JAXA

Magnetic field variations are regarded as major causes of relativistic electrons in the inner magnetosphere. The Pc5 ULF waves cause the radial diffusion of electrons and consequent acceleration. The whistler waves can accelerate electrons by the energy transfer from the waves to the electrons.
It is told that the radial diffusion process is insufficient to interpret the observed increase of the relativistic electrons. Some comparisons between the measurements and numerical simulation have shown that both radial diffusion by ULF waves and whistler waves would contribute to the increase of the relativistic electrons (Ma+, 2018).
The EMIC waves are considered as the effective process to loss the relativistic electrons by the pitch angle scattering. Meanwhile, magnetic field variations around and above proton cyclotron frequency have not studied in view of the acceleration of the electrons. The magnetospheric disturbance phenomena, e.g., dipolarization and bursty bulk flow from the night-side plasma sheet, are often accompanied by the broadband magnetic field variation. The magnetic field variation in this frequency range has the potential for factor of the rapid increase of the relativistic electrons in the inner magnetosphere.
The magnetic field variations between a few Hz and a few tens Hz are measured by MGF, fluxgate magnetometer, onboard the Arase satellite. For the precise measurement of the magnetic field variation, we have worked to reduce the artificial noises caused by the linearity error of the analog-to digital conversion, inaccuracy of the satellite spin phase at the sampling, and inaccuracy of the satellite clock. The data after reduction of artificial noises enable us to study the magnetic field variation in the frequency range of interest.
We will present the method and benefit to reduce the artificial noise from the magnetic field data. The remaining noise and its effect to the scientific results are studied as well. Based on the knowledge about the restriction to evaluate the magnetic field disturbance, we will discuss the characteristics of the magnetic field variations in view of the acceleration of electrons in the inner magnetosphere.

R006-63
Zoom meeting B ：11/4 PM1 (13:45-15:30)
14:15-14:30

Application of MI Sensor to Geomagnetic Field Measurements for Constructing Distributed Arrays of Small Instruments (DASI)

#Hiroshi Nomura[1)], Masahito Nose[1)], Hitoshi Aoyama[2)], Takeshi Kawano[2)], Hiroshi Ichihara[3)], Masafumi Hirahara[1)]
[1)]ISEE, Nagoya Univ.,[2)]Aichi Steel Corporation,[3)]Nagoya University

Magneto-impedance (MI) effect was discovered about 25 years ago and micro-size magnetic sensors that utilizes this effect become commercially available. MI sensors are much less expensive than fluxgate sensors. We are developing a low-cost system to measure the geomagnetic field using the MI sensor, which is named MIM-Pi. MIM-Pi includes a Raspberry Pi, low-cost 24-bit AD converters, and power supply circuits for generating a stable power supply voltage.
For the period of June 17 to June 25, 2020, we conducted experimental observations of geomagnetic field variations with MIM-Pi at Inabu observation site in Japan (26.8 degrees, -152.5 degrees in geomagnetic coordinates). Inabu observation site is operated by Nagoya University. Data obtained with MIM-Pi were compared with those from the fluxgate magnetometer that has been working at the site. Results showed that MIM-Pi recorded Sq variations and geomagnetic pulsations with amplitudes of ~2 nT that were also detected with the fluxgate magnetometer.
In presentation, we will show long term observations by MIM-Pi and discuss the possibility of using this system for construction of Distributed Arrays of Small Instrument (DASI). We will also show the result of an attempt to remove artificial noises by placing multiple observation systems at neighboring observation points and performing independent component analysis.

R006-65
Zoom meeting B ：11/4　PM1　(13:45-15:30)
14:45-15:00

電子温度と密度を測定する Thermal Noise Receiver のチップ化に向けた検討

#伊藤　友哉[1)],小嶋　浩嗣[2)],栗田　怜[3)],頭師　孝拓[2)]
[1)]京大 生存圏,[2)]京大・生存圏,[3)]京都大学 生存研

Evaluation of thermal noise spectra in unmagnetized and magnetized plasmas for development of future noise receiver

#Tomoya Ito[1)], Hirotsugu Kojima[2)], Satoshi Kurita[3)], Takahiro Zushi[2)]
[1)]RISH, Kyoto Univ.,[2)]RISH, Kyoto Univ.,[3)]RISH, Kyoto Univ.

Observation of electron temperature and density by satellites is important to consider physical phenomena in space plasma. Various kinds of particle detectors have been installed to Japanese scientific satellites to measure these parameters. However, it is difficult to obtain the temperature and density of cold plasmas whose energies are below the spacecraft potential. On the other hand, in Europe, the plasma wave receiver called “thermal noise reciever" has been widely used to obtain the cold electron temperature and density from the spectral shape around the plasma frequency [1]. The thermal noise receiver is required to observe faint voltage fluctuations induced by thermal motion of the plasma. Thus the noise level of the receiver needs to be much lower than the voltage fluctuation. In order to reduce the noise level of the receiver, a low noise amplifier and a narrow band filter are essential, while use of the commonly-used amplifier and narrow band filter make the total size of the receiver large. The purpose of this research is to reduce the size of the thermal noise receiver by utilizing the ASIC technology so that the receiver can be installed to miniaturized spacecraft. In this paper, in order to consider the specifications required for future miniaturized thermal noise receiver, we derive the signal level of the thermal noise which is induced in the electric field antenna based on the theoretical and numerical analysis [2][3]. We assumed two kinds of plasma distribution; one is a single Maxwellian distribution and the other is two Maxwellian distributions consisting with “cold" and “hot" plasmas. For each case, we assumed that the magnetic field has a large influence (magnetized plasma, for example, the inner magnetosphere) [4], and the magnetic field has no influence (weak) (unmagnetized plasma, for example, the solar wind and the tail of the earth's magnetosphere) [5][6]. From the derived voltage spectra, the noise level required for the receiver is evaluated using the characteristics of the antenna. The assumed electric field antenna is a dipole type antenna traditionally used in Japan. From this result, we will discuss the design policy of the amplifier and filter that can be installed in the thermal noise receiver.

宇宙プラズマの衛星観測における計測パラメータとして電子温度、密度は物理現象を考える上で重要である。日本ではこれらのパラメータを計測する観測器として粒子観測器やラングミュアプローブを衛星に搭載し、測定している。ただし、粒子観測器から衛星の帯電ポテンシャル以下の cold 電子の温度や密度を求めることは難しい。一方、欧州中心にプラズマ波動観測器によって、プラズマ周波数や高域混成周波数付近のスペクトル構造から、電子温度、プラズマ密度を求める手法が開発されてきた[1]。プラズマ波動の分散関係とアンテナ特性を用いて電子温度、密度を求めるこの手法は、衛星が与える周辺プラズマの変化に影響を受けにくく、他の測定器では観測することの難しい、cold プラズマのパラメータを求めることができる。このようなプラズマ波動観測器は Thermal Noise Receiver と呼ばれており、最近のミッションとしては、日欧協力で行われている水星探査衛星 BepiColombo のプラズマ波動観測器にフランスから提供されたコンポーネントとして搭載されているが、我が国で開発された例はない。Thermal noise receiver では、プラズマの熱的な動きが、電界アンテナに誘起する電圧を捉え、その周波数スペクトル構造から電子温度や密度を求めるため、非常に低いレベルのスペクトルまで観測する必要がある。そのため、その観測器のノイズレベルを十分に抑えなくてはならない。受信器のノイズレベルを抑えるために、低ノイズアンプ、狭帯域フィルタが必須となるがそのために、受信器の規模が大きくなってしまう。このように大きなリソースを要求する受信器を、アナログ ASIC を用いて、小型化することを本研究の目的としている。まず、本稿ではチップに要求されるスペックを求めるため、理論と数値解析により、想定されるプラズマ状態において、電界アンテナに誘起される信号レベルを導出する[2]。想定されるプラズマの状態として 1 成分のマクスウェル分布電子プラズマ、2 成分のマクスウェル分布電子プラズマとしている。またそれぞれの状態に対して、磁場の影響が大きい場合(例えば内部磁気圏)[4]、磁場の影響がない(弱い)場合(例えば、太陽風、地球磁気圏尾部)[5][6]の計 4 つの場合を想定して算出する。算出した誘起電圧レベルから、アンテナの特性を用いて、受信器に要求されるノイズレベルを求め、アナログ ASIC の設計方針についての検討を行う。
References:
[1] MAKSIMOVIC, M., et al., J. Geophys. Res., 100.A10: 19881-19891, 1995.
[2] SCHIFF, M. L., Radio Science, 5.12: 1489-1496, 1970.
[3] SENTMAN, D. D., J. Geophys. Res., 87.A3: 1455-1472, 1982.
[4] MEYER‐VERNET, N., J. Geophys. Res. 84.A9: 5373-5377, 1979.
[5] MEYER‐VERNET et al., J. Geophys. Res.,　94.A3: 2405-2415, 1989.

R006-66
Zoom meeting B ：11/4　PM1　(13:45-15:30)
15:00-15:15

波形・スペクトル双方の観測が可能な小型プラズマ波動観測器の開発

#頭師　孝拓[1)],小嶋　浩嗣[2)]
[1)]奈良高専,[2)]京大・生存圏

Development of the new plasma wave instruments capable of both waveform and spectrum observation.

#Takahiro Zushi[1)], Hirotsugu Kojima[2)]
[1)]National Institute of Technology, Nara College,[2)]RISH, Kyoto Univ.

Recently, the miniaturization of the instruments onboard scientific satellites is required because of the diversification of observation targets and the use of microsatellites. In order to reduce the size of the plasma wave instruments, we have been working on the integration of analog circuits. Developing analog circuits of the plasma wave instruments as Application-Specific Integrated Circuits (ASICs) enables significant miniaturization. In this study, we propose a miniaturized plasma wave instruments for both waveforms and spectrum using an ASIC with variable frequency characteristics to further reduce the size of the plasma wave instruments.
Plasma wave instrument is classified into two types: waveform type and spectrum type. Since these two types of instruments play complementary roles, it is common to have both types of instruments in recent scientific missions. These two types of instruments required different analog circuits, which led to the increase in size of the instruments. The analog circuits of the waveform type are required to have a wide bandwidth to cover the entire frequency coverage, while the spectral receiver is required to have a narrow bandwidth. The dedicated integrated circuit for the new instruments is designed to select from several cutoff frequencies of the band-limiting filter. This makes it possible to measure waveforms with a wide bandwidth when using as waveform type and with a narrow bandwidth when using as spectrum type. The new plasma wave instruments will be realized by combining such externally controllable analog circuits and digital circuits that perform the signal processing required for both the waveform and spectrum type instruments.
In the presentation, we will describe the detail design and performance of the new plasma wave instruments and analog circuit.

近年、観測対象の多様化による搭載機器の増加や超小型衛星の利用により衛星搭載機器の小型が求められており、プラズマ波動観測器についても同様である。我々は、プラズマ波動観測器の小型化のため、大型になりがちであったアナログ回路の集積化に取り組んできた。従来ディスクリート部品により構成されていたアナログ回路を専用集積回路として実現することにより、一つのチップで置き換えられ、大幅な小型化が可能になった。本研究ではプラズマ波動観測器のさらなる小型化に向け、周波数特性を可変とした専用アナログ集積回路を用いた、波形・スペクトル両用の小型プラズマ波動観測器を提案する。
プラズマ波動観測器は波形を観測する波形捕捉型と、周波数スペクトルを観測するスペクトル型の 2 種類に分類することができる。これらは相補的な役割を果たすため、近年の理学観測においては両方を搭載することが一般的である。この 2 種類の観測器において、それらの利点を最大限活かすためにはそれぞれ異なったアナログ回路を搭載する必要があり、それが観測器の大型化を招いていた。本研究では、これらの両方に対応可能なアナログ回路を専用集積回路として設計し、それを用いて 2 種類の観測が可能な観測器を開発する。波形捕捉型観測器のアナログ回路においては観測帯域全体をカバーする広帯域が求められ、スペクトル型受信器においては狭帯域であることが求められる。そのため、専用集積回路は帯域制限フィルタのカットオフ周波数を複数から選択できるよう設計している。これにより、波形を観測する際は広帯域で、周波数スペクトルを観測する際は狭帯域で測定することが可能となる。このような外部から制御可能なアナログ回路と、波形捕捉受信器、スペクトル受信器のそれぞれで必要となる信号処理を行うディジタル回路を組み合わせることで観測器を実現する。
発表においては、新型観測器の性能および設計の詳細について述べる。

R006-67
Zoom meeting B ：11/4　PM2　(15:45-17:30)
15:45-16:00

地球磁気圏 X 線撮像計画 GEO-X に向けた超軽量 X 線望遠鏡のプラズマ原子層堆積法による Pt 膜付加工

#伊師　大貴[1)],江副　祐一郎[1)],石川　久美[2)],沼澤　正樹[3)],福島　碧都[1)],鈴木　光[1)],湯浅　辰哉[1)],内野　友樹[1)],作田　紗恵[1)],稲垣　綾太[1)],上田　陽功[1)],廣本　悠透[1)],満田　和久[4)]
[1)]東京都立大,[2)]JAXA 宇宙研,[3)]理研,[4)]国立天文台

Pt-coated light-weight X-ray optics prepared by plasma atomic layer deposition on-board GEOspace X-ray imager (GEO-X)

#Daiki Ishi[1)], Yuichiro Ezoe[1)], Kumi Ishikawa[2)], Masaki Numazawa[3)], Aoto Fukushima[1)], Hikaru Suzuki[1)], Tatsuya Yuasa[1)], Tomoki Uchino[1)], Sae Sakuda[1)], Ayata Inagaki[1)], Yoko Ueda[1)], Haruyuki Hiromoto[1)], Kazuhisa Mitsuda[4)]
[1)]Tokyo Metropolitan Univ.,[2)]ISAS/JAXA,[3)]RIKEN,[4)]NAOJ

We have been developing light-weight X-ray optics for future astronomical and planetary exploration missions (Ezoe et al. 2010 MST). Microscopic pores with a width of 20 μm and a depth of 300 μm are formed by deep reactive ion etching on silicon substrates. The sidewalls of micropores are utilized as X-ray reflectors. The substrates are annealed at high temperatures to obtain sub-nm rms surface roughness and deformed into a spherical shape to focus X-rays from celestial objects. We have demonstrated X-ray reflection and imaging with micropore sample optics (Ogawa et al. 2017 MST). Our micropore optics will be on-board GEOspace X-ray imager (GEO-X; Ezoe et al. 2018 JATIS), which aims at X-ray imaging of the Earth's magnetosphere. Silicon is relatively easy to process with micro-machining technologies, while heavier materials such as Au and Pt can obtain higher reflectivity. Therefore, we focused on atomic layer deposition (ALD) as a means to coat micropore sidewalls with such a heavy metal. This thin-film deposition technique is based on self-limiting surface reactions alternately, providing high uniformity and good conformality on high-aspect-ratio micropore structures.
We previously verified X-ray reflection from Ir- and Pt-coated micropore sample optics prepared by thermal ALD (Ogawa et al. 2013 Appl. Opt., Takeuchi et al. 2018 Appl. Opt.). However, in the case of Pt, its surface roughness was estimated to be 2.2 ± 0.2 nm rms which did not meet a required micro-roughness of GEO-X (<2 nm rms). To achieve better surface roughness, we newly tested plasma ALD. The higher reactivity of plasma species can promote more active surface reactions. Using $Pt(Cp^{Me})Me_3$ as metal precursors and O_2 plasma instead of O_2 gas as reactants for oxidization decomposition of precursor ligands, we coated Pt films with a thickness of 20 nm following our previous protocol. The estimated surface roughness was 1.6 ± 0.1 nm rms and significantly better than our previous results (Ishi et al. 2020 Appl. Phys. Express). This result is acceptable for the requirement of GEO-X. Furthermore, we found that a maximum achievable surface roughness was 1.0 ± 0.1 nm rms from Pt films on a silicon substrate surface. The similar surface roughness is expected to be achieved in our micropore optics. Here we report on characterization of Pt-coated light-weight X-ray optics and other coating results of currently considered materials such as Co, Ni, and light-elements, e.g., SiC and BN.

我々は微細加工技術を用いた独自の超軽量 X 線望遠鏡を開発している（Ezoe et al. 2010 MST)。半導体加工技術の一つであるドライエッチングで厚み 300 μm の Si 基板に幅 20 μm の微細穴を多数開け、側壁を X 線反射鏡として利用する。X 線反射に必要な数 nm rms の滑らかな側壁を高温アニールで実現した後、基板を球面に塑性変形することで天体からの平行 X 線を集光する。基板が薄いため、世界最軽量であり、我々は本手法で世界初の X 線反射・結像を実証してきた（Ogawa et al. 2017 MST)。本望遠鏡は世界初の地球磁気圏 X 線撮像を目指す超小型衛星 GEOspace X-ray imager（GEO-X; Ezoe et al. 2018 JATIS）に搭載が予定されている他、JAXA 宇宙科学技術ロードマップにて「獲得すべきキー技術」にも選出され、重量・サイズ制限の厳しい将来惑星探査に対する多彩な応用可能性を秘めている。Si は加工が容易な反面、X 線反射率は Au や Pt などの重金属と比べて低いため、高アスペクト微細穴の金属成膜技術が欠かせない。そこで我々は原子層堆積法（Atomic Layer Deposition: ALD）に着目した。重金属を含むガスと酸化ガスを交互に流し、表面化学反応の自己制御性を利用して 3 次元構造体に純金属を一層ずつ成膜できる。
我々は 200-300 度の高温下における熱的反応性を利用するサーマル ALD 方式で微細穴側壁の Ir および Pt 成膜に成功してきた（Ogawa et al. 2013 Appl. Opt., Takeuchi et al. 2018 Appl. Opt.)。ALD 成膜による X 線反射率の向上は実証したが、成膜初期の核形成遅延が無視できず、表面粗さは Pt の場合 2.2 ± 0.2 nm rms と GEO-X 衛星の要求値（<2.0 nm rms）に対して更なる改善が求められていた。そこで酸化ガスに O_2 プラズマを用いるプラズマ ALD 方式を新たに試した。サーマル ALD 方式で使用していた O_2 ガスに比べてラジカルの高い反応性を利用でき、成膜初期の核形成を促進できる。我々は原料ガスに $Pt(Cp^{Me})Me_3$ を用いてサーマル ALD 方式と同様に Pt を 20 nm 成膜することに成功した。X 線反射率から求めた表面粗さは 1.6 ± 0.1 nm rms とサーマル ALD 方式に比べて有意に改善しており（Ishi et al. 2020 Appl. Phys. Express)、なおかつ GEO-X 衛星の要求値も十分に満たしている。下地となる Si 側壁を滑らかにすれば、表面粗さは 1.0 ± 0.1 nm まで達成可能であることも突き止めた。本講演では、GEO-X 衛星に搭載予定の超軽量 X 線望遠鏡のプラズマ ALD 方式を用いた Pt 膜付結果を報告すると

ともに、その他の反射材として現在検討している Co や Ni 成膜および SiC や BN などの軽元素オーバーコーティングの結果についても紹介する。

R006-68
Zoom meeting B ：11/4　PM2　(15:45-17:30)
16:00-16:15

LAMP ロケット実験搭載多波長オーロラ観測カメラの開発現状

#川村　美季[1)],坂野井　健[2)],浅村　和史[3)],岩田　直子[8)],柴野　靖子[8)],三好　由純[4)],細川　敬祐[5)]
[1)]東北大学,[2)]東北大・理,[3)]宇宙研,[4)]名大 ISEE,[5)]電通大,[6)]GSFC/NASA, USA,[7)]University of New Hampshire, USA,[8)]宇宙航空研究開発機構

Current status of development of multi-spectral auroral cameras on the LAMP experiments

#Miki Kawamura[1)], Takeshi Sakanoi[2)], Kazushi Asamura[3)], Naoko Iwata[8)], Yasuko Shibano[8)], Yoshizumi Miyoshi[4)], Keisuke Hosokawa[5)], Jones Sarah L.[6)], Lessard Marc[7)]
[1)]TU,[2)]Grad. School of Science, Tohoku Univ.,[3)]ISAS/JAXA,[4)]ISEE, Nagoya Univ.,[5)]UEC,[6)]GSFC/NASA, USA,[7)]University of New Hampshire, USA,[8)]JAXA

We are developing the multi-spectral auroral camera (AIC2) installed on the LAMP rocket which is scheduled to be launched in Alaska in the winter of 2021. We report the current status of development and future plan of AIC2. Chorus waves generated in the magnetospheric equatorial region are thought to cause the pitch angle scattering of electrons in a wide energy range (several keV -1 MeV and more). Since the pulsating aurora is caused by several keV to tens keV electrons and 'microburst' is the electron precipitation with a relativistic energy range, the generation process of pulsating aurora is possibly the same as that of microburst, and therefore, the positive relationship between pulsating aurora and microbursts is expected. However, there is no simultaneous observation between them. The purpose of the LAMP rocket is to clarify the relationship between pulsating aurora and microbursts by particle and electromagnetic wave measurement and auroral optical observation. The project Pl is Dr. Jones of NASA/GSFC. Instruments measuring thermal electrons, low energy electrons, medium energy electrons and magnetic field are provided from institutes in US, and the instrumental package called PARM2 (Pulsating AuRora and Microburst 2) is provided by the Japanese team. In addition, we plan to carry out the ground network observation using an ultra-high-speed phantom camera, high speed EMCCD imager, all-sky CMOS imagers, magnetometers at Poker Flat, Venetie, Fort Yukon, and Toolik stations. AIC2 is a one of the PARM package which consists of two CMOS detectors called AIC-S1 and S2, and the data processing electrics AIC-E, and will perform auroral imaging at two wavelengths simultaneously. Concerning the design, AIC2 is characterized by a low noise (1.6 e-RMS) and wide dynamic range sampling capability (12bit A/D) using the consumer CMOS sensors (ZWO AS1183MM). AIC-S1 targets the E region N2 1PG aurora with an interference filter (Andover, CW 670 nm, FWHM 20 nm) and a fast objective lens (SpaceCom JF17095M, f= 17 mm. F/0.95, field of view 29 deg x 29 deg). AIC-S2 is designed to observe the F-region OI 844.6 nm aurora with an interference filer (Andover, CW 846 1 mm, FWHM 4.4 nm) and a wide-angle objective lens (SpacaCom HF3.5M-2, f= 3.5mm, F/1.6, field of view 106 deg x 106 deg). To gain S/N and reduce data size, binning is performed to an original 3660 pix x 3600 pix image, and a 60 bin x 60 bin image is produced. AIC2 is mounted on a despun platform of the rocket to cancel a rocket spin. Combining the despun platform with the rocket attitude control, AIC-S1 will point to the magnetic footprint to perform simultaneous observation between the fine structure of pulsating aurora and precipitating electrons. AIC-S2 will point slantingly west covering the wide area from the limb of the earth to nadir to obtain the height profile of O 844.6 nm emission as well as the pulsating auroral distribution. The time resolution of each camera is 10 frames/s. At the apex altitude (-450km), the spatial resolution at nadir is 3.0 km x 3.0 km for AlC-S1 (E-region), and 6.3 km x 6.3 km for AIC- S2 (F-region). The AIC-E consists of two NanoPi M4 board computers, two FPGAs, and power supply to handle a large amount of image data produced by the two cameras. We newly developed a heat pipe unit to cool the two CPUs of NanoPiM4. Total weight and power of AIC2 are 2.6kg and 20W, respectively. On the development of AIC2, we carried out electrical function and system evaluation tests, such as 1) evaluation of time accuracy of the image data, 2) sensitivity calibration, and 3) data communication via a despan platform. Regarding (1), we suspected that there might be discrepancy between recorded time of image data and actual time since the camera images are taken by self-produced timing without trigger synchronization. Thus, we evaluated the accuracy of time of image data recorded with NanopiM4 by the following test. Since the time recorded by AIC2 and other instruments on the LAMP rocket is required to be sufficiently consistent with the ground-based instruments to examine high-frequency variations in pulsating aurora and microburst, such as 3Hz modulation. In the test, we fixed a continuous LED light on an aluminum disk, and rotated the disk accurately with a period of 420ms using a stepping motor. From the analysis of data taken for more than one hour, we found that the time of image data is precisely proportional to the rotation angle of LED which equals to the timing, and finally conclude that the time of AIC2 is sufficiently accurate to compare with other rocket and ground instruments. Regarding (2), a calibration test was carried out with an integrated sphere in the National Institute of Polar Research. We obtained the relationship between the counts in image data and absolute intensity in Rayleigh, and the dynamic ranges AIC-S1 and S2 are 0-480kR and 0-360kR, respectively. Data is recorded in a logarithmic scale with a sensitivity resolution in the range of 6-100R. We found that the read noise is negligibly small, and the photon shot noise is dominant. Regarding (3), we installed the AIC2 on the flight model of despun platform and carried out the data communication test via rotating terminal in the despun platform with a spin rate of 1Hz for approximately one hour. As a result, we had no error in the image data, and

could demonstrate the data communication with the despun table. In summary, from the function and calibration tests described in 1)- 3), we evaluated the optical and electrical performance of AIC2 quantitatively, and confirmed that they satisfy the scientific requirements. We are conducting electrical test of the improved AIC-E and AIC2 including the heat pipe. In the presentation, we give the latest results of AIC2, such as the vacuum test with the heat pipes, thermal cycle test, and focus adjustment.

私たちは北米アラスカから打上げが予定されている LAMP ロケット搭載オーロラ観測用多波長カメラ(AIC2)の開発をしている。本講演では AIC2 の開発の現状と、今後の開発予定について報告する。コーラス波は磁気赤道面近傍において広いエネルギー帯の電子(数 keV-1Mev 以上)とのピッチ角散乱を発生させることが理論的に指摘されている。したがって、数〜10keV の電子で発光する脈動オーロラと相対論的高エネルギー電子降下「マイクロバースト」は関係性があると期待される。しかし、それらの同時観測をした例は今までにない。LAMP ロケットは、粒子・電磁波動計測とオーロラ光学観測により、脈動オーロラと「マイクロバースト」の発生過程の関係性を明らかにすることを目的として、北米アラスカ・ポーカーフラットより 2021 年の冬に打ち上げられる。プロジェクト PI は NASA/GSFC の S. Jones 博士で、日本側からは多波長オーロラカメラ（AIC2）、高エネルギー電子計測器（HEP）、磁場計測器（MIM）からなる PARM2(Pulsating AuRora and Microburst 2)パッケージが提供される。一方、米国側からは熱的電子計測器、低エネルギー・中間エネルギー電子計測器、磁場計測器が搭載される。さらに、地上では複数の観測拠点にファントムカメラによる超高速撮像、EMCCD による高速撮像、全天カメラ撮像、地磁気・電磁波計測のネットワーク観測が計画されている。AIC2 は 2 台の CMOS 検出器（AIC-S1、AIC-S2）と信号処理エレクトロニクス（AIC-E）で構成される。CMOS 検出器には低ノイズ(1.6 e-RMS)かつ広いダイナミックレンジ(12bit A/D)に特徴がある ZWO 社 ASI-183MM を採用した。AIC-S1 は E 領域の N2 1PG 発光（中心波長 670 nm, FWHM 20 nm)を視野 29 deg x 29 deg（対物レンズ SpaceCom JF17095M, f= 17 mm, F/0.95)で撮像する。また、AIC-S2 は F 領域の OI 発光(中心波長 846 1 mm, FWHM 4.4 nm)を広角視野 106 deg x 106 deg（対物レンズ SpacaCom HF3.5M-2, f= 3.5mm, F/1.6)で撮像する。カメラはロケットスピンを打ち消すデスパンプラットフォームに搭載され、姿勢制御を組み合わせて視野の制御を行う。具体的には、S1 は磁力線フットプリント周辺の N2 オーロラ微細構造（Apex 高度 450km における空間分解能 3 km x 3 km）を捉え、オーロラ発光と粒子同時計測を行う。また、また S2 は磁力線フットプリント(Apex 高度 450km における空間分解能 6 km x 6 km)からリムまでをカバーし、脈動オーロラの広範囲分布に加えて F 領域発光の高度分布(高度分解能 2 km)を得る。2 台のカメラは 10 frames/s で同時撮像する。CMOS の元々の画素は 3660pix x 3660pix だが、S/N を上げ、かつデータ通信レート条件を満たすためにオンボードでビニング処理し、60bin x 60bin 空間分解画像（1bin あたり 16bit 深さ）とする。AIC-E は 2 台のボードコンピュータ NanopiM4 と 2 台の FPGA 回路、電力供給等で構成される。AIC2 全体の重量は 2.6kg、電力は 20W である。NanopiM4 基板上で局所的に高温になる CPU の冷却には新開発のヒートパイプを用いる。私たちはこれまで AIC2 の主な開発課題として、(1)記録される時刻精度の検証、(2)感度較正、(3)デスパンプラットホームを介したデータ通信検証などの性能評価に取り組んできた。(1)について、カメラの撮像は時刻同期をしない自走式で行われており、NanopiM4 上で記録される時刻データが実際の時刻と食い違う可能性があった。このため、私たちは、NanopiM4 が記録する時刻データが、実際に撮像された時刻とどれだけのずれがあるか実験により評価した。特に AIC2 をはじめとする LAMP ロケット搭載機器と地上観測期は脈動オーロラやマイクロバーストに見られる 3Hz モジュレーションを計測することを目標としている。このため、AIC2 データの時刻と地上機器の時刻の時刻は、この現象が十分な精度で整合的である必要がある。実験では、オシレーターをもちいて LED を台に固定し、この台をステッピングモーターで正確に回転（回転周期 420ms）する回転光源を製作した。この撮像実験の結果、LED 光源の回転角度と画像時刻の関係には良好な比例関係があり、AIC2 の時刻は、脈動オーロラの 3 Hz モジュレーションなどの高速変調の現象観測において、LAMP ロケットの搭載機器や地上機器と比較するのに十分な精度を持っていることを確認した。(2)について、国立極地研究所において、積分球を用いた較正実験を行った。この結果、ダイナミックレンジは AIC-S1 で 0-480kR、AIC-S2 で 0-360kR であることを示した。感度分解能は、対数圧縮記録のため明るさにより異なるが、6-100R であり、十分小さく、またリードノイズ成分は無視出来るほど小さい。 (3)についてフライトモデルのデスパンプラットフォームを用いて、カメラ撮像試験を行った。この試験では、デスパン部を 1rev/s で回転させ、デスパンプラットフォーム内の回転端子を介してカメラ撮像を連続 1 時間実施し、取得データ通信に抜けやエラーが発生しないことを確認した。以上まとめると、課題（1）〜（3）について AIC 光学的・電気的性能を実験により検証し、科学目的を満たすことを示した。現在、AIC-E の改良を進めており、改良された AIC-E とヒートパイプを含めた AIC2 の統合的な電気試験を行っている。講演では、最新の電気試験と、宇宙科学研究所等の真空チャンバ設備をもちいてヒートパイプの動作検証を含む真空中の動作試験、大気中での熱サイクル試験、およびフォーカス・アライメント調整などの結果について報告する。

R006-69
Zoom meeting B ：11/4 PM2 (15:45-17:30)
16:15-16:30

Experimental results on performance of an engineering model of a “double-shell" type of electrostatic plasma particle analyzer

#Masafumi Hirahara[1)], Tomomi Takei[1)], Shoichiro Yokota[2)], Tomoki Yanagimachi[3)]
[1)]Institute for Space-Earth Environmental Research, Nagoya University,[2)]Graduate School of Science, Osaka University,[3)]Creator Ryu

In these few decades, the demonstrative space plasma physics communities in the world have been conducting the intensive research and development activities for the instrumental miniaturization because compact and lightweight sensors are required for installation on micro/small satellites and cubesats in ongoing and future space exploration missions. We, therefore, have also been leading the designs and developments of several types of electrostatic plasma particle analyzers providing us with cutting-edge in-situ observational results. Recently, some novel types of space plasma instrument capable of simultaneous measurements of low-energy(less than a few tens of keV) electrons and ions with a single sensor head are being designed to cover a wide field-of-view(FOV), i.e., a full planar FOV similar to that of the prevailing top-hat type or a hemispheric FOV referring to the case of the "SELENE-PACE" analyzers, and the fabrication of the first engineering model succeeded for experimental performance tests in our electron/ion beamline facility of ISEE, Nagoya Univ. In these development activities for evolving in-situ observations of the space plasmas, the most significant viewpoint is to realize completely simultaneous measurements of electrons and ions over wide FOVs in one sensor head with a unique electrostatic energy analysis configuration for charged particles. Two separate/independent electrostatic field distributions, produced in our “double-shell" structure based on the top-hat type configuration by one high-voltage supply unit, are individually applied for electron/ion energy analyses. In the case of the engineering model reported in this presentation, the analyzer constant, the ratio of the measured particle energy to the applied voltage, is approximately four, and the full planar FOV is achieved. According to the data by the two-dimensional position-sensitive detection system, the experiments on the energy/angular analyses show good agreements with our numerical design. Since we use the electron and ion beams for the realistic space measurement situation in the actual performance tests, the detailed characteristics of the double-shell electrostatic energy analyzer can be obtained for the further improvements. These experimental results will be given here for investigation and discussion.

R006-70
Zoom meeting B ：11/4　PM2　(15:45-17:30)
16:30-16:45

波動粒子相互作用解析装置における粒子検出用高速応答回路の集積化に関する研究

#菊川　素如[1)],小嶋　浩嗣[1)],浅村　和史[2)],齋藤　義文[3)]
[1)]京大・生存圏,[2)]宇宙研,[3)]宇宙研

Development of the High-Speed Current Detection Circuits in Particle Sensors Dedicated to Wave-Particle Interaction Analyzer

#Motoyuki Kikukawa[1)], Hirotsugu Kojima[1)], Kazushi Asamura[2)], Yoshifumi Saito[3)]
[1)]RISH, Kyoto Univ.,[2)]ISAS/JAXA,[3)]ISAS

In the radiation belts, there are many high-energy particles. These particles can cause severe damage to spacecraft. Therefore, it is very important to understand their acceleration mechanism [Reeves et al., 2003]. The physical interaction between plasma waves and particles, which is considered to be the acceleration process of particles, is called "wave-particle interaction". However, it has been difficult to observe the wave-particle interaction. At present, we have only found a temporal correlation between trapped high energy particles and waves [Li et al., 2014]. This was due to the lack of temporal resolution and processing speed of conventional instruments, which prevented us from determining the energy conversion amount between waves and particles. Then, the concept of Wave-Particle Interaction Analyzer (WPIA) was proposed by Fukuhara et al. [2009]. The WPIA is designed to obtain the phase relationship between the velocity and wave vectors of each particle onboard a satellite, and it calculates the energy conversion amount directly. The WPIA was launched in 2016 as a trial installation on the Arase satellite in Japan, and is still in operation [Miyoshi et al. 2018]. However, the WPIA has some problems with respect to the physical scale of the system. Since wave-particle interaction is spatially and temporally localized and dynamically fluctuating phenomenon [Li et al., 2009], it is necessary to realize simultaneous multipoint observations by multiple small satellites to carry out accurate observations. However, satellites carrying WPIA is limited to mid-size or larger such as Arase satellite in Japan and MMS satellites in USA, and for this reason the simultaneous multi-point observation is not realistic in view of the necessary cost. Therefore, it is important to make the WPIA system small enough to be mounted on small satellites such as CubeSat [Nakaya et al].

The WPIA consists of particle observers, wave observers and the processing circuits that calculate energy conversion amount. Although it is necessary to miniaturize each part of the WPIA, we have tried to integrate the particle detection circuits inside the particle detectors that output the incoming signal of plasma particles. Since the number of detection circuits is the same as that of the particle sensors, the detection circuits are one of the largest components of the WPIA. For example, in the Arase satellite, there are 16 particle sensors to detect particles arriving from all directions, and the total size of the particle detection circuits is over 10 cm square. The subject of this study is to miniaturize and integrate the entire detection circuits on a 5 mm square chip. For integration, we will use application-specific integrated circuit (ASIC) technology, which enables us to realize a high-performance circuit specialized for a particular application.

The particle detection circuit should be able to detect one million arrivals per second. In this study, we designed three circuits: (1) a high-speed amplifier for particle detection, (2) a comparator and (3) a peak-hold circuit. In the high-speed amplifier for particle detection (1), weak current pulses generated by the particle sensor are amplified and converted into a voltage signal. The comparator (2) is used to distinguish noise from the incoming particle signal. The peak-hold circuit (3) is necessary to synchronize the reset timing of the incoming signal between 16 channels. Then we designed a prototype chip and measured it. A single detection circuit is less than 0.2 square millimeters, which makes it possible to fit 16 channels on a 5mm-square chip. The measurement results show that the rise delay time of the signal is about 30 ns and the response delay of the entire circuit is less than 50 ns at most. These results show that this circuit satisfies the prescribed conditions. In this presentation, we present the details of the WPIA system and the results of operational measurements.

地球近傍の宇宙空間には、MeV 以上の高エネルギー粒子の集まりである放射線帯が存在している。これらの粒子は航行する宇宙機へ深刻なダメージを与えうることから、その加速メカニズムの解明は工学的に重要な意味を持つ[Reeves et al., 2003]。粒子の加速過程として考えられているプラズマ波動・粒子間の物理的作用を広く"波動粒子相互作用"と呼ぶが、従来、これを観測的に捉え実証することは困難であった。目下、観測上の実績としては、捕捉された高エネルギー粒子と波動との間に時間的な相関があることを明らかにしたのみである[Li et al., 2014]。これは従来の観測器の時間分解能や処理速度が不足しており、波動・粒子間のエネルギー変換量を求めることができないことに原因があった。そこで、Fukuhara et al.[2009]により、波動粒子相互作用解析装置(WPIA: Wave-Particle Interaction Analyzer)のコンセプトが提案された。これは、人工衛星上で各粒子の速度ベクトルと波動ベクトルの位相関係を取得し、ここからエネルギー交換量を直接計算することを企図して設計されている。WPIA は 2016 年に打ち上げられた我が国の Arase 衛星へ試験的に搭載され、現在も観測を行っている[Miyoshi et al., 2018]。ところが、現用の WPIA には、そのシステムの物理的な規模に関して改善すべき課題が存在する。磁気圏中の粒子およびプラズマ波動は時空間的に局在しており、かつダイナミックに変動している[Li et al., 2009]ため、精確な観測を実施するには広範囲に投入された複数の小型衛星による同時多点観測を実現する必要がある。しかし、現状 WPIA を搭載しうる衛星は上述

した JAXA の Arase 衛星や NASA の MMS 衛星のような中型以上のものに限られ、それらを複数打ち上げることによる同時多点観測の実現は必要コストを鑑みると現実的ではない。したがって、CubeSat[Nakaya et al., 2003]等に代表される小型衛星に搭載可能なほど WPIA システムを小型化することが同時多点観測の実現のために重要であると考えられる。

WPIA は粒子観測器と波動観測器、およびそれらが取得したデータを処理する演算回路から成る。これらの各部分を小型化することが必要であるが、本研究が現在までにターゲットとして小型化を試みているのは、粒子観測器の内部にあってプラズマ粒子、とりわけ放射線帯電子の到来信号を逐次出力する粒子検出回路である。その機能上、粒子センサと同数の検出器が必要となり、WPIA の構成要素の中でも大規模なものの 1 つであった。例えば、Arase 衛星には全方向から到来する粒子を検出可能なように 16 個の粒子センサが搭載されており、それに伴う粒子検出回路の大きさは総体で 10 cm 四方を超える。本研究の目的は、この検出器の全体を 5 mm 四方の基板上に小型、集積化することにある。集積化には、専用の用途に特化した高性能な回路を実現することが可能な特定用途向け集積回路(ASIC: Application Specific Integrated Circuit)技術を用いる。

粒子検出回路には、1 秒間に 100 万個の粒子到来が検出可能であることが求められる。そこで、本研究では次に示す 3 つの回路、すなわち(1)粒子検出用高速アンプ、(2)コンパレータ、(3)ピークホールド回路を設計し、試作チップの測定を行った。 (1)は、粒子センサが発生する数百?A の電流パルスを増幅した上で電圧信号に変換し、後段のコンパレータに接続する回路である。(2)のコンパレータによって雑音と粒子の到来信号とが峻別される。(3)の回路は、到来信号のリセットタイミングを 16 チャンネルの間で同期させるために必要となるものである。測定の結果、信号の立ち上がり遅延時間は高々30 ns であり、回路全体の応答遅延時間も最大で 50ns 以下であった。また、検出回路 1 チャンネルの専有面積は 0.2 平方ミリメートルに満たず、これは 16 チャンネルを 5mm 角のワンチップに収納することも可能な大きさである。以上の結果はいずれも所定の条件を十分に満足するものであるといえる。

本発表では、この粒子検出回路システムの詳細と動作試験の測定結果を紹介する。また、WPIA システム全体の小型化に向けた今後の開発計画について述べる。

R006-71
Zoom meeting B ：11/4　PM2　(15:45-17:30)
16:45-17:00

FPGA を用いたプラズマ波動観測器向け定常雑音除去機能の開発

#大場　崚平 [1)],笠原　禎也 [1)],尾崎　光紀 [1)]
[1)]金沢大

Development of stationary noise reduction function for plasma wave instruments using FPGA

#Ryohei Oba[1)], Yoshiya Kasahara[1)], Mitsunori Ozaki[1)]
[1)]Kanazawa Univ.

Various types of plasma waves are important clues to understand the dynamics in space plasma. A number of scientific satellites have been equipped with plasma wave instruments and electromagnetic waveforms and high-resolution spectra have been obtained. Recently, the miniaturization of satellites and instruments is strongly required to realize simultaneous observations using multiple satellites. It is necessary to reduce the size of plasma wave instrument while further improving the onboard signal processing speed and performance in order to achieve more detailed observation. For this purpose, we have been developing a wave receiver composed of FPGA (Field Programmable Gate Array) with lower power consumption and higher processing speed than CPU.

In general, measured data by plasma wave instruments include artificial noise from the other onboard components in the satellite. In order to avoid the artificial noises, magnetic field sensors has to be mounted at the top of a boom. The miniaturization of satellites, however, makes it difficult to place the sensors at a sufficient distance from the satellite body. In the present study, we aim to suppress such artificial noise by on board signal processing technique implemented in the onboard FPGA to enable us to observe natural waves clearly.

Spectral subtraction (SS) method has been developed for VLF emissions observed at ground stations to suppress only stationary noise [1]. They applied the SS method to the acquired data on a computer, while we develop a noise suppression function using the SS method as an FPGA module for real-time processing on board satellite.

In the presentation, we introduce an overview of the noise reduction module, and show the evaluation results of the module using the data obtained by the PWE on board the Arase satellite.

[1] Dejima et al., The 140th SGEPSS fall meeting abstracts, 2016.

宇宙プラズマ空間で観測される様々な種類のプラズマ波動は、プラズマ中のダイナミクスを知る重要な手がかりである。これまで、数多くの科学衛星に波動観測器が搭載され、電磁界波形や高分解能スペクトルが取得されてきた。近年は、複数衛星による同時観測を実現するために、衛星や観測器の超小型化が求められている。プラズマ波動観測器においても、このような超小型化を実現しつつ、従来以上の高速かつ高度な信号処理を衛星機上で行うことで、より詳細なプラズマ波動観測の需要が高まっている。その実現のために我々は CPU に比べて、低消費電力・高速処理が可能な FPGA(Field Programmable Gate Array)を用いた波動受信器の開発を進めている。

科学衛星が機上でプラズマ波動を観測する際、観測データには観測機器や衛星内の他の搭載機器による定常的な雑音が含まれる。これらの人工的な雑音を回避するため、従来は長い伸展物の先に磁界センサを搭載していたが、衛星の小型化によりセンサを衛星から十分離して設置することが難しくなる。本研究ではこのような定常雑音を機上信号処理で抑圧し、本来の観測対象である自然波動を良好に観測できるようにすることを目指している。

先行研究[1]において、地上の観測点で観測された VLF エミッションに対して、音声信号処理技術を用いて、定常雑音のみを取り除くスペクトルサブトラクション(SS)法が開発されている。同研究では、取得済みのデータに対し、パソコン処理によって雑音除去を行っているが、本研究では機上でのリアルタイム処理を目指し、同 SS 法を FPGA モジュールとして開発する。

本発表では、FPGA による定常雑音除去システムの概要と、あらせ衛星に搭載されたプラズマ波動・電場観測器(Plasma Wave Experiment; PWE)の観測データを用いた信号処理の評価結果を示す。

[1] 出島ほか, 第 140 回地球電磁気・地球惑星圏学会予稿集, 2016.

R006-72
Zoom meeting B ：11/4 PM2 (15:45-17:30)
17:00-17:15

Electric Field Sensor Impedance in Magnetized Plasma by Particle-in-Cell Simulation

#Ibuki Fukasawa[1)], Hirotsugu Kojima[2)], Yohei Miyake[3)], Hideyuki Usui[4)], Satoshi Kurita[5)]
[1)]RISH, Kyoto Univ.,[2)]RISH, Kyoto Univ.,[3)]Kobe Univ.,[4)]System informatics, Kobe Univ,[5)]RISH, Kyoto Univ.

A dipole antenna?has been commonly used as electric-field sensors to observe plasma waves in space plasma. To calibrate electric field measurements, we have been using the assumption that wavelengths are much longer than antenna lengths. However,?in the next generation of satellite projects,?it is possible that the wavelength is comparable to antenna length and?it?significantly?affects the interpretation of the observation results. Understanding of?the electric field sensor response to plasma waves with short wavelengths is significant in evaluating intensities and phases of targeted electrostatic waves. In this research, we simulated the antenna impedances of electric field sensors in magnetized plasmas over electromagnetic waves with short wavelengths. We conducted Particle-In-Cell simulations with electric field sensors as inner boundaries.
The results were evaluated considering the linear dispersion relations in magnetized plasmas.?According to the calculation results, when the wave number of the antenna resonance is large enough, it is estimated that the resonances are seen at the frequencies of the electron cyclotron harmonics, which are frequently observed in the magnetized plasmas. The results show in some situations that at near the UHR frequency, one or two peaks of?the antenna impedance was observed. When the wave number is small enough, the resonances frequencies are shifted to slightly high.
As results of the PIC simulations, the resonances were seen at harmonics of the electron cyclotron frequency when their wave numbers were large. When the wave number was small, no resonance was observed.
In the present paper, we discuss the characteristics of electric field sensors in plasmas over plasma waves with short wavelengths that are comparable with lengths of electric field sensors.

R006-73
Zoom meeting B ：11/4 PM2 (15:45-17:30)
17:15-17:30

Onboard impedance measurement of the wire-probe antennas aboard Arase

#Shoya Matsuda[1)], Yoshiya Kasahara[2)], Hirotsugu Kojima[3)], Yasumasa Kasaba[4)], Atsushi Kumamoto[5)], Fuminori Tsuchiya[5)], Yoshizumi Miyoshi[6)], Iku Shinohara[1)]
[1)]ISAS/JAXA,[2)]Kanazawa Univ.,[3)]RISH, Kyoto Univ.,[4)]Tohoku Univ.,[5)]Planet. Plasma Atmos. Res. Cent., Tohoku Univ.,[6)]ISEE, Nagoya Univ.

The Plasma Wave Experiment (PWE) is one of the science instruments aboard Arase to measure the electric field and magnetic field in the inner magnetosphere. PWE consists of three receivers: Electric Field Detector (EFD), Waveform Capture and Onboard Frequency Analyzer (WFC/OFA) and High Frequency Analyzer (HFA), and two sensors: a couple of dipole wire-probe antenna (WPT) and a tri-axis magnetic search coil (MSC).
It is well known that the impedance of the electric field antenna in space change depending on the plasma parameters (e.g., plasma density, temperature, etc.) We have developed the onboard antenna impedance measurement system (Onboard SoftWare CALibration function; SWCAL) and implemented as a part of the onboard software of the PWE. The system uses multiple square waves as the calibration signals. It performs fast Fourier transforms (FFT) on the signal output from the A/D converters and collects frequency responses of the fundamental and that of the odd-numbered harmonics below 32768 Hz. The transfer function can be derived on the ground by dividing observed responses into the reference square wave in the frequency domain. The antenna impedance can be derived by comparing the observed total-circuit response (including the effect of the antenna impedance) and the internal-circuit response.
We have operated SWCAL measurements more than 6000 times since Arase was launched. In this study, we introduce the technique of the SWCAL function and report results from the statistical survey of the SWCAL measurements. We successfully obtained a clear relationship between the measured antenna impedance and the ambient plasma density derived from the upper hybrid resonance (UHR) frequency measurement. This result provides an important factor for the precise calibration of observed electric field data.